JPRS-UMS-92-014
13 October 1992

JPRS Report

Science & Technology

Central Eurasia: Materials Science

Science & Technology
Central Eurasia: Materials Science

JPRS-UMS-92-014 13 October 1992

CONTENTS

CORROSION

FERROUS METALS

NONFERROUS METALS, ALLOYS, BRAZES, SOLDERS

NONMETALLIC MATERIALS

PREPARATIONS

TREATMENTS

WELDING, BRAZING, SOLDERING

EXTRACTIVE METALLURGY, MINING

MISCELLANEOUS

Solubility of Fe-Ni Alloys in Liquid Aluminum

927D0251F Kiev POROSHKOVAYA METALLURGIYA in Russian No 7, Jul 92 (manuscript received 9 Jan 91) pp 58-62

[Article by V.I. Dybkov, Ye.S. Meshkov, V.V. Kovylyayev, and G.Z. Omelchenko, Institute of Problem in Materials Science at Ukrainian Academy of Sciences, Kiev; UDC 532.739.2:541.012.3]

[Abstract] The solubility of Fe-Ni alloys in liquid aluminum at 700°C temperature was studied in an experiment with 13 such alloys containing respectively 5-10-15-20-25-30-40-50-60-65-75-80-90 % Fe. These alloys were produced by melting 99.98 % extra-pure carbonyl iron and 99.98 % extra-pure electrolytic nickel in an electric-arc furnace, then pouring the melt into copper molds. The ingots were turned down to 5-6 mm long cylinders 11.27-11.29 mm in diameter with a threaded stem for mounting in a graphite holder. The alloy composition was checked by chemical sample analysis and for homogeneity by x-ray microanalysis with an electron microprobe in a "Jeol Superprobe-733" analyzer. Metallographic examination revealed a monophase structure of all alloys except of the 90 Fe - 10 Ni alloy, which contained traces of a second phase. All alloys became γ-phase solid solutions at 700°C, also the 90 Fe - 10 Ni (its $\alpha \rightarrow \gamma$ transformation temperature being 640°C). The test procedure included use of a flux containing mainly halides of alkali metals to prevent oxidation of the aluminum melt, preheated solid alloy specimens being immersed into the flux and then 10 mm deep into the aluminum melt. After their temperature had stabilized, they were removed from the melt for cooling first in liquid nitrogen and then in water. The aluminum alloys which had formed during the dissolution process were removed from the surface of the specimens, the bulk mechanically and the remainder by chemical etching with 10 % NaOH or KOH solution. These alloys were then analyzed chemically for Fe and Ni content. On the basis of the test data have been plotted isothermal solubility diagrams for Fe + Ni in liquid aluminum, dissolution of Fe-Ni alloys being nonselective despite the large difference between the solubility of Fe and of Ni individually. Measurements and calculations have, moreover, yielded data indicating how the Fe concentration in liquid aluminum depends on the length the of Fe-Ni alloy dissolution time $\tau = N_{St}/v$ (N_{St}- Stanton number, v- immersion rate) and how the combined Fe + Ni saturation concentration in liquid aluminum depends on the initial Fe content in a Fe-Ni alloy at 700°C. Figures 3; tables 3; references 4.

Mesoscopic Structure of Metallic Glasses

927D0207D Kiev METALLOFIZIKA in Russian Vol 14 No 3, Mar 92 (manuscript received 5 Aug 91) pp 79-83

[Article by V.L. Naberezhnykh, O.N. Beloshov, B.I. Selyakov, and V.M. Yurchenko, Institute of Engineering Physics at Ukrainian Academy of Sciences, Donetsk; UDC 539.219:539.37]

[Abstract] Processes in binary glassy alloys during quench hardening and subsequent annealing are analyzed according to Konobeyevskiy's theory (S.G. Konobeyevskiy; ZHURNAL EKSPERIMENTALNOY I TEORETICHESKOY FIZIKI Vol 13 No 6, 1943) for a binary solid solutions in the continuous medium approximation, the kinetics of the strain profile ε(x,t) and the kinetics of the defect concentration profile obeying Fick's law and being described each by the corresponding equation for the diffusion rate. This model is applied to two processes; 1) "ascending" diffusion caused by internal stresses during quench hardening, which results in formation of mesoscopic n-type and p-type defects with identical, on the average, atomic contents; 2) relaxation of internal strains during annealing, which results in segregation of the two kinds of atoms so that defects become converted into globules of the different alloy components during annealing. The defects are assumed to be one-dimensional and to be equidistantly spaced, with n-type and p-type defects alternating. The two kinds of atoms in the alloy are characterized by their unequal respective radii r(A) and r(B). Simultaneous relaxation of strains which external stresses induce and superposed on the internal strains is also analyzed according to this model, particularly noteworthy being the relaxation kinetics of elastic induced strains by diffusion alone below the quenching temperature and thus in the absence of Newtonian viscous flow. The authors thank V.I. Tkach for helpful discussions. Figures 6; references 12.

Electronic and Crystal Structures of Y-Ba-Cu-O Superconductor Films With Anomalous Lattice c-Parameter

9270207B Kiev METALLOFIZIKA in Russian Vol 14 No 3, Mar 92 (manuscript received 30 Jan 92) pp 12-17

[Article by V.V. Nemoshkalenko, E.M. Rudenko, A.P. Shapovalov, Yu.M. Boguslavskiy, A.V. Zhalko-Titarenko, A.A. Sushchik, S.V. Pavlovskiy, A.Ya. Perlov, and V.N. Antonov, Institute of Metal Physics, G.G. Gridneva, V.S. Melnikov, and N.P. Pshentsova, Institute of Geochemistry and Mineral Physics, Ukrainian Academy of Sciences, Kiev; UDC 539.379.3]

[Abstract] A technique of producing epitaxial $YBa_2Cu_3O_y$ superconductor films by high-frequency magnetron sputtering with a short rather than long subsequent annealing has been developed, such films with a cheemical composition corresponding to $y = 7$ having been found to have an anomalously large $\bar{c}$ lattice parameter. The apparatus for this process consists of a VUP-5 universal vacuum station with fore pumps and diffusion pumps pulling the pressure down to the 10 μtorr level, a generator of 13.5 MHz high-freqency voltage with output power regulation over the 50-200 W range, and a magnetron with an $Ar+O_2$ plasma producing gas mixture. The sputtering targets are 40 mm in diameter disks of stoichiometric 123-phase Y-Ba-Cu-O ceramic. The high-frequency discharge is stabilized by insertion of a metal reflector plate into the plasma at a 45° angle to the

target surface. Substrates are disposed edgewise at a 90° angle rather than parallel to the target surface, such a noncoaxial configuration minimizing the high-energy fraction in the flux of deposited particles. Substrates are preheated by quartz lamps to a temperature within the 650-750°C range, their temperature then being stabilized within 1-5°C by a VRT-111 high-precision temperature regulator and measured with a platinum thermocouple. Films are deposited in the $Ar+O_2$ atmosphere under any pressure within the wide 0.5-200 mtorr range, the substrate temperature being sufficiently high to ensure a mobility of absorbed atoms necessary for formation of a perovskitic structure and to ensure thermodynamically favorable conditions for growth of an oriented film structure with the $\bar{c}$-axis normal to the substrate surface. The films are then annealed in an oxygen atmosphere at a temperature within 400-450°C for only 3-5 min. An electron probe microanalysis of thus produced thicker than 100 nm epitaxial films has established that the Y:Ba:Cu = 1:2:3 is maintained, within 3-5 % variation, throughout the given ranges of gas pressure and substrate temperature. On the p-1/T diagram (T- absolute temperature in deg K) is indicated the region of thermodynamic stability of the perovskitic $YBa_2Cu_3O_7$ structure, along with the existence ranges for the $Y_2Ba_3CuO_5$+$BaCuO_2$ +Cu_2O high-temperature low-pressure phase, the tetragonal YBa_2C_{3y} ($y \geq 6.0$) phase, the orthorhombic-II $YBa_2Cu_3O_y$ ($y \geq 6.3$) phase, and the low-temperature high-pressure orthorhombic-I $YBa_2Cu_3O_y$ ($y \geq 6.6$) phase. The crystal structure of all epitaxial $YBa_2Cu_3O_y$ films was examined by the x-ray diffraction method. Subsequent calculations by the method of least squares have revealed an anomalous temperature dependence of their $\bar{c}$ lattice parameter, its magnitude varying over the 1.170-1.182 nm range at 88 K. This anomaly can be explained either by an anomalous superconductivity of films with a low (close to y = 6) oxygen content or by the crystal structure of films which differs from that of bulk ceramic. The crystal structure of $YBa_2Cu_3O_7$ films is evidently one where the configuration of layers is the same as in the lattice of $YBa_2Cu_3O_7$ bulk ceramic. The electrophysical properties of the films were measured by the standard current-voltage method at temperatures covering the "0"-300 K range and thus including the critical superconducting transition temperature T_c (81-85 K depending on the conditions of the film deposition process) for films produced under various pressures. A critical current density of up to 10 MA/cm^2 indicates an excellent superconductivity, in comparison with that of bulk ceramic. The electronic structure of films with an anomalous $\bar{c}$ lattice parameter was determined on the basis of calculations by the LMTO (Linear Combination of Tin Muffin Orbitals) method. The results indicate the same maximum density of electronic states associated with Cu-O chains in "ordinary" and "anomalous $YBa_2Cu_3O_7$ films, the difference between them being principally due to different structures of the p-states of oxygen ions in the "corrugated" lattice layers. Figures 4; references 5.

Electronic and Magnetic Properties of TiB_2 Doped With 3d-Metals

927D0207A Kiev METALLOFIZIKA in Russian Vol 14 No 3, Mar 92 (manuscript received 16 Dec 91) pp 8-11

[Article by R.F. Sabiryanov and A.L. Ivanovskiy, Institute of Solid-State Chemistry, Ural Department, Russian Academy of Sciences, Yekaterinburg; UDC 541.16]

[Abstract] The electronic structure of TiB_2 with substitutional 3d-metal impurity atoms was systematically analyzed by the self-consistent method of Green's LMTO (Linear Combination Muffin Tin Orbitals) functions. The total and local densities of states calculated by this method for the basic ideal TiB_2 compound indicate that its valence band includes not only two ground subbands of states formed respectively by B2s (higher energy) and B2p (lower energy) response functions but also Ti3d 4s and and Ti3d 4p states, the Fermi level being located close to the deep minimum density of states that separates the subband fully occupied by hybrid Ti3d and B2p states from the conduction band with Ti3d and 4p states. The total and partial impurity density of states in the TiB_2:M system (M = all 3d metals) were calculated for Sc,V,Cr,Mn,Fe,Co,Ni,Cu atoms replacing a Ti atom. The data on Sc and V atoms indicate that both have nearly the same orbital energy as a Ti atom, an energy which gives rise to a local impurity density of states and completely overlaps with the nonmetal subbands in TiB_2. While replacement of Ti atoms with Sc or V atoms will evidently destabilize the system of interatomic bonds in a TiB_2 crystal, their replacement with a Cr, Mn, Fe, or Co atoms will lower the one-electron energy and thus make the bonding between these impurity atoms stronger what it was between the replaced Ti atoms. Inasmuch as a 3d impurity element with a higher atomic number has a lower energy, its is evident from the data that in TiB_2 the energy of Sc and V (lowest atomic numbers in this series) is free and the energy of Cr is almost at the Fermi level, these states then becoming partly occupied when Mn or Fe is added and fully occupied when Co or Cu is added. This trend of the local impurity density of states leads to eventual spin polarization and attendant splitting of energy bands with opposite spin orientations: a small magnetic moment appearing first on Cr atoms (about 0.05 μ_B), a much stronger one on Mn atoms (about 1 μ_B), a weaker one on Fe atoms (about 0.6 μ_B), and again none on Co, Ni, and Cu. This consistent with the Stoner criterion of high density of states near the Fermi level as one of the prerequisites for formation of local magnetic moment centers in a crystal. Figures 3; references 10.

Low-Temperature Diffusion in Macrocrystalline Epitaxial Ni:Cu and Pd:Ag Films

927D0207E Kiev METALLOFIZIKA in Russian Vol 14 No 3, Mar 92 (manuscript received 16 Dec 91) pp 91-93

[Article by A.N. Bekrenev and A.D. Vasilyev, Samara Polytechnic Institute; UDC 539.219.3]

[Abstract] An experimental study was made concerning diffusion of substrate atoms into macrocrystalline thin epitaxial Ni:Cu and Pd:Ag films at temperatures within the (0.35-0.40)T_{melt} range, this range being 570-670 K for Ni:Cu films and 520-620 K for Pd:Ag films. The effective diffusion coefficient pertaining to condensate films of both kinds did not exceed 10^{-15} cm^2/s when the dislocation density in the substrate was about 10^6 cm^{-2}, but increased with increasing dislocation density in the substrate and decreased with rising film temperature. This effective diffusion coefficient was found to be 6-8 orders of magnitude larger than the diffusion coefficient referred to the volume of Ni or Pd grains respectively and in the case of the Ni:Cu pair to be only slightly smaller than the diffusion coefficient pertaining to fine-disperse films. The energy activating diffusion of Cu in Ni films and diffusion of Ag in Pd films was found to be 1.1 eV and 0.85 eV respectively. These data indicate that diffusion in such films takes place principally across defects in the crystal structure of the films, namely dislocations and grain boundaries. Measurements have yielded the temperature dependence of the effective diffusion coefficient for substrate atoms within the region containing 90-95 % film atoms. The mean concentration of substrate atoms fully occupying the boundaries of 40 μm large film grains did not exceed 0.2 %. After diffusion annealing at 670 K for 4 h, meanwhile, the mean Cu content in epitaxial Ni films was 30 % and the mean Ag content in epitaxial Pd films was higher than 80 %. Metallographical examination has revealed an extremely small mobility of grain boundaries, according to which the mean concentration of diffusing substrate atoms should not exceed a few percent. Their much higher measured concentration confirms that their diffusion takes most likely place across glissile dislocations in the film, dislocations which intersect the diffusion zone. Figures 2; references 4.

Effect of Molybdenum on Oxygen Diffusion and Distribution in Niobium Alloys

927D0207C Kiev METALLOFIZIKA in Russian Vol 14 No 3, Mar 92 (manuscript received 6 Aug 91, final version received 4 Jan 92) pp 47-56

[Article by N.P. Kushnareva, S.E. Snezhko, and I.P. Yarosh, Institute of Metal Physics at Ukrainian Academy of Sciences, Kiev; UDC 539.65:669.018.45:660.786]

[Abstract] In an experimental study of Nb-Mo-O alloys concerning the effect of Mo-O interaction, measurements of the logarithmic decrement of internal friction $\delta = 1/Q$ in alloys with an up to 50 atom.% Mo content were made by the inverted pendulum method. Specimens of these alloys had been produced by smelting 99.99 % pure Nb and Mo in an electric-arc furnace with a nonconsumable tungsten electrode in a pure Ar atmosphere. After primary annealing at 1200-1500°C for 2-5 h and supplementary final annealing at 950-1000°C for 1 h the oxygen content was different in different alloys but the nitrogen content was within 0.005-0.007 wt.% in all of them. Measurements were made at temperatures covering the 120-320°C (2.7-1.5 1/K) range, with the frequency of pendulum oscillations varied from 3 Hz to 10 Hz. An analysis of the temperature dependence of internal frictions and its δ peaks due to oxygen relaxation as a result of Mo-O interaction reveals no changes as the Mo-content increases from 0 to 1 atom.%, a slight asymmetry of the O-peak as the Mo-content increases to 1.5 atom.%, and an increasing this asymmetry of this peak as the Mo-content increases to 2.5 atom.%. The form of this peak and the δ_{max} temperature depend on the oxygen content. Another peak (2) appears when the Mo-content reaches 8 atom.% and there are four peaks (0,1,2,3) when the Mo content reaches 25 atom.%, the 0-peak then disappearing when the Mo content reaches 50 atom.%. For verification, the oxygen content in alloys with a known maximum δ was determined on the basis of chemical analysis and then also correlated with the impurity relaxation theory. The results of this study reveal the distribution of oxygen atoms among octahedral interstices positioned nearest to lattice nodes with different numbers of Mo atoms. They also yield data needed for calculating the Mo-O bond energy, which is positive and very low not exceeding 1.4 kJ/mole within the 150-300°C temperature range so that the repulsion of oxygen atoms from Nb atoms is weak. This indicates that the diffusion activation energy for oxygen atoms in Nb becomes higher not because of added Mo and strengthened Mo-O bond but because of the higher energy required by oxygen atoms at the upper point of the potential barrier for surmounting as they attempt to jump over it. Figures 4; references 25.

Effect of Cold Plastic Working on Austenite Grain Size in Steel

927D0211A Moscow METALLOVEDENIYE I TERMICHESKAYA OBRABOTKA METALLOV in Russian No 3, Mar 92 pp 2-4

[Article by S.S. Dyachenko, Ye.A. Kuzmenko, Kharkov Automotive Engineers Institute; UDC 669.14.018.298:620.184.82]

[Abstract] The inconsistency of published data on the effect of cold plastic working on the austenite grain size is attributed to the fact than in various studies, samples with different straining methods and degrees, initial states, and heating conditions are used. Consequently, the effect of cold plastic deformation on the austenite grain size is examined using samples from steel 15Kh with critical points of 740 and 840°C; in hot rolled samples shipped for the tests, the original ferrite grain size corresponds to No. 8 (15 μm or fine grain). Some samples annealed at 1,100°C for 1.5 h had a grain size No. 4-5 (40 μm or coarse grain). The samples are strained to a 5-80% degree and heated to various temperatures at a rate of 1-2°C/min (slow), 100°C/min (accelerated), and 50°C/min (fast). The α-phase grain size is recorded before the start of the $\alpha \rightarrow \gamma$ transformation. The dependence of the ferrite grain size at 730°C on the straining degree of steel 15Kh, the

austenite grain size in fine grain steel 15Kh at 830°C as a function of the straining degree, the austenite grain size behavior in strained fine grain steel under slow heating, and the dependence of the austenite grain size at 900°C on the straining degree in fine and coarse grain steel 15Kh are plotted. An analysis indicates that the ferrite grain size depends on the straining degree ε and the original grain size. In fine grain steel, the initial austenite grain size is the same as the α-phase grain size at the first critical point regardless of the straining degree while in the austenitic areas, highly strained steel in which a fine grain has formed before the α→γ transformation displays a greater grain growth tendency regardless of the heating conditions. The commonly held assumption of the austenite structure refining in strained steel is refuted by the findings for fine grain steel. Figures 4; references 6.

Effect of Dy Additions on Aluminum Structure and Properties

927D0211J Moscow METALLOVEDENIYE I TERMICHESKAYA OBRABOTKA METALLOV in Russian No 3, Mar 92 pp 33-35

[Article by I.N. Fridlyander, Ye.M. Sokolovskaya, Ye.N. Zimina, Ye.A. Tkachenko, M.S. Artemova; UDC 669.715'863'864:620.17:620.18]

[Abstract] The ability of small additions of transition metals to greatly affect the structure and properties of aluminum and its alloys by affecting the processes of crystallization, supersaturated solid solution decay, and recrystallization prompted an investigation of the effect of yttrium subgroup rare earth metal (RZM) elements, particularly Dy or Tb, in a 0.3% amount on the structure and properties of A99 aluminum in order to determine the possibility of using them for doping aluminum alloys. To this end, alloys are smelted in a crucible electric furnace and added to the melt at 760°C in the form of an alloying composition of Al+3.64% Tb and Al+7.72% Dy; the resulting alloy contains 0.32% Tb and 0.35% Dy. Then 25 mm dia. ingots are made by casting into a pig iron mold and 70 mm dia. ingots by casting into a water-cooled mold; the ingots are subsequently cut into 25x10 mm templates for examining their structure and determining their hardness and conductivity in the cast state and after various types of heat treatment. The dependence of the HB hardness and electric resistivity of the cast alloy with 0.35% Dy on the hardening reheat temperature with a 30 min exposure, the dependence of the HB hardness of the cast alloy with 0.35% Dy on the hardening reheat exposure, and the dependence of the recrystallized grain size of the aluminum sheet and aluminum alloys with 0.32% Tb and 0.35% Dy on the annealing temperature with a 15 min exposure are plotted. An analysis of the findings demonstrates that spherical intermetallic compounds with a 2 μm diameter form in the alloys as a result of heat treatment while the addition of 0.32% Tb or 0.35% Dy decreases the grain size in the ingots by twofold and up to sixfold in cold rolled sheets. Moreover, the lower bound of the solidification range rises by 50°C while the rupture strength increases by 50% with a slight decrease in ultimate strength. Both additions have a virtually identical effect on the alloy properties. Figures 3; tables 1; references 5: 3 Russian, 2 Western.

Structure and Properties of Microcrystalline Ni-Fe-Nb(Mo) System Alloys

927D0211I Moscow METALLOVEDENIYE I TERMICHESKAYA OBRABOTKA METALLOV in Russian No 3, Mar 92 pp 28-33

[Article by V.V. Sosnin, A.M. Glezer, O.M. Zhigalina, Central Scientific Research Institute of Ferrous Metallurgy imeni I.P. Bardin; UDC 669.24'1'293:620.17:620.182]

[Abstract] The phase composition, structure, texture, and mechanical and magnetic characteristics of Ni-Fe and Ni-Fe-Nb(Mo) system alloys commonly used in instrument-making due to a favorable combination of properties are examined in the initial state and after annealing and the effect of rapid quenching on the structure, phase composition, and magnetic and mechanical properties of microcrystalline alloy tapes on the basis of the Ni-Fe system are studied. To this end, alloy blanks are smelted in an induction furnace and cast into a stainless steel mold with a 20 mm diameter; the alloy tapes are made by the spinning method in an Ar shielding atmosphere using a closed-type Rotor-3M unit resulting in a 10 mm wide and 60-80 μm thick tape. Binary Ni+25% Fe and Ni+20% Fe alloys as well as Ni-Fe-Nb and Ni-Fe-Nb-Mo alloys with up to 8% Nb and 2.5% Mo are investigated. The alloy compositions are summarized and the dependence of the mean grain size and microhardness on the alloy annealing temperature and the dependence of the coercive force and effective magnetic permeability at a 1 MHz frequency in a 0.08 A/m field on the alloy annealing temperature are plotted. The study reveals a change in the crystallization mechanism from cellular to dendritic when binary alloys are doped with Nb, a high density of the dislocation loop defects of the quenching origin, a mean grain size stabilization, and a crystallographic texture characterized primarily by the ξ100ξ and <OVW> orientation. The use of rapid quenching by spinning makes it possible greatly to improve the mechanical characteristics compared to the alloys produced by conventional methods while maintaining a high level of magnetic properties. Figures 6; tables 1; references 12: 7 Russian, 5 Western.

Structure Formation Patterns of Phase Cold Worked Steel 50N25 Under Slow Heating

927D0211C Moscow METALLOVEDENIYE I TERMICHESKAYA OBRABOTKA METALLOV in Russian No 3, Mar 92 pp 6-8

[Article by P.Yu. Volosevich, V.V. Girzhon, V.Ye. Danilchenko, Institute of Physics of Metals, Kiev; UDC 669.15'24:669-172.620.181]

[Abstract] The diffraction patterns forming during the slow heating of phase cold worked samples of steel 50N25 to the temperature of the end of the $\alpha \rightarrow \gamma$-transformation and the solid Debye γ-phase lines observed in addition to the initial single crystal lattice spots attesting to the development of a polycrystalline component are discussed and the formation of this polycrystalline component in carbon-containing Fe-Ni alloys where carbon precipitation from the γ-solid solution with cementite formation is observed under slow heating is studied. To this end, samples of steel 50N25 smelted in a microwave (TVCh) furnace using the V-3 carbonyl iron, N-1 electrolytic nickel, and synthetic pig iron are used as the charge. The melt is slowly cooled to 1,100°C in order to produce large crystal grains, then the ingots are water-quenched, as a result of which an austenite structure is formed. An X-ray diffraction study in an RKV-66 chamber in Fe*K* radiation and an analysis of the pole figures as well as electron microscopy studies under a PREM-200 microscope reveal that the appearance and subsequent transformation of the polycrystalline γ-phase line are due to the successive development of the recrystallization process whereby the reverse austenite stability behavior in relation to the subsequent direct martensitic transformation is due not only to a change in its structural state but also to the carbon precipitation from the γ-solid solution with the cementite particle formation. Figures 2; references 5.

Twinning During Polymorphous $\alpha \rightarrow \gamma$-Transformation in Fe and High-Speed Steels

927D0211B Moscow METALLOVEDENIYE I TERMICHESKAYA OBRABOTKA METALLOV in Russian No 3, Mar 92 pp 5-6

[Article by Yu.N. Taran, V.A. Shcherbatykh, P.F. Nizhnikovskaya, L.M. Snagovskiy, Dnepropetrovsk Metallurgical Institute; UDC 669.1:669.14.252.3:620.186]

[Abstract] The $\alpha \rightarrow \gamma$-transformation in high-purity carbonyl iron and annealed high-speed commercially smelted steels R6M5K5 and R6M5F3 under continuous heating conditions at a 0.4°C/s rate is investigated. To this end, ion bombardment-etched samples are placed in the high-temperature NM-4 microscope chamber for directly observing the polymorphous transformation stages; the process is recorded on tape. The samples are cooled in argon after the end of the transformation process. The findings reveal that austenite twins in ferrite form and grow in Fe and high-speed steel under heating, leading to a nondiffusing ferrite reordering into austenite; moreover; this twin growth does not correspond to existing notions of the packing defect arrangement in a BCC (OTsK) lattice. A structural analysis of the heat-treated samples shows that in high-speed steels, austenite is shaped as layers and petals. The coherent austenite boundary rate and displacements during the twinned rectilinear boundary formation are a function of the ferrite grain orientation. The study confirms that the nondiffusing $\alpha \rightarrow \gamma$-transformation is the principal austenite-forming process in steel and iron. Figures 3; references 5.

Resistance to Brittle Failure

927D0210F Moscow METALLOVEDENIYE I TERMICHESKAYA OBRABOTKA METALLOV in Russian No 2, Feb 92 pp 21-26

[Article by A.P. Gulyayev; UDC 539.56]

[Abstract] The mechanism of brittle failure in metal alloys is reviewed on the basis of numerous published sources and a technique for determining the brittle strength of a material with internal defects is proposed. The spread of experimental data on the ultimate rupture strength under viscous and brittle failure, the energy behavior during brittle failure, the stress distribution at the notch apex, the brittle strength curves for a material with an internal crack, and the crack growth mechanism at the notch mouth are plotted. An analysis of the failure mechanisms makes it possible to derive a formula for determining the brittle strength of iron alloys as a function of the crack apex radius and crack length. The formula is easy to use since it does not take into account the energy expended by the growing crack to overcome the principal obstacle—microplastic deformation. It is shown that under brittle failure, the grain boundaries are more plastic than its bulk and vice versa under viscous failure. A. Griffiths' contribution to developing the brittle failure mechanism is recognized. Figures 8; references 48.

Nitriding Electrodeposited Iron Coats

927D0211L Moscow METALLOVEDENIYE I TERMICHESKAYA OBRABOTKA METALLOV in Russian No 3, Mar 92 pp 43-44

[Article by Li Tie-Xiong, Peoples Republic of China; UDC 621.785.53]

[Abstract] Electrolytic iron plating (and peeling) tests of 40x15x5 mm samples of steel A3 saturated in an electrolyte consisting of a 35% aqueous solution of $FeCl_2$ x $4H_2O$ resulting in a 0.7 mm thick coat are described and the coat's grain structure as well as the matrix and coat behavior under heat treatment are discussed. The iron plated steel samples are then nitrided under varying conditions. The micro- and macrostructure of the surface layer after iron plating and nitriding is examined and the surface layer hardness distribution in the layer after iron plating and nitriding under various conditions and for various durations is plotted. The study shows that a white grid forms in the nitrided layer over old microcracks and a solid white layer is observed in the longitudinal cross section, attesting to the fact that the microcracks are cured. The nitrided layer on the iron plated steel samples forms rather rapidly due to the presence of these microcracks which speed up propagation and due to the small grain size. It is recommended that the iron plated steel coats be nitrided at 440°C for 6 h or at 480°C for 3 h for optimum results; in any case, the nitriding temperature should not exceed 480°C. Figures 6; tables 1.

Certain Structure and Property Characteristics of Titanium Carbide on Steels and Hard Alloys

927D0223F Moscow METALLOVEDENIYE I TERMICHESKAYA OBRABOTKA METALLOV in Russian No 5, May 92 pp 32-34

[Article by B.V. Zakharov, A.N. Minkevich, E.R. Tone, A.I. Kovalev, Moscow Railroad Engineers Institute and Central Scientific Research Institute of Ferrous Metallurgy imeni I.P. Bardin; UDC 621.793.6:669.295'24]

[Abstract] Three methods of producing titanium carbide coats currently used today are reviewed and it is noted that the properties of titanium carbide coats vary within a broad range depending on the production method. Consequently, titanium carbide coats produced by the Moscow Railroad Engineers Institute (MIIT) and Moscow Hard Alloy Works (MKTS) technologies in a vacuum in the presence of a titanium sponge and CCl_4 vapors entering the working chamber at a 1,000-1,100°C temperature are studied. To this end, carbon steel and sintered hard alloys on the basis of tungsten carbide (TT10K8B, TT7K12, and VKS) are used as the base. The lattice parameter is measured by a DRON-0.5 X-ray diffractometer in Co*K* radiation; in addition, the chemical composition of the coats on the TT10K8B alloy produced by the former technology and the chemical vapor deposition (CVD) method is examined using X-ray photoelectron spectroscopy (RFS) in an LHS10 Zeibold Heraus spectrometer. The effect of the carbon concentration in austenite on the layer thickness and the dependence of the titanium carbide coat surface microhardness on steel with 1.2% C on the coat thickness and indentor load are plotted. The findings reveal that the more the carbon concentration in steel, the greater the surface hardness and the lower its microhardness. Structural analyses show that the coat produced on high carbon steel has a fine grain columnar structure with a prevalent growth orientation along the (100) plane and a high lattice constant while the TiC coat produced on a sintered hard alloy is characterized by larger grains and a lower lattice constant and has no growth orientation. The CVD coat has a higher oxygen content. Figures 3; tables 1; references 7: 6 Russian, 1 Western.

Wear Resistance of Heat-Treated Eutectic Iron Alloy Ion-Plasma Coatings

927D0251D Kiev POROSHKOVAYA METALLURGIYA in Russian No 7, Jul 92 (manuscript received 21 Jun 90) pp 40-44

[Article by O.V. Mikulyak, V.Ye. Panarin, and A.K. Shurin, Institute of Metal Physics at Ukrainian Academy of Sciences, Kiev; UDC 621.891]

[Abstract] The effect of high-temperature annealing on the tribological characteristics of two eutectic steel ion-plasma coatings was studied in an experiment with 12Cr18Ni9Ti (NiV15) steel and 120Mn13 (MnV7) steel coatings containing a VC (vanadium carbide) interstitial hardener phase. They were deposited by the ion-plasma process ensuring the necessary dispersion of structural components on the substrate at a temperature not higher than 150°C. They were annealed at a 1173 K temperature under a vacuum of 10 mPa for 0.5 h, 1.5 h, and 5 h, no oxides having formed in this process. They were then tested for wear resistance in dry sliding friction against quenched nitrided 28CrMoAl steel, a cylinder of this steel rubbing against a flat coating in oscillatory motion with an amplitude of 200 μm at a frequency of 50 Hz for a period of 1 h under a load of 300 MPa initial contact pressure. The wear was measured on profilograms of friction tracks. The microhardness of coatings was measured before and after annealing, heat treatment of even a short duration (0.5 h) having been found to decrease the microhardness of both coating materials to nearly one half and to nearly double their wear. The increase of the wear of MnV7 coatings was almost fully compensated by a corresponding decrease of the wear of the cylinder material. The increase of the wear of NiV15 coatings was accompanied by an almost equal increase of the wear of the cylinder material. The results of this study thus indicate that annealing decreases the wear resistance of eutectic steel ion-plasma coatings. The amount by which it decreases was found not to depend much on the length of the annealing time. Figures 2; tables 1; references 5.

Ceramic Composites

927D0210I Moscow METALLOVEDENIYE I TERMICHESKAYA OBRABOTKA METALLOV in Russian No 2, Feb 92 pp 36-40

[Article by I.N. Fridlyander, V.Ya. Shevchenko, S.M. Barinov, Scientific Production Association of the All-Union Institute of Aviation Materials and Interbranch Scientific Research Center of Engineering Ceramics; UDC 621.763]

[Abstract] The development of ceramic composites reinforced with various types of fibers and whiskers in different countries is reviewed and today's state of the ceramic composite technology is evaluated. Special attention is focused on the reinforcing elements, primarily silicon carbide filamentary crystals or fibers, the principal elements of the ceramic composite production methods, the mechanical properties of reinforced ceramic composites, and ceramic composite applications. The dependence of the crack resistance improvement of ceramic composites on the filamentary silicon carbide crystal concentration in materials with various brittle matrices and the tensile strain diagram of a ceramic composite reinforced with continuous silicon carbide fibers and the tensile strain diagram of the matrix ceramics are plotted. The conclusion is drawn that the principal method of attaining a high crack resistance—the parameter which largely determines the material's operating reliability—is to develop a heterogeneous composite structure; these structures make it possible to realize the energy-consuming processes of dissipating the work of fracture and reach a crack resistance level of over 300 $N/mm^{3/2}$ and a strength of over 500 N/mm^2. Figures 2; references 6: 2 Russian, 4 Western.

Effect of Reinforcing Filler on Structure of Castings From Al+12% Si Alloy

927D0210J Moscow METALLOVEDENIYE I TERMICHESKAYA OBRABOTKA METALLOV in Russian No 2, Feb 92 pp 40-42

[Article by T.A. Chernyshova, L.I. Kobeleva, Metallurgy Institute imeni A.A. Baykov; UDC 621.763]

[Abstract] The interaction between the Al-Si alloy matrix and the reinforcing filler fibers and the effect of the alloy temperature and exposure prior to casting, the pressure application duration during the solidification, and the presence of solid carbon particles in the melt on the Si solubility in Al, the change in the eutectic concentration, and the silicon phase morphology and dispersion in silumin alloys are discussed and the effect of these factors on the matrix structure under the vacuum-compression impregnation conditions is investigated. To this end, 30x50x120 mm samples from a composite consisting of the AL2 alloy and carbon fibers produced by vacuum-compression impregnation in an autoclave are tested and the material structure is studied under a scanning electron microscope; an X-ray microanalysis is carried out using a Camebax unit. An analysis of the composite structure demonstrates the possibility of improving the properties of composite products by carbon fibers thus reaching a higher structural heterogeneity of the matrix due to increasing the silicon content in the matrix melt. This lowers the Al_4C_3 carbon phase concentration and improves corrosion resistance and the mechanical properties. The reinforcing carbon fibers change the silumin matrix structure by developing primary Si crystal near the fiber surface and increasing the dendrite parameter and eutectic colony dispersivity. It is also shown that the material properties may be improved by modifying the melt or overheating it prior to delivering it to the impregnation mold. Figures 4; references 10: 6 Russian, 4 Western.

Electron Microscopy of Fracture of TiB_2-Fe Composites

927D0251G Kiev POROSHKOVAYA METALLURGIYA in Russian No7, Jul 92 (manuscript received 30 Oct 90) pp 83-86

[Article by R.A. Andriyevskiy, I.F. Bayman, V.N. Paderno, A.N. Pilyankevich (deceased), and L.I. Dyachenko, Institute of New Problems in Chemistry at Russian Academy of Sciences, Chernogolovka; Institute of Physics at Kyrgyz Academy of Sciences, Bishkek; Institute of Problems in Materials Sciences at Ukrainian Academy of Sciences, Kiev; UDC 621.762]

[Abstract] Fracture of TiB_2 + 25-40 % Fe composites at temperatures ranging from 20°C to 1350°C (eutectic point of TiN_2-Fe system 1340°C) was studied under scanning and transmission electron microscopes by the method of replicas, these composite materials having been produced by hot pressing of thermosetting mixtures. Fracture of specimens was tested in flexure, transition from brittle to plastic state known to begin at about 600°C. The examination revealed no particular changes in the TiB_2 phase as the temperature of fracture tests was raised from 20°C to 1250°C but did reveal increasing isolation of TiB_2 grains as the temperature of fracture tests was raised further to 1350°, these grains occasionally growing into large faceted crystals in the process of recrystallization through the liquid phase. Both intercrystalline and transcrystalline cracking mechanisms were found to play a role in fracture, the mechanism changing at about 600°C owing to change in the behavior of the binder phase and of the interphase boundaries with attendant decrease of strength and increase of plasticity at 900-1100°C temperatures. Figures 2; references 9.

Production and Properties of Corrosion-Resistant TaC-Base Material

927D0251H Kiev POROSHKOVAYA METALLURGIYA in Russian No 7, Jul 92 (manuscript received 18 Sep 90) pp 101-106

[Article by T.N. Shishkina, V.V. Podlesov, and G.N. Komratov, Institute of Structural Macrokinetics at Russian Academy of Sciences, Chernogolovka; UDC 621.762:621.7.011]

[Abstract] A new wear-resistant tantalum carbide material also highly resistant to nitric acid has been produced by the "self-propagating high- temperature synthesis" extrusion process, this process already being used for production of not so corrosion-resistant hard tool alloys. The only other material highly resistant to nitric acid in this class is chromium carbide Cr_3C_2, but it can be produced only from Cr, C oxides and therefore requires the "self-propagating high-temperature synthesis" casting process. The advantage of tantalum carbide TaC is that it can be produced directly from tantalum and carbon without their prior oxidation. As the base material has been selected $TaC_{0.85}$, this carbide burning faster than any other in the Ta-C system and the slight carbon deficit ensuring that no free carbon will appear in the combustion products. Cr18Ni9Ti stainless steel has been selected as binder material because of its excellent adhesion to carbide grains. Inasmuch as dilution of a Ta-C mixture with an inert combustion product leads to incomplete combustion, the heat effect can be enhanced by addition of titanium powder and carbon black to the charge so that they will combine into titanium carbide TiC during the high-temperature combustion process. This carbide will enhance the hardness of the end product and only a solid solution of (Ta,Ti)C carbides, which is likely to form in the process, will ensure high resistance to nitric acid (TiC alone not being resistant to nitric acid). Formation of this solid solution was verified by x-ray phase analysis, the results confirming that all grains contained only the (Ta,Ti)C carbide phase rather than two TaC and TiC carbide phases. Electrodes made of this new material were tested 24 h for corrosion resistance in boiling 74 % and 37 % HNO_3 solutions, respectively not more than 1.7 % and 2.35 % of the electrode material having dissolved. Their corrosion resistance in boiling 96 % and 48 % H_2SO_4 solutions was also but not quite as high, respectively 5.15 % and 11 % of the electrode material having dissolved. In boiling 21.5 % $HClO_4$ solution 64 % of the electrode material dissolved. In boiling 89 % and 44.5 % H_3PO_4, 21.5 % $HClO_4$, 37 % and 18.5 % HCl solutions the electrode material became pulverized. The authors thank Yu.A. Galchenko (deceased) for assisting in the microstructural examination of the electrodes, N.S. Samoylenko for performing the x-ray phase analysis, and A.M. Stolin for helpful suggestions. Figures 5; references 8.

On Existence of Nonsegregating Alloy Group With Constant Solidification Temperatures in Fe-C-Si System

927D0210B Moscow METALLOVEDENIYE I TERMICHESKAYA OBRABOTKA METALLOV in Russian No 2, Feb 92 pp 3-8

[Article by V.A. Ilinskiy, L.V. Kostyleva, M.N. Litvinenko, All-Union Scientific Research Institute of Mechanical Engineering, Volgograd; UDC 669.15'782-194]

[Abstract] The inconsistency of the published data on the dendritic segregation of silicon in ternary Fe-C-Si alloys and the notion that the segregation surface is essentially planar in the hypoeutectic section of the Fe-C-Si constitution diagram and the lack of reliable data on the concentration boundaries of the silicon microsegregation behavior range prompted an analysis of the specific features of the equilibrium Fe-C-Si constitution diagram under relatively pure experimental conditions in order to explain the discrepancy between the boundary areas of the direct and inverse silicon segregation and use the resulting patterns for optimizing the structure and properties of real steel and pig iron castings. Fifty-one ternary alloys with various component concentrations are examined whereby the broad concentration ranges of elements are simulated for most commercial steels and alloys. Specially pure carbonyl iron powder, spectral graphite, and high-purity silicon are used as the charge materials. The experiments revels the existence in pure Fe-C-Si alloys of a saddle line which is the *locus* of the figurative points of the nonsegregating ternary alloys with constant solidification temperatures; it is noted that the existence of such alloys cannot yet be experimentally confirmed and their solidification temperatures cannot be measured. It is also stressed that the existence of this saddle line is not unique to Fe-C-Si alloys; it is speculated that the line may also be found in Fe-C-Ni, Fe-C-Cu, and Fe-C-Al system. Figures 8; references 10: 5 Russian, 5 Western.

Phosphide Eutectics in Hadfield Steel Structure

927D0210A Moscow METALLOVEDENIYE I TERMICHESKAYA OBRABOTKA METALLOV in Russian No 2, Feb 92 pp 2-3

[Article by D. Shulik, L. Karamash, Ya. Vilchko, P. Dzugas, VTSh, Kosice, Slovakia; UDC 669.15'74-194:620.186.1]

[Abstract] The structure of Hadfield steel ingots (G13) cast into green sand molds consisting of austenite, phosphide eutectics, secondary carbides, and troostite with nonmetallic inclusions and micropores before heat treatment and uniform austenite after heat treatment is discussed and an earlier study of the phosphide eutectics in Hadfield steel is continued due to the fact that phosphide eutectics have a negative impact on the steel properties. To this end, a 2% nital pickling reagent is used to reveal the structure of phosphide eutectics—the only structure retained in the metal together with austenite after hardening. The study shows that the form and quantity of phosphide eutectics in Hadfield steel depend primarily on the cooling rate after casting, the heat treatment conditions, and the chemical composition. The effect of these individual factors is examined and the effect of the phosphorus and oxygen concentration on the quantity and form of the eutectic formations is analyzed. The conclusion is drawn that both the oxygen and phosphorus concentration affect the phosphide eutectics morphology. It is recommended that the Hadfield steel heating temperature be confined within a 1,030-1,050°C range. Figures 3; references: 2 Western.

Structure and Mechanical Properties of Low Carbon Structural Steels Hardened in Mill Line

927D0211F Moscow METALLOVEDENIYE I TERMICHESKAYA OBRABOTKA METALLOV in Russian No 3, Mar 92 pp 13-17

[Article by P.D. Odesskiy, D.P. Khromov, Central Scientific Research Institute of Building Structures and Central Scientific Research and Design Institute of Steel Structures; UDC 669.14.018.29:620.17:620.17:620.182]

[Abstract] The difficulty of using steel St3 and similar brands in building structures due to its insufficient strength and the shortcomings of existing hardening methods prompted an investigation of the structure forming process in low carbon steels during in-line heat treatment in the mill. To this end, commercial batches of 6 and 8 mm thick rolled low carbon steel sheets produced in wide strip mill 2000 at the Cherepovets Integrated Iron and Steel Works (CherMK) with heating to a 1,240-1,260°C temperature for rolling are examined; this heat treatment technology is compared to the method used at the Azovstal Works for 10-30 mm thick sheets made in mill 3600 and shape sections in-line heat-treated in mill 450 at the Western Siberian Integrated Iron and Steel Works (ZSMK). The HV hardness distribution in the rolled stock cross section is plotted. An analysis of the findings shows that a structure which ensures a yield strength of at least 350 N/mm^2 combined with sufficient cold resistance is formed by in-line heat treatment while in order to attain a higher yield strength of 400-600 N/mm^2, it is better to use rapid surface cooling at a 600-800°C/s rate, leading to tempered martensite with a varying degree of hardness. Subgranular and grain-boundary hardening, age hardening, and the dispersion of the pearlitic component are the main factors increasing the low carbon steel hardness. Theoretically the maximum attainable yield point of low carbon steel is 800-900 N/mm^2. Figures 4; tables 2; references 13.

Effect of Thermal Cycling on Structure of Hardened Ti-Ta-Nb System Alloys

927D0211H Moscow METALLOVEDENIYE I TERMICHESKAYA OBRABOTKA METALLOV in Russian No 3, Mar 92 pp 25-27

[Article by M.I. Petrzhik, S.G. Fedotov, Yu.K. Kovneristyy, N.F. Zhebyneva, Metallurgy Institute imeni A.A. Baykov and NIID; UDC 669.295.5'294'293:621.789]

[Abstract] The crystal lattice restructuring during the heating of α"-martempered titanium alloys and the criteria which determine the α"-martensite behavior in Ti-Ta-Nb ternary alloys are discussed and an attempt is made to establish a correlation between the crystal lattice parameters of α"-martensite and the degree of its stability to reversible 20-900°C thermal cycling. To this end, an alloy mixture containing titanium iodide, Ta, and high-purity Nb is cast into 0.8 kg ingots by five- to sevenfold remelting in an electric arc furnace with a nonconsumable electrode in a He atmosphere in a water-cooled copper mold. The chemical composite is maintained within 1% (atomic). The chemical composition, phase composition, and endothermal and exothermal transformation characteristics and lattice constants are summarized and thermograms of Ti-Ta-Nb alloys are plotted. A differential thermal analysis (DTA) of the heating-cooling process and X-ray diffraction analysis of thermal cycling (TTsO) under normal temperature show that depending on the lattice parameters, α"-martensite may undergo both reversible and irreversible phase transformations under thermal cycling. The reversible transformations are observed predominantly in alloys where Ta atoms are dominant among the alloying additions and α"-martensite has a certain degree of rhombic lattice distortion. The upper bound of the reversible phase transformations can be either 900°C or 500°C, depending on the lattice structure. Figures 1; tables 3; references 4: 2 Russian, 2 Western.

Transformations During Isothermal Treatment of VT35 Pseudo-β-Ti Alloy

927D0211G Moscow METALLOVEDENIYE I TERMICHESKAYA OBRABOTKA METALLOV in Russian No 3, Mar 92 pp 22-25

[Article by N.I. Moder, V.N. Moiseyev, A.I. Antipov, A.K. Bezrukova, L.M. Sukhorosova, Scientific Production Association of the All-Union Aviation Materials Institute and Verkhnyaya Salda Machining Production Association; UDC 669.295.5:621.785.3]

[Abstract] The properties of pseudo-β-Ti alloys in the hardened state—a promising material for various commercial applications—are discussed and the behavior of the new VT35 pseudo-β-Ti alloy (Ti-Al-V-Cr-Sn-Mo-Zr-Nb system) with $K = 1.5$ developed for making semifinished sheet products under isothermal treatment (phase transformations) are investigated. To this end, an 11.7 mm sheet produced under commercial conditions from a 920 kg ingot is examined. The polymorphous transformation and recrystallization annealing temperature are measured. The VT35 alloy hardness after isothermal exposures to various temperatures and durations and the phase composition of the alloy after exposures to various temperatures and durations are summarized and the diffraction patterns of VT35 alloy samples after an exposure to 450°C for various durations are plotted; the isothermal decay diagram of the VT35 alloy and the curves of its cooling in various media are plotted. An analysis of the curves shows that the β-solid solution decay is preceded by stratification which is more pronounced after cooling from the β-areas with subsequent isothermal exposure rather than after hardening and aging. The final decay product are the α- and β-phases. Figures 6; tables 2; references 5: 1 Russian, 4 Western.

Reversible Hydrogen Doping and Straining of VT6 Titanium Alloy

927D0210K Moscow METALLOVEDENIYE I TERMICHESKAYA OBRABOTKA METALLOV in Russian No 2, Feb 92 pp 43-45

[Article by L.I. Anisimova, Yu.A. Aksenov, M.G. Badayeva, N.V. Vasko, V.L. Kolmogorov, V.S. Mozhayskiy, Mechanical Engineering Institute at the Urals Department of Russia's Academy of Sciences and Scientific Production Association of the Machine Building Plant imeni M.I. Kalinin; UDC 621.785.53:669.295'5]

[Abstract] The effect of hydrogen on the ductility of the nonwrought VT6 titanium alloy containing 5.7% Al and 5.3% V with the final α+β→β transformation temperature of 970°C and the maximum initial volume β-phase concentration of 7% is investigated. To this end, the dependence of the yield strength of the VT6 alloy with various hydrogen concentrations is plotted and the structure, phase composition, and mechanical properties of the alloy treated by reversible hydrogen doping, hot straining, and subsequent dehydrogenation annealing (OLVOD) are studied. The metallographic analysis is performed using a Neophot-21 optical microscope and X-ray diffraction studies are carried out in a DRON-2 diffractometer in CuK radiation. The findings show that an addition of 0.3-0.5% H to the alloy makes it possible to lower the stamping and forging billet temperature from 950 to 750°C without increasing the straining force and reveal that hydrogen saturation leads to the development of α"-martensite in the alloy structure. Straining in the β-area results in the development of a lamellar structure in the alloy at an 800-750°C temperature. Thus, the use of the OLVOD technology makes it possible to substantially increase the alloy ductility without reducing the strength properties. It is suggested that VT6 alloy blanks with 0.3-0.5% H be stamped at an 800°C in order to attain the optimum range of mechanical properties. Figures 4; tables 2; references 3.

Structural and Substructural Changes During Alloy Brass Heat Treatment

927D0210C Moscow METALLOVEDENIYE I TERMICHESKAYA OBRABOTKA METALLOV in Russian No 2, Feb 92 pp 9-10

[Article by L. Ramiandravola, I. Lukach, T. Grigerova, Czech and Slovak Republic; UDC 669.5'3'71'1'74: 620.18]

[Abstract] The processes accompanying heat treatment of alloy brass doped with manganese, aluminum, and iron—a high-strength corrosion-resistant casting brass—are discussed and the specific structural and substructural transformations in Cu-Zn-Al-Fe-Mn brass under heat treatment are examined. To this end, the microstructure of alloy brass in the cast state and after hardening and tempering is investigated by a metallographic analysis and an electron microscopy study; local chemical analysis is carried out using a LINK type EDX instrument. The findings indicate that tempering at a 400-600°C temperature helps form an equilibrium $\alpha+\beta'$-structure with an α-phase and iron precipitation from the supersaturated solid solution; the α-phase precipitates in the form of acicular crystals with the cast structure's crystallographic orientation. During diffusion annealing, only a small part of disperse precipitates which remain in the solid solution after hardening passes to the solid solution while after tempering, only noncoherent disperse particles unevenly distributed in the matrix are observed in the alloy brass structure Figures 1; references: 4 Western.

Assessment of Thermally Expanded Graphite Molding Process by Strain Spectral Analysis

927D0197F Moscow TSVETNYYE METALLY in Russian No 3, Mar 92 pp 38-40

[Article by Yu.A. Nikitin, I.G. Chernysh, M.L. Pyatkovskiy, Surface Chemistry Institute at the Ukrainian Academy of Sciences; UDC 539.621]

[Abstract] The role of advanced methods of assessing and monitoring the quality of materials in the study of molding processes is discussed and the process of one-sided molding of thermally expanded graphite (TRG) is examined by investigating and evaluating the structure formation process with the help of the strain spectral methods of micromechanical testing and visual optical microscopy; in addition, the compressive strength of compacted thermally expanded graphite samples is measured. The physical essence of the strain spectral analysis technique is explained and the tribospectral characteristics of the surface layer of thermally expanded graphite during molding, the behavior of the maximum spectral density of the tribospectral characteristics during molding, and the dependence of the compressive strength of thermally expanded graphite samples on their apparent density are plotted. An analysis of the findings confirms that the use of the strain spectral method makes it possible to establish the process conditions and monitor the one-sided molding of thermally expanded graphite products with a stable uniform surface strength structure at an apparent density of 300-600 and 900-1,300 kg/m^3 and shows that the methods is suitable for assessing the structure formation of the powder material surface. The tribospectral characteristics are sensitive to bulk molding processes while their parameters may also be used as criteria for comparative estimates of powder material fabrication. Figures 4; references 2.

Cathode Cells for Aluminum Electrolyzers With Pasted Current Leads

927D0197E Moscow TSVETNYYE METALLY in Russian No 3, Mar 92 pp 32-33

[Article by G.D. Vergazova, G.A. Sirazutdinov, M.Ya. Mintsis, GosNIIEP, SaAZ, NkAZ; UDC 541.135:621. 792.053]

[Abstract] The high capital outlays and cost of using pig iron filling of cathode cells for fastening them to the bottom of the electrolytic units and the high level of thermal and mechanical stresses developing in the binding layer which lead to cracking are discussed and a paste developed for binding the electrode rods to the bottom units which hardens at room temperature and also makes it possible to eliminate the consequences of thermal shocks and lower the thermal and mechanical stress level in the binding layer is described. The pastes consist of a solid filler, a synthetic liquid resin or a mixture of several resins, and a hardening agent; the paste is rammed into the space between the unit and the steel current lead rod. The physical and mechanical properties of pastes are summarized, the dependence of the electric resistivity of the paste on its roasting temperature is plotted, and the principal process parameters of the pilot electrolyzer unit operation are cited. An analysis reveals that the pastes are characterized by practical feasibility, good adhesion to steel and carbon, and high strength properties in the cured state and are capable of equalizing the thermal expansion of units and rods. Tests of the pilot units did not reveal any negative changes in the electrolyzer performance. Figures 1; tables 2; references 2.

Sorptive Copper Recovery From Circulating Pyrite Cinder Hydroremoval Solutions

927D0197D Moscow TSVETNYYE METALLY in Russian No 3, Mar 92 pp 26-28

[Article by L.Ye. Slobtsov, State Nonferrous Metals Institute; UDC 669.33]

[Abstract] The outcome of exploratory research in the use of sorption to recover copper from the circulating pyrite cinder hydroremoval solutions in the mineral fertilizer industry is discussed. The conditions and results of four experimental efforts to recover copper from the cinder and the indicators of copper and zinc

desorption by sulfuric and orthophosphoric acid solutions are summarized and a flow chart of the copper recovery technology is cited; the so-called semi-counterflow method calls for neutralizing the pulp by lime, separating it into several flows according to the number of pulp agitators, and merging the flows after settling and sending it to the circulation system; then copper is recovered using the ANKB-35 ampholytic unit by acid solutions which are used for making first eluate, then mineral fertilizers (ammophos) with microelement additions, thus eliminating the the desorption reagent outlays and making the process more economical. Figures 2; tables 2; references 3.

Viscosity of SiO_2-Na_2O-CaO-Cu_2O-ZnO System Slag Melts

927D0197C Moscow TSVETNYYE METALLY in Russian No 3, Mar 92 pp 25-26

[Article by L.S. Strizhko, A.I. Ridel, L.B. Stepanov, Moscow Steel and Alloy Institute; UDC 669.046.58: 532.13]

[Abstract] The viscosity of synthetic slags of the SiO_2-Na_2O-CaO-Cu_2O-ZnO system is examined in order to help select the optimum slag composition of the pyrometallurgical processing of secondary silver-containing raw materials. The study is carried out in a lab unit consisting of a vibratory viscometer with a shaft furnace, a self-excited oscillator with a power supply source, and an instrument. The viscometer spindle is made out of nickel-plated steel in order to avoid the interaction between the spindle material and the metal. The viscometer is calibrated using model cold liquids with a known viscosity. The dependence of the slag viscosity on temperature at various Cu_2O concentrations, the dependence of the slag viscosity on the slag-forming component ratios, and the dependence of the slag viscosity on the zinc oxide concentration at various temperatures are plotted. The findings indicate that the slags have an insignificant viscosity at a 40-45%:35-40%:20-25% component ratio of SiO_2:Na_2O:CaO which is five- to sixfold lower than that of real slags in existing smelteries, making it possible to draw the conclusion about the expediency of using slags of this composition for making silver bullion. Figures 3; references 1.

Nickel Matte Processing in Horizontal Converters With Tuyeres in Protective Shells

927D0197B Moscow TSVETNYYE METALLY in Russian No 3, Mar 92 pp 12-13

[Article by N.M. Barsukov, Yu.A. Korol, M.R. Rusakov, A.A. Halnbeck, A.A. Pashkovskiy, A.F. Pronin, State Nickel Industry Design Institute and Leningrad State University; UDC 669.045.5:669.243]

[Abstract] The limited life cycle (6-7 days) of nickel matte converters due to the need to replace the converter lining in the tuyere belt area while the remaining lining areas remain fully serviceable prompted an examination of methods of applying an oxygen-poor blast by using tuyeres with a protective shell (FZO). To determine the optimum performance variables of the protective shell tuyere method for the blast unit operation in a horizontal nickel matte converter, studies are carried out using water-model simulation of the blast hydrodynamics of a submerged lateral tuyere with a protective shell at the Yuzhuralnikel Smeltery and State Nickel Industry Design Institute. The study is conducted at a specific blast rate typical of existing converters. The principal parameters of the blast unit are summarized and a schematic diagram of the blast unit with a protective shell tuyere is cited. The use of FZO in converters makes it possible to stabilize the temperature conditions of the process and eliminate sharp local thermal shocks on the lining which usually occur at the initial blast stage. As a result, the mean converter campaign reaches 16 days, an increase of 2.3 times over the conventional method. It is stressed that the procedure can also be used for copper and copper-nickel matte. Figures 1; tables 1; references 4.

Problem of Waste-Free Processing of Solid Industrial Waste at Ferrous and Nonferrous Metallurgy Enterprises

927D0198A Moscow TSVETNYYE METALLY in Russian No 2, Feb 92 pp 4-7

[Article by V.I. Chalov, L.N. Tauzhnyanskaya, L.N. Dorokhina, Central Scientific Research Economics and Information Institute; UDC 504.064.43:669]

[Abstract] The large quantity of solid production waste accumulating in ferrous and nonferrous metallurgy enterprise spoil heaps, e.g., overburden and enclosing rock, dressing tailings, slags, sludges, etc., which can serve as a potential source of nonferrous and rare metals and building materials prompted an investigation of a waste-free method of processing solid industrial waste; the problem is further aggravated by the need for additionally alienating land for waste disposal. The outcome of research and feasibility studies conducted by a number of industry institutes is summarized and a number of proposals for implementing waste-free processing technologies are described. The need to develop a specific program of action in order to assist each individual plant in this endeavor on the basis of a market economy is emphasized. As a result of the study, a database is developed at the Chermetinformatsiya Institute and Central Scientific Research Economics and Information Institute, listing all existing sources of solid waste in the ore dressing and metallurgy industries and possible trends of their utilization and metal recovery. References 6.

Study of Refractory Compound-Based Composition Stability Under Aluminum Electrolysis Conditions

927D0198F Moscow TSVETNYYE METALLY in Russian No 2, Feb 92 pp 36-37

[Article by Yu.V. Borisoglebskiy, M.M. Vetyukov, M.I. Karimov, Leningrad State Engineering University; UDC 669.713]

[Abstract] The rising demand for aluminum prompted a study of ways of improving the efficiency of electrolytic aluminum smelting by developing new refractory compounds (TS) for the electrolyzers, preferably from the easily available and inexpensive titanium and zirconium nitrides, carbides, and borides. Consequently, the stability of the TiB_2-TiC and TiC-TiN compositions in the cryolite-alumina melts and aluminum is investigated. To this end, the solubility of the TiB_2-TiC and TiC-TiN compositions is examined by the chemical analysis method; in so doing, an experiment is conducted to determine the effect of the melt and metal mass on the Ti content. The dependence of the Ti content in Al and cryolite-alumina melt on the exposure duration, the dependence of the Ti content in the electrolyte on the temperature and on the cryolite ratio, and the dependence of the Ti concentration in the metal on the electrolysis duration are plotted and the Ti concentration in the Al-cryolite-alumina melt system as a function of the Al and cryolite sample weight is summarized. The studies demonstrate that the stability of the TiB_2-TiC and TiC-TiN compositions in aluminum and cryolite-alumina melts is sufficient; as a result, these compositions are recommended for use as the aluminum electrolyzer cathode. Figures 5; tables 1; references 2.

Copper and Cobalt Activity in Slag Melts

927D0198E Moscow TSVETNYYE METALLY in Russian No 2, Feb 92 pp 25-27

[Article by M.L. Sorokin, V.Ya. Zaytsev, A.I. Dabayev, Ya.Ya. Zayonts, Moscow Steel and Alloy Institute; UDC 669.33+669.253]

[Abstract] The issue of copper and cobalt solubility in iron silicate slags and the mutual effect of these metals on their distribution between the slag and the Co-containing copper matte raised in *Tsvetnyye metally* No. 3, 1991, is discussed and the thermodynamic characteristics of Cu and Co, namely, their activity and activity coefficients in iron and silicate melts, are investigated. The study is performed in an O_2-controlled atmosphere at a 1 x 10^{-6} Pa pressure and a 1,525K temperature using a circulation procedure; the thermodynamic characteristics are analyzed by using Yazawa'a component isoactivity diagram. The effect of the Cu concentration in the matte on the thermodynamic characteristics of Cu dissolved in the slag in an oxide and sulfide form and the effect of the Cu content in the matte on the Co distribution between the slag and the matte and on the CoO activity coefficient in the slag are plotted and the experimental data on the Co solubility in the slag and copper as a function of the copper concentration in the matte are summarized. Two practical aspects of the study are emphasized: the desire to attain superhigh-grade matte and even smelted copper in NGMK smelteries will inevitably lead to a sharp increase in the concentration of dissolved copper and cobalt in the slag; and the cobalt concentration in the copper matte proposed by Yazawa (using the phase stirring method with subsequent refining to remove cobalt) should not pose serious difficulties due to the favorable cobalt distribution between the high-grade copper matte and the converter slag. Figures 2; tables 1; references 9: 6 Russian, 3 Western.

Electrochemical Indium Refining Through Thin Fused Electrolyte Layers

927D0198D Moscow TSVETNYYE METALLY in Russian No 2, Feb 92 pp 22-25

[Article by A.A. Omelchuk, V.T. Melekhin, L.A. Kazanbayev, M.N. Kozlov, A.M. Marchenko, General and Inorganic Chemistry Institute at the Ukrainian Academy of Sciences and ChETsZ; UDC 621.357.1:669.872]

[Abstract] The characteristic features of the indium refining process stages and the difficulties of controlling the refining process stage are discussed and the new principles of electrochemical indium refining in fused electrolytes which are free of the shortcomings of the traditional methods are investigated. The method of using a thermally stable silica cloth and a porous septum for separating the salt and metallic phases are compared. The effect of the electrolysis conditions on the indium transport from the anode to the cathode in a unit with a porous septum is examined, the effect of the current density on the refining ratio (removal of Sn impurities from In) is plotted, and the dependence of the In refining ratio on the ammonia chloride content in the fused electrolyte is computed. The comparative characteristics of various electrochemical indium refining methods are summarized. An analysis of the findings shows that the use of new refining processes makes it possible to increase the process stage efficiency by threefold while maintaining a high a high refining quality and reduce the amount of In in circulation as well as completely eliminate the use of Hg and the iodide Cd removal operation. The methods makes it possible to perform the procedure at an electrode spacing on the order of 5 x 10^{-4} m. Figures 2; tables 3; references 9.

Comprehensive Alkali Semiproduct Processing in Lead Refining

927D0198C Moscow TSVETNYYE METALLY in Russian No 2, Feb 92 pp 20-22

[Article by B. Nikolic, Kirilo Savic Institute, Yugoslavia; UDC 669.443]

[Abstract] Various methods of processing the numerous intermediate lead alkali products forming during the lead refining by various methods—primarily sodium hydroxide and sodium nitrate—used in Yugoslavia are reviewed and a block diagram of the generic lead bullion refining process is cited. The chemical composition of the intermediate products is summarized and the metal balance of the Na-Sb-slag and alkaline bismuth dust processing with lead chloride in a drum furnace is calculated. Laboratory tests of the processing technique indicate that the maximum sodium recovery from the slag components reaches 88.9-91.4%, depending on the method. The leaching residue contains 20% Sb and 7% Pb whose quality depends not only on the leaching conditions but also on the slag quality. Figures 1; tables 2.

Using Vanyukov's Process for Smelting Low-Sulfur Auriferous Concentrates

927D0198B Moscow TSVETNYYE METALLY in Russian No 2, Feb 92 pp 13-15

[Article by V.V. Galushchenko, A.V. Tarasov, T.A. Bagrova, V.A. Generalov, State Nonferrous Metals Institute; UDC 669.213]

[Abstract] The increasing gold consumption in industry in particular and the national economy in general and the constant depletion of the placer and quartz vein auriferous ore deposits prompted a study of the efficiency of Vanyukov's process for smelting low sulfur ore-containing concentrates, e.g., pyrite concentrates which are gaining an increasing share of the market. To this end, the process of matte smelting of pyrite concentrates is examined in detail. The problem of preventing the gold contained in such concentrates from being "spread" among various products by converting all silver and gold to the ferruginous matte is discussed and it is emphasized that in order to maintain the thermal balance of autogenous smelting, it is necessary to use a certain amount of carbon-containing fuel which, in turn, lowers the advantages of this type of smelting. Consequently, the material and thermal balance of both the electric smelting and Vanyukov's smelting processes are analyzed, the dependence of the comparative equivalent fuel consumption on the sulfur concentration in the concentrate is plotted, and the pyrite concentrate composition in seven Leninogorsk deposits is summarized. The findings show that the specific equivalent fuel rates curve of the two processes intersect at a sulfur concentration of 15-20% in the concentrate; at a lower S content, the electric smelting process is more efficient but not universally so since in each case considered in the study, there are ways of compensating for the heat losses. It is stressed that the possibility of using cheap and available coal fuel makes Vanyukov's process especially economical. Figures 1; tables 1; references 10.

Spend Molding Sands as Fine Concrete Aggregate

927D0228F Moscow BETON I ZHELEZOBETON in Russian No 7(448), Jul 92 pp 29-30

[Article by S.D. Semenyuk, R.P. Semenyuk, Mogilev Mechanical Engineering Institute; UDC 691.327.32: 666.97]

[Abstract] A shortage of quartz sand which meets existing standards and is traditionally used as a fine concrete aggregate and the shortcomings of fine sands which lead to an excessive cement consumption and poor quality of reinforced concrete structures prompted an investigation into the possibility of using spent molding sands as a fine concrete aggregate pursuant to GOST 27006. To this end, class V10-V22.5 concrete compositions are selected in a trial and error experiment in which spent molding sands are used as the fine aggregate while granite gravel of the corresponding size is used as the coarse aggregate. Altogether, 12 cubic batches with a 10 cm edge each containing at least 90 cubes are made for tests. The composition of spent molding sands from three plants and the compositions of concrete mixes and their principal characteristics are summarized and a formula is derived for calculating the behavior of concrete strength in time. Concrete subjected to thermal-moisture treatment displays a 30% increase in strength at early stages and a 5-10% increase later while the proposed concrete has an elevated frost resistance (by 20-30%) compared to the standard value. Tests of slabs made from the new concrete reveal that they meet the requirements of GOST 8829 for strength, rigidity, and crack resistance and have a safety margin of 1.4-1.67. Tables 2.

Manufacture of Gypsum-Cork Concrete as Thermal Insulation Material

927D0219C STROITELNYYE MATERIALY in Russian No 6, Jun 92 pp 11-12

[Article by N.I. Osminin, candidate of technical sciences, L.A. Goncharova, engineer, I.V. Paskonnov, engineer, and I.M. Tishchenko, engineer, Odessa Institute of Construction Engineering; UDC 691.322]

[Abstract] An experimental study has established the feasibility of combining β-0.5$CaSO_4$ gypsum as binder and cork tailings as fine filler into a light-weight grade of concrete useful as thermal insulation material. The raw slurry consists of 38-40 wt.% gypsum + 30.3- 37.35 wt.% cork tailings + 20-26 wt.% water. To the slurry are added a hardener consisting of 0.5-0.7 wt.% DEG-1 epoxy resin + 0.05-0.07 wt.% polyethylene-polyamine resin and, to ensure biostability of cork, 0.1-0.3 wt.% of the bactericide-fungicide catapin. Test specimens in the form of 40x40x160 mm^3 bars and 100x100x400 mm^3 prisms were produced by casting the slurry into plastic molds and subsequent, after 8-10 h, removal of the cakes from the molds for drying to a not more than 2 wt.% residual water content. The test results qualify this material as one with an average density within 330-370 kg/m^3, compressive strength and flexural strength of 7.1-8.4 MPa and 4.1-4.6 MPa respectively, a thermal conductivity of only 0.07-0.1 W/(m x °C), and a water absorption capacity of 27-29 wt.%. The biocide is highly active, harmless to humans, and compatible with the concrete mix. Specimens of the concrete were tested for biostability in a Petri dish with Capek-Dox culture medium for spores of six fungi (Aspergillus niger, A. terreus, Stemphyrius ilicis, Penicillium brevi-compactum, Trichoderma Lignorum, P. funicolosum) in aqueous suspension. These fungi were incubated in the dish at a 29°C temperature, whereupon the micelle growth on concrete was estimated on a 0-6 scale and found not to exceed 2 on that scale. Tables 2.

Fireproof Structural Plastic Materials

927D0219A Moscow STROITELNYYE MATERIALY in Russian No 6, Jun 92 pp 2-3

[Article by V.N. Kirillov, candidate of technical sciences, and B.F. Pronin, candidate of technical sciences, Scientific-Industrial Association "Kompozit(Composite)"; UDC 578.06:678.674-415:69.024.15]

[Abstract] Considering that structural materials with organic content are not absolutely fireproof and that addition of halogen or phosphorus compounds can even raise the toxicity of the combustion products, two glass-plastic materials "Deks" and "Mineplen" have been developed whose gaseous combustion products have a minimal toxic and asphyxiating effect on the human organism. The filler in both is aluminum borosilicate glass cloth. According to the results of standard combustibility tests, "Deks" with an organic binder (KM-9K organosilicon resin, up to 5 % volume fraction of organic radicals) qualifies as a hardly combustible material and "Mineplen" with a mineral binder (chromium-aluminum phosphate) qualifies as a noncombustible one. Following optimization of their technology, both materials were tested for thermal stability in a "Puraky" analyzer and heating from 30°C to 750°C was found to increase their loss of mass monotonically to not more than 5 %. Thermogravimetric analysis and gas chromatography at 20-40°C revealed no significant escape of volatile organic substances within this temperature range. Thermogravimetric analysis at temperatures up to 1000°C simulating conditions of fire revealed an only 4.2-4.7 % loss of mass, evidently owing to escape of water vapor through pores. Both materials are thus not only fireproof but also safe from the hygienic standpoint, "Mineplen" having an HCL_{50} index of 300 g/m^3 and "Deks" also having one higher than the minimum acceptable 120 g/m^3 (amount of volatile products causing 50 % of laboratory test animals to die within 30 min). Decorative surface coating of "Deks" and "Mineplen" can be done by several methods: 1) hot pressing together with a decorative sheet impregnated with an organosilicon resin, or with a decorative glass cloth impregnated with a melamine-formaldehyde or organosilicon resin; 2) dyeing the surface; 3) implanting mineral dyes in the binder. Tables 3; references 10.

Composites Based on Vermiculite for Intumescent Fireproof Coatings

927D0219B Moscow STROITELNYYE MATERIALY in Russian No 6, Jun 92 pp 7-11

[Article by P.P. Gedeonov, candidate of technical sciences, Izhevsk Institute of Mechanics; UDC 666.691.62-761.691.278]

[Abstract] An experimental study of four intumescent fireproof coating materials (VOZP = Intumescent Fire-Proof Coating) with vermiculite alone as filler and together with other mineral filler components was made, for the purpose of determining the effect of three different types of additional filler components on the mechanical strength of such a coating. The basic components of all four materials were 14 wt. units of fresh vermiculite ore concentrate, 2.8 wt. units of vermiculite calcined at 500-600°C, 0.9 wt. units of vermiculite calcined at 800-900°C, and 30 or 40 wt. units of liquid sodium glass as binder. The first material VOZP-1, with a compressive strength of 5 MPa, contained 30 wt. units of liquid glass alone as binder and no additional filler component. The second material VOZP-2, with a compressive strength of 8.9 MPa and a fire resistance 11.4 % higher than that of VOZP-1, contained 40 wt. units of liquid glass alone as binder and 1.6 wt. units of crushed asbestos fiber as additional filler component. The third material VOZP-3, with a compressive strength of 14.3 MPa and a fire resistance 8 % lower than that of VOZP-1, contained 30 wt. units of liquid glass + 10 wt. units of urea-formaldehyde resin as binder and 2.7 wt. units of zinc oxide + 7.5 wt. units of dicyandiamide as additional filler components. The fourth material VOZP-4, with a compressive strength of 13.7 MPa and a fire resistance 11.2 % higher than that of VOZP-1, contained 40 wt. units of liquid glass + 10 wt. units of urea-formaldehyde resin as binder and 1.6 wt. units of crushed asbestos fiber + 2.7 wt. units of zinc oxide + 7.5 wt. units of dicyandiamide as filler. For the purpose of determining the role of fibrous filler materials, the amount of asbestos fiber in a plain mix of vermiculite ore and liquid glass in a 1.03:1 ratio was varied from 5 % to 30 % of the binder mass. Asbestos fiber was then replaced successively with mineral wool and with kaolin fiber, the amount of each substitute being also varied over the same 5-30 % of binder mass range. All materials were tested not only for compressive strength but also for flexural strength and bonding strength. Coatings of VOZP-4 were then tested for fire resistance on steel plates during during heating from 0°C to 900°C, fire resistance being measured in terms of time required for heating the coating to that high at temperature. They were tested without and with either sodium fluorosilicate or nepheline-antipyrene in various amounts up to 20 wt.% having been added as hardening catalyst. The data indicate that VOZP-4 coatings with 20 wt.% crushed asbestos fiber and without catalyst or with small amounts of nepheline-antipyrene are most fire-resistant and thus most effectively slow down heating of steel plates. Both catalysts make VOZP coatings stick to the protected surface, but only nepheline-antipyrene in amounts not larger than 5 wt.% does not lower their fire resistance. Sodium fluorosilicate in any amount degrades the mechanical strength of these coatings at high temperatures and, therefore, is not recommended. Figures 7; tables 2; references 8.

Using TransCarpathian Volcanic Rock as an Active Mineral Additive in Cement

927D0217B Moscow BETON I ZHELEZOBETON in Russian No 6, Jun 92 pp 6-7

[Article by G. B. Girshtel and S. V. Glazkova, candidates in the technical sciences, M. V. Gaken, P. I. Belik, and A. I. Komarov, engineers (Scientific Research Institute of Structural Design), and M. M. Saldugey, candidate in the technical sciences (Kievinzhtsiment Institute of Problems of Cement); UDC 691.54.001.1]

[Abstract] The feasibility of using a binder made with uncalcined perlite in finely ground multi-component cement was studied to determine whether such a formulation would increase the amount of concrete yielded. The binder was made from portland cement slag from the Kamenets-Podol cement plant (TU 21-13-2-88), crushed perlite from the Beregov quarry in the TransCarpathian Oblast (GOST 25226; density 2.25 to 2.4 g/cu cm), and gypsum (GOST 4013). All the components were ground together. The addition of the perlite significantly changed the chemical composition of the binder: SiO_2 content went from 21 to 42%, Al_2O_3 from 6 to 8%, and CaO from 60 to 37%. The activity of the binder was not affected. Test batches of the cement were made with a perlite content of 25 to 79% in a laboratory ball mill. The concentration of the other components was held constant. The addition of up to 50% perlite did not affect concrete strength; thus binder with 50% perlite was used in the experimental production of V7.5 to V55-grade concretes, some of which were made with C-3 superplasticizer and some without. The binder was used in quantities of 200, 300, 400, 500, and 600 kg/cu m; the consistency factor was 4 to 6 cm. All specimens were steam cured for (2)+3+6+2 hours at an isothermal heating temperature of 80°C. Strength was virtually unaffected by the addition of the perlite, and the addition of the plasticizer increased strength from 7 to 15%. Calculations of concrete yield showed that, in comparison with ordinary slag cement, up to twice as much concrete can be obtained from 1 ton of cement made with the new binder. Cement made with the new binder is now in commercial production. Figures 1, tables 4.

Quick-Setting Keramzit Concrete for Winter Concrete Pouring

927D0217C Moscow BETON I ZHELEZOBETON in Russian No 6, Jun 92 pp 12-14

[Article by A. V. Ferronskaya, doctor of the technical sciences, V. F. Korovyakov and L. D. Chumakov, candidates in the technical sciences, and S. V. Melnichenko, engineer, Moscow Institute of Construction Engineering; UDC 691.327:666.973.2:693.547.3]

[Abstract] The feasibility of using a water-resistant gypsum binder that requires little water to make Keramzit concretes for winter pouring conditions was evaluated. The cement was made using two ratios of ordinary/water-resistant binder: 65/35 and 50/50. The formula also included G-511B gypsum binder, a hydraulic additive, and a 0.06-% quantity of VRP-1 that was added with the curing water to delay setting-up time by 40 to 50 minutes. It was found that using the water-resistant gypsum binder in place of ordinary gypsum and portland cement (Voskresenya plant) binders makes it possible to sharply reduce binder consumption, decrease the initial moisture content and the amount of curing water required to obtain a smooth-flowing concrete mixture, and to increase the initial pouring speed, compressive strength and water and frost resistance of the concrete. Tests of the hardening kinetics of 10-cm cubic specimens of Keramzit concrete made with this binder were performed at temperatures between 5 and -30°C. These tests showed that the concrete sets up and hardens very rapidly at low and negative temperatures. All of the aforementioned characteristics of concrete made with the water-resistant gypsum binder make this concrete more suitable for pouring concrete and constructing limited-story housing during the winter. Figures 1, tables 3; references 2: Russian.

Water-Dispersed Film-Forming Compositions for Concrete Used in Hot, Dry Weather

927D0217D Moscow BETON I ZHELEZOBETON in Russian No 6, Jun 92 pp 15-17

[Article by Professor B. A. Krylov, doctor of the technical sciences (NIIZhB [Scientific Research Institute of Reinforced Concrete]), L. G. Chkuaselidze, candidate in the technical sciences (Zarubezhstroy Production Association), G. V. Topilskiy, candidate in the technical sciences (All-Union Scientific Research Institute of Reinforced Concrete), and V. P. Rybasov, candidate in the technical sciences (NIIZhB); UDC 691.327(213)]

[Abstract] The application of a water-dispersed film-forming composition to the exposed surfaces of freshly cured concrete was studied to determine whether this procedure enhanced the service properties of concrete structures. The composition was applied with either a 7000 NA high-pressure paint sprayer, a KRP-1 pneumatic sprayer, or an OGU-3 hydrodynamic sprayer to reinforced concrete piles (16 x 0.4 x 0.4 and 12 x 0.3 x 0.3 m) immediately after the surface of the newly set concrete had been repaired. In all, five piles were made in the same thermal mold, three of which were treated with the film-forming composition and two in the conventional manner with polyethylene film, burlap, and water. In the mold, the specimens were conductively steam cured at temperatures of 50 to 70°C for 3+4+8+2 hours. The V27.5 concrete from which the piles were made consisted of, in kg/cu m, 400-440 units of cement, 620 of sand, 1140 of crushed rock, 176 of water, and 3.08 of S-3 superplasticizer. A tear-away and shearing test performed two days after treatment showed that the strength of the concrete treated with the film-forming composition was 25 MPa, versus 20 MPa for the conventionally treated piles. Application of the new film also reduced moisture loss 1.5 to 2-fold and reduced water absorption from 8.5 to 6-6.5%. Different modifications of the new composition were used in different applications, all with satisfactory results in terms of improved strength and service characteristics. It was also shown that application of the new composition requires 2.5 man-hours of labor, versus 35.4 man-hours for conventional maintenance, and saves up to 70 cu m of water per week. Figures 4, tables 1.

Predicting the Frost Resistance of Concrete

927D0217E Moscow BETON I ZHELEZOBETON in Russian No 6, Jun 92 pp 25-27

[Article by V. P. Sizov, candidate in the technical sciences; UDC 691.327:536.485]

[Abstract] A new quantitative method of predicting concrete frost resistance was proposed. This method is based on a formula that incorporates a cement-to-water ratio coefficient as the primary determinant of frost resistance: $F = AR_{cement}(C/W - 0.5)$. This formula obviates calculations for the various types of porosity that heretofore have been used in quantitative models of cement frost resistance. By using this formula in conjunction with the reference cement composition detailed in the study, frost resistance can be predicted when a particular cement composition is actually being formulated, rather than having to physically test concrete specimens. Application of the formula showed that, in addition to controlling the cement-to-water ratio, concrete frost resistance can be enhanced by formulating the cement with air-entraining and pore-forming additives. Figures 1, references 6: Russian.

Desorption of Moisture From Portland Stone During Irradiation

927D0217A Moscow BETON I ZHELEZOBETON in Russian No 6, Jun 92 pp 2-4

[Article by Ye. B. Sugak, A. V. Denisov, L. P. Muzalevskiy, candidates in the technical sciences, Moscow Institute of Construction Engineering; UDC 666.9.015.44:691.327]

[Abstract] Moisture desorption from irradiated portland stone was studied. Portland cement made by the Belgorod and Sebryakov plants was used, as were the basic minerals of portland cement slag synthesized by the Scientific Research Institute of Cement. Specimens of one of the various compositions studied were steam-cured at a temperature of 80 to 85°C and held in a chamber for normal curing for up to 28 days. The remaining compositions were allowed to cure for 28 days in humid conditions, and the slag minerals in water. Afterwards, all specimens were stored in normal temperature and moisture conditions. Prior to irradiation, the portland stone was dried to a constant mass at 105°C. The stone was irradiated in BR-10 and BOR-60 fast neutron laboratory reactors and in an AM reactor. The results of the experiment showed that the C_2S and C_3S lost a great deal of moisture during irradiation; residual moisture content was 0.053 and 0.033 g/g, respectively. The moisture content of the C_3A and C_4AF was 2 to 6 times higher than the other minerals. After irradiation, the residual moisture content in the portland stone was 4 to 11% of the mass of the binder, with moisture loss increasing as radiation and temperature were increased. Moisture loss was greatest in the steam-cured specimens. It was concluded that, during irradiation, the structure of the portland stone gives up free, capillary, interlayer, and pore-absorbed water, and part of the chemically bound moisture as well. The residual moisture is gel-pore and chemically bound moisture, primarily C-S-H water and $Ca(OH)_2$. Tables 5; references 5: Russian.

ZrO_2-Based Concrete Body With Barium Aluminozirconate Cement

927D0221A Moscow OGNEUPORY in Russian No 3, Mar 92 pp 2-3

[Article by A.G. Karaulov, N.G. Ilyukha, Ukrainian Scientific Research Institute of Refractories; UDC 666.974.2:666.762.52]

[Abstract] A zirconate concrete body with a maximum 5 mm grain size on the basis of fused zirconium dioxide stabilized with calcium oxide and barium aluminozirconate cement developed at the Ukrainian Scientific Research Institute of Refractories (UkrNIIO) together with the Kharkov Polytechnic Institute is discussed and the properties of barium aluminozirconate cement with various barium aluminate:barium zirconate (BA:BZ) ratios are summarized. Production of the new concrete in rotary kilns and the cement dehydration procedure are considered and the properties of the concrete body at a 20°C temperature and the characteristics of mortar made from barium aluminozirconate cement are examined. An analysis of the findings shows that the concrete body containing only 10% of cement is sufficiently strong while an increase in the cement concentration to 20% does not lead to an increase in strength; on the other hand, it is suggested that 20% of cement be added to the mortar in order to increase its shear strength at temperatures of up to 1,200°C. The new concrete body is tested in high-temperature combustion chambers at the High Temperature Institute at the Academy of Sciences (IVTAN) at gas temperatures of 2,000-2,600°C and flow rates of 400 m/s. The test results make it possible to recommend the concrete body for use at the Kaustic Association at temperature of 2,500°C. The annual economic impact from its implementation reaches 273 million rubles. Figures 1; tables 3; references 8: 6 Russian, 2 Western.

Investigation of Heat Resistance of Silica Brick Products for Coke Ovens by Panel Method

927D0221C Moscow OGNEUPORY in Russian No 3, Mar 92 pp 10-13

[Article by A.I. Portnova, V.L. Bulakh, R.F. Rud, T.S. Penzeva, Ukrainian Scientific Research Institute of Refractories; UDC 666.762.2.017:536.495]

[Abstract] The negative impact of thermal, chemical, physical, and mechanical factors on the operation of coke oven battery brickwork and the abrupt and sharp cooling of the wall brickwork during the charging prompted a study of the heat resistance of silica brick products in coke ovens; the study is carried out by the panel (test bench) method which simulates the operating conditions of silica brick and makes it possible to investigate the effect of air and water cooling on the silica brick's thermal resistance. The behavior of the thermal resistance indicator as a function of open porosity in silica brick products of various densities is plotted and the properties, chemical and phase composition, and quality indicators before and after air and water thermal cycling are summarized. An analysis reveals that the heat stability of silica brick products is lower under water cooling than under air cooling while a decrease in the absolute value of the design heat stability indicator C attests to an increase in the thermal stability of silica brick items and is borne out by an experiment by the test bench method. Silica brick products with a 19-21% open porosity and a ≤ 2.37 g/cm^3 density have an elevated heat resistance and are capable of increasing the resistance of high-capacity coke ovens. The resulting property indicators are incorporated in coke oven battery silica brick standards. Figures 2; tables 6; references 14.

Basic and High-Alumina Refractory Production Monitoring by Nondestructive Testing

927D0221E Moscow OGNEUPORY in Russian No 3, Mar 92 pp 19-21

[Article by L.I. Nerubashchenko, N.I. Novikova, G.A. Belokrys, L.V. Puzik, N.K. Senyavin, I.D. Tochilnikova, Zaporozhye Industrial Institute, Zaporozhye Refractories Plant, and All-Union Refractories Institute; UDC 666.76:620.111.3]

[Abstract] A sound-probing nondestructive testing method of monitoring the quality of refractories and their production and a special standard (or standard

sample) developed at the All-Union Refractories Institute (VIO) together with the Zaporozhye Industrial Institute and Zaporozhye Refractories Plant in order to certify sonic nondestructive testing units in laboratories are discussed and the instruments necessary for carrying out the procedure are described. The operations involved in certifying refractory products using alignment charts plotted on the basis of regression equations are outlined and the statistical data on the mass, frequency, apparent density, open porosity, and compressive strength of KhP-1 chromite periclase refractories measured in 50 samples are summarized and the nomographs for determining the apparent density, compressive strength, and open porosity of KhP-1 products are plotted. Test results obtained by destructive and nondestructive methods and the convergence of results are compared. The study confirms the possibility of using nondestructive testing for monitoring the production and quality of periclase chromite, chromite periclase, and high-alumina refractories. The method has been implemented, making it possible significantly to shorten the test duration, minimize labor-intensive operations, prevent the products from destruction, and certify the products with greater confidence. Figures 2; tables 3; references 4.

Magnetic Susceptibility of Refractories

927D0221D Moscow OGNEUPORY in Russian No 3, Mar 92 pp 13-14

[Article by L.B. Khoroshavin, V.A. Perepelitsin, Eastern Refractories Institute; UDC 666.762.017:537.621]

[Abstract] The magnetic characteristics of refractories—magnetization, magnetic field strength, magnetic permittivity, magnetic susceptibility, etc.—which determine the molding and wear indicators of refractories are discussed and special attention is focused on the magnetic susceptibility (and apparent density) of refractories which provides important data on the structure of materials and often depends on the amount of ferromagnetic components, grain size, the type of grain defects, and the temperature and pressure. The minerals used in refractories are classified by their magnetic susceptibility into nonmagnetic, weakly and highly magnetic, diamagnetic, paramagnetic, and ferromagnetic; the specific magnetic susceptibility and bulk density of various fractions of sintered periclase powder and fraction mixtures, the effect of the ferric and ferrous oxide concentration on the magnetic susceptibility of caustic magnesium oxide in various states, and the effect of the periclase mixture concentration on the magnetic susceptibility of samples after drying and roasting and the gas permeability and maximum carbon burnout rate are plotted; it is shown that roasting increases the gas permeability and carbon burnout rate. The specific magnetic susceptibility of various refractory materials is examined. The need for a detailed study of the magnetic properties of refractories at conventional and especially high temperatures is recognized. Figures 3; tables 2; references 4: 3 Russian, 1 Western.

Principles of Determining Composition of Low Water Consumption Binder-Based Concrete

927D0226A Moscow BETON I ZHELEZOBETON in Russian No 4(445), Apr 92 pp 6-7

[Article by Yu.M. Bazhenov, L.A. Alimov, V.V. Voronin, Moscow Civil Engineers Institute; UDC 691.972]

[Abstract] The development of efficient binders with a low water demand (VNV) and an elevated superplasticizer concentration and various fillers calls for using special concrete composition analysis methods for each specific type of such binder. The existing principles of determining the composition of concrete on the basis of low water consumption binders developed at various research institutes do not make it possible to identify the basic patterns of the concrete mix composition variation as a function of principal factors; consequently, an attempt is made to clarify the main correlations necessary for selecting the VNV-based concrete composition. To this end, the VNV-100 and VNV-50 binders with a quartz aggregate and the S-3 superplasticizer are used. The Staryy Oskol and Belgorod portland cement are used as the VNV basis while medium-sized quartz sand and granite gravel with a 5-10 and 4-40 mm fraction are used as the fine and medium aggregate. The cement:water ratio, cement consumption, and sand fraction in the aggregate mix are varied. The dependence of the concrete mix fluidity and rigidity on the water rate is examined and the dependence of the concrete strength on the cement:water ratio is measured; the rheological properties of concrete are analyzed using a special cylindrical device with a 6 dm^3 volume. Statistical processing of the results makes it possible to derive two-factor square-law models which describe the relationship between the concrete rigidity or fluidity and the C:W ratio and the settling which characterize the mix moldability. The findings indicate that that concrete mixes and concrete on the basis of low water consumption binders have similar patterns and only the position of curves and the resulting quantitative data change. Consequently, the low water consumption binder-based concrete composition can be determined by a unified method used for determining the portland cement-based concrete composition. References 2.

Generalized Analysis of Slab Squirting Strength Using Domestic and Foreign Standards

927D0226B Moscow BETON I ZHELEZOBETON in Russian No 4(445), Apr 92 pp 11-13

[Article by K.Ye. Yermukhanov, Dzhambul Reclamation Irrigation Engineering Institute; UDC 624.073]

[Abstract] The methods of measuring the punching failure of concrete slabs resting on columns or other point supports under the effect of a concentrated load applied to a small area whereby the limiting state is characterized by the development of a truncated pyramid or cone whose smaller base is circumscribed by the load area contour and whose generator lines are inclined

at a 45° angle (30° in Great Britain) are discussed and the foreign and domestic standards used in analyzing the squirting strength of reinforced concrete slabs from heavy concrete without lateral reinforcement are presented. The differences in the punching fracture mechanisms are noted despite the generality in the structure of the foreign standards and methods used in analyzing the limited state, and the lack of a unified approach to strength analysis is mentioned. The characteristic features of the foreign strength analysis standards are reviewed and various strength methods used in the United States, Great Britain, Germany, France, and the USSR are compared quantitatively. The comparison reveals that Building Standards and Rules (SNiP) set higher limiting punching force levels than comparable foreign standards while the latter are somewhat more versatile than the SNiP's. The expediency of coordinating the SNiPs with foreign standards, especially with respect to the linear element analysis by the inclined cross section and the slab punching strength analysis, by expanding the scope of the issues necessary for practical designs is discussed. Figures 4; references 6: 2 Russian, 4 Western.

Frost and Salt Resistant Concrete

927D0226C Moscow BETON I ZHELEZOBETON in Russian No 4(445), Apr 92 pp 18-20

[Article by V.V. Gurskis, Scientific Research Institute of Reinforced Concrete; UDC 691.327:666.972.53]

[Abstract] The severe effect of the freezing and thawing cycle in a salt solution on the strength and performance of concrete and various mechanisms of concrete fracture under the composite effect of frost and salt solutions are discussed and the results of an experimental investigation of fine-grain concrete samples with Sebryakovskiy Plant 500 portland cement and Chelyabinsk Aluminum Smelter's microalumina as a binder are presented. The study is aimed at determining the reasons for concrete failure and developing concretes which are resistant to the combined salt-and-frost exposure. To this end, prismatic samples are made and dried at 60°C to a constant mass, then saturated with an aqueous NaCl solution of varying concentrations. The W:C ratio is manipulated in order to produce concretes with different structures while the S-3 superplasticizer and the PPF air entraining admixture are added. The component concentrations and their properties and the water absorption as a function of the W:B ratio and entrained air volume are summarized. The relative change in the bending strength of concrete prismatic samples saturated with water and aqueous NaCl solutions as a function of the freezing temperature is plotted. The strength of samples at subzero temperatures of up to -50°C is measured. The findings show that the strength variation patterns of the salt solution-saturated frozen concrete affect the accelerated concrete failure under a complex exposure. It is recommended that highly efficient chemical and active mineral additives which increase strength and decrease permeability be used to increase the concrete strength by preventing the crystalline ice formation and the resulting hydraulic pressure as well as lime leaching. Figures 1; tables 3; references 5.

Specifying and Correcting Concrete Composition

927D0226D Moscow BETON I ZHELEZOBETON in Russian No 4(445), Apr 92 pp 24-26

[Article by V.A. Pirogov, Kiev Construction Design Office; UDC 693.542[006]]

[Abstract] The steps necessary for adhering to state standard GOST 18105 (Concrete. Strength Control Rules) so as to ensure that the specified and design concrete resistance is maintained while minimizing the cement outlays, usually taken while specifying the mean concrete strength level allowing for its class and strength variation at a specific entity during a specific time and then periodically correcting the concrete composition while monitoring its other properties, are outlined. The shortcomings of the existing manual with respect to fixing the composition are mentioned and it is speculated that the task can be solved most efficiently using the experimental-analytical method (EAM) based on a cybernetic control model combined with statistical monitoring and strength control at the output. The EAM is based on the classical pattern of the dependence of the requisite C:W ratio on the cement activity and concrete strength as well as the dependence of the concrete strength on the informative factors. An alignment chart of the C:W ratio as a function of the cement activity and concrete strength is plotted. An example of the C:W ratio calculation for the specific values of parameters is cited. Stored program control of an automated process using the EAM algorithm makes it possible to shorten the differentiated concrete activity and discrete cement strength intervals to 1 MPa and create the conditions for comprehensive utilization of the potential technical and economic impact of GOST 18105. Figures 1; references 3.

On Standardizing Concrete Testing and Quality Control Methods

927D0226E Moscow BETON I ZHELEZOBETON in Russian No 4(445), Apr 92 pp 26-28

[Article by G.L. Gershanovich, Bratsk Hydroelectric Plant Construction Office; UDC 693.542(006)]

[Abstract] The need for further standardization in the construction industry and the excessive number of regulatory documents as well as the shortcomings common to all existing standards for concrete, particularly with respect to concrete classification, are discussed and the specific drawbacks of several individual standards are summarized. Special attention is focused on the lack of uniformity in control and acceptance rules and the issue of aggregate and nonmetallic rock product standardization. The inadequacy of the frost resistance standards, strength testing methods, rheological property measurements, and the handling of rejects are outlined. It is stressed that the list of issues addressed in the article is far from exhaustive. The conclusion is drawn that the system of standard preparation and enactment must be updated and that many shortcomings could be overcome

by submitting draft standards to engineers and other experts for approval prior to publication and enactment.

Floating Method of Reinforced Concrete Structure Erection for Nuclear Power Industry

927D0228A Moscow BETON I ZHELEZOBETON in Russian No 7(448), Jul 92 pp 12-14

[Article by K.Z. Galustov, A.B. Pavlov, Scientific Research Institute of Power Industry Construction; UDC 624.012.45]

[Abstract] The negative impact of the low level of power generation in poorly developed regions of the Far North, Far East and Central Russia on the development of extractive and processing industries and migratory processes of ore resource shipment from the central areas and the resulting high cost of power transmission lines prompted the development of new methods of power plant construction. A large-panel prefabricated construction method whereby power plant generating units are erected at a contractor yard under batch production conditions while ready-for-operation nuclear power plant panels are delivered on pontoons is considered and attention is focused on the structure module configuration as a single unit and the reliability of erection and assembly operations. Versions of nuclear power plants configured from transportable units and the design of the floating module of the main nuclear power plant structure on a pontoon foundation are shown. The effect of the structure rigidity on the taut strained state of the pontoon section of the floating module and floating module bottom panel sag are plotted. The advantages of using prestressed structures are discussed. The configuration and design of small nuclear power plant modules make it possible to develop mobile power plants intended for remote regions with a severe climate while at the same time addressing the issues of safety and reliability. Figures 5; references 3

Maximum Economic Efficiency Conditions of Columns With Tendons

927D0228B Moscow BETON I ZHELEZOBETON in Russian No 7(448), Jul 92 pp 15-16

[Article by D.R. Mailyan, Rostov Architectural Institute; UDC 624.075.23.003.13]

[Abstract] The utilization efficiency of high-strength reinforcement in short rigid elements under small lateral force eccentricity can be increased by prestressing the tendons which transfer the prestress to the concrete. The specific case of II-04 columns with a 40x40 cross section from class V30 concrete and with At-VI tendons is considered from the viewpoint of maximizing the economic efficiency of their utilization. Formulas are derived for calculating the cost of reinforcement bars under various conditions and the economic indicators of reinforced concrete columns with tendons and nonstressed reinforcement bars as a function of the steel consumption and tension conditions are plotted; the curves show that the economic efficiency of columns with tendons increases with an increase in the prestress and a decrease in the relative content of the nonstressed reinforcement. Given an identical length of the stressed and nonstressed reinforcement at a fixed cost ratio, the steel consumption and outlays decrease with an increase in the tendon proportion. Thus, prestressing of reinforcement bars makes it possible to lower the lateral reinforcement bar rate by 50% and reduce financial outlays by 45%. The findings are useful for determining the conditions under which elements with mixed reinforcement are especially effective. Figures 1; tables 1; references 2.

Assessment of Normal Section Strength of Reinforced Concrete Tendons

927D0228C Moscow BETON I ZHELEZOBETON in Russian No 7(448), Jul 92 pp 19-20

[Article by A.M. Boldyshev, V.S. Plevkov, Tomsk Civil Engineers Institute; UDC 624.012.4]

[Abstract] Despite the fact that the use of high-strength tendons makes it possible to considerably improve the performance and economic indicators of reinforced concrete structures, the procedures used today for analyzing the bent and eccentrically loaded tendons are inadequate for determining the real safety margins or designing optimum reinforcement under the effect of several combinations of lateral forces and bending moments. Consequently, an attempt is made to asses the normal section strength of reinforced concrete tendons and identify limiting states. The force and stress diagrams of six types of reinforced concrete tendons under various combinations of lateral forces and bending moments and the domains of relative strength of normal sections of nonstressed and prestressed reinforcement bars under various conditions are plotted. The resulting analytical and graphic relationships make it possible to check the strength of reinforced concrete elements under various types of reinforcement and determine the optimum element reinforcement. Figures 3; references 3.

Predicting Enterprise's Economic Indicators Under Transition to Market Economy

927D0228D Moscow BETON I ZHELEZOBETON in Russian No 7(448), Jul 92 pp 21-23

[Article by N.M. Bolshakov, Komi Branch of TsNIIEUS; UDC 69.003:658.011.8]

[Abstract] The importance of economic forecasting at an enterprise level for efficient economic management during the transition to a market economy and the principal components of the market mechanism are discussed and an attempt is made to substantiate theoretically and confirm in practice the efficiency of economic forecasting at a construction industry enterprise. To this end, forecasting is defined as determining the

economic indicators of the enterprise's activity on the basis of their development patterns at which the enterprise's potential and capabilities are controlled on the one hand by the market mechanism, i.e., competition, and on the other—by the state's economic regulation power. Attention is focused on economic forecasting under the condition of state property divestment, the appearance of numerous new forms of property, and the disappearance of existing enterprises. It is shown that the forecasting task calls for determining the economic indicators which largely determine the enterprise's existence and development, then the indicators over which the enterprise has no control, i.e., taxes, interest rates, insurance premiums, industry standards, etc. The importance of separating fixed costs from variable costs is stressed and a formula is derived for calculating the break even point. The role of price and other indicators on profitability—the most important factor in a market economy—is summarized and the conditions necessary for ensuring profitability are addressed. It is emphasized that prediction of economic indicators during the transition period will enable construction enterprises to meet production efficiency goals. Tables 1; references 1.

Resistance of Multicomponent Fine-Milled Binder-Based Concrete

927D0228E Moscow BETON I ZHELEZOBETON in Russian No 7(448), Jul 92 pp 24-26

[Article by V.G. Dovzhik, V.N. Tarasova, All-Union Scientific Research Institute of Reinforced Concrete; UDC 691.327:620.191.1]

[Abstract] The use of finely milled multicomponent cement binders (TMTsV) with various types of mineral aggregates for saving cement and increasing the production volume and the effect of TMTsV on the concrete resistance are discussed. The outcome of a concrete resistance study carried out at the All-Union Scientific Research Institute of Reinforced Concrete (VNIIZhB) using samples on the basis of the TMTsV-50 binder with a specific surface of 4,600-4,900 cm^2/g are described; the binder is made by joint ball mill grinding of the Zhuguli OTs 400-D20-B cement, Lyubertsy quartz sand, and Novo-Tulskiy granulated slag in a 1:1 ratio. The behavior of the concrete strength under various storage conditions is plotted and the strength of various compositions of concrete in a water saturated state after 28 days and after 50 and 100 moistening and drying cycles as well as the compressive strength, prism strength, tensile strength, modulus of elasticity, Poisson's ratio, and plasticity coefficient are summarized. An analysis demonstrates that the use of finely milled cement binder with a 50% substitution of the clinker component with slag and sand in a 1:1 ratio combined with an addition of a superplasticizer makes it possible to produce class V15-V30 concrete whose strength and normal life are equal to, or exceed, similar indicators of concrete with portland cement under various conditions. Figures 1; tables 3; references 5.

Structure of SiC Powders Produced by Interaction of Silica and Carbon Black

927D0251E Kiev POROSHKOVAYA METALLURGIYA in Russian No 7, Jul 92 (manuscript received 4 Dec 90) pp 47-52

[Article by M.V. Vlasova, D.P. Zyatkevich, N.G. Kakazey, G.S. Oleynik, A.A. Rogozinskaya, and A.I. Kharlamov, Institute of Problems in Materials Science at Ukrainian Academy of Sciences, Kiev; UDC 541.1-16.661.2.661.68]

[Abstract] A structural study of SiC powders produced by reduction of SiO_2 and subsequent synthesis of Si with carbon black in an argon atmosphere at temperatures ranging from 1473 K to 2073 K was made, the silica having been obtained from H_2SiO_3 powder and a total reaction time of 3 h having been allowed at each temperature. The end products of the reaction were examined by several methods: elemental chemical analysis, x-ray structural and quantitative x-ray phase analyses in a DRON-0.5 diffractometer, EPR spectroscopy in an RE 1306 radio-frequency spectrometer, infrared spectroscopy in a UR-20 spectrometer, and under a transmission electron microscope combined with a HU-200 microdiffractometer. Interaction of silica and carbon black began at 1473 K, with formation of subdisperse β-SiC. Interaction at higher temperatures up to 1773 K produced powder containing not only monophase β-SiC aggregates but also polyphase SiC+SiO_2+C aggregates. As the reactor temperature was raised further, the oxygen content in the SiC powder decreased linearly from 8 wt.% (synthesis at 1773 K) to zero (synthesis at 1973 K) while the carbon content increased from 22 wt.% (synthesis at 1773 K) to 28 wt.% saturation level (synthesis at 2073 K). The phase composition of the powder was also found to depend on the reactor temperature, the fraction of the major phase β-SiC increasing to maximum (synthesis at 2073 K) and the fraction of the minor phase α-SiC decreasing to zero (synthesis at 2073 K) while the α-SiO_2 (cristobalite) content peaked to a maximum (synthesis at 1773 K) and then decreased to zero (synthesis at 1873 K). Figures 4; tables 2; references 15.

New Boron-Bearing Raw Materials for Glassmaking

927D0236C Moscow STEKLO I KERAMIKA in Russian No 4, Apr 92 pp 9-10

[Article by Yu.Ya. Keyshs, V.G. Chekhovskiy, Yu.S. Plyshevskiy, N.V. Garkunova, Leningrad Technological Institute and Riga Engineering University; UDC 666.112.7:666.122.4]

[Abstract] The decreasing availability of B-bearing raw materials traditionally used in glassmaking prompted a search for new materials. The phase and structural transformations occurring during the heat treatment of the danburite (KD) and sayak (KS) concentrates at a temperature which corresponds to the initial stage of the

glassmaking process—the silicate formation—as well as in the glass founded from these concentrates without an addition of other materials to the charge are examined. To this end, glass is founded at a temperature of about 1,300°C and exposed to it for 1.5 h in corundum crucibles. A thermographic study is carried out in a Paulik, Paulik, & Erdei differential thermal analyzer, X-ray diffraction patterns are recorded in DRON-2.0 and URS-50IM units in Cu*K* radiation using a Ni filter, and infrared spectra are recorded in a UR-20 spectrometer; the differential thermograms of the concentrates and glass produced from them are plotted. The mass percentage of boron, silicon, aluminum, iron, calcium, magnesium, arsenic, and trace element oxides of the KD and KS concentrates (mined in Pamir and eastern Kazakhstan) is summarized. The findings show that KS glass is opacified, yet no structural features responsible for it could be identified; is it speculated that opaqueness is due to the presence in KS glass of As whose compounds serve as opacifying additions. The study also confirms that the KS and KD concentrates may be used as raw materials in preparing charge compositions for borosilicate glass, glaze, and enamels. The need to eliminate body defects in the form of crystalline inclusions is stressed. Figures 1; tables 1; references 4: 2 Russian, 3 Western.

Improving Uviol Glass Quality

927D0236D Moscow STEKLO I KERAMIKA in Russian No 4, Apr 92 pp 11-12

[Article by A.B. Atkarskaya, V.I. Borulko, F.A. Tkachenko, S.Z. Khripunov, Yu.V. Shevchenko, L.P. Yurchuk, Scientific Research Institute of Automotive Glass; UDC 666.246.1.002.237]

[Abstract] The glass body contamination with staining impurities and the resulting unacceptable increase in the short-wave light absorptance of the US-11449 optical glass prompted an investigation of the specific refractive index (UPP) of eight staining elements—Fe, Cu, Cr, V, Ce, Ti, Ni, and Co—in the ultraviolet spectrum and an attempt to assess the possibility of lowering the number of grains in the glass. The specific refractive indices of the staining impurities at various wavelengths from 200 to 400 nm, the founding conditions and fusion quality of eight batches of glass, and the relative fraction of various inclusions are summarized. The glass used in the study is founded in a lab electric furnace with silicate heaters in quartz glass crucibles while the melt is stirred by a quartz impeller. The light transmission is measured by an SF-26 instrument and the number and size of grains is measured under a MIN-8 microscope. The findings demonstrate that the use of the synthetic charge with the OSCh 8-4 silica with a 1,480°C charging temperature, a 1.0 h charging duration, a 1,500°C founding temperature, a 1.0 h founding duration, and with clarification for 1.5 h at 1,520°C makes it possible to produce glass without charge grains and with good optical properties. Tables 3.

Using Flotation Polishing Principle for Machining Optical Glass Parts

927D0236E Moscow STEKLO I KERAMIKA in Russian No 4, Apr 92 pp 13-16

[Article by S.I. Zakharov, O.V. Tapinskaya, A.A. Frolov, Optika Scientific Production Association; UDC 666.22:666.1.053.5:681.7]

[Abstract] The methods of high-quality flotation polishing of planar surfaces of optical and other special materials developed in the early 80's by the Japanese researchers are discussed and the advantages and shortcomings of flotation polishing practices are outlined. An attempt is made to modify the flotation polishing principle for uses in traditional mechanical designs of equipment for machining optical glass parts. The design calls for delivering the lubricant-coolant fluid (SOZh) either under pressure or in a mixture with an abrasive material. A schematic diagram of the optical glass machining principle is cited and a tribohydrodynamic problem is formulated whereby the flow of the coolant-lubricant flow with an abrasive material is simulated by a flow of a viscous liquid. The wear profile of the machined surface in various cases is plotted. An analysis of a spherical surface machined by the new method is carried out on an IBM PC/AT microcomputer by the Synchrospeed method developed by the Lon company (Germany). The study confirms the feasibility of using the principle of machining the surface by a flow of fluid with abrasive particles directed at a high speed along the surface profile; the machining efficiency virtually does not change along the tool surface. Figures 3; references 6: 1 Russian, 5 Western.

Amorphous Silicon Oxide-Based Ceramic Materials

927D0236F Moscow STEKLO I KERAMIKA in Russian No 4, Apr 92 pp 24-26

[Article by F.Ya. Boroday, Tekhnologiya State Scientific Production Enterprise; UDC 666.762.2]

[Abstract] The need for materials characterized not only by a high heat resistance but also by a certain combination of dielectric, thermal, and strength properties led to the development of amorphous silicon oxide-based ceramic materials which possess these qualities. The dependence of the dielectric constant on porosity—a standard used in engineering analyses—is derived and the production practices for making ceramic materials with a porosity of 0-95% and the methods of making lamellar and combined products from dense and porous amorphous silicon oxide-based ceramic materials are described. The properties and production methods of such materials with a varying porosity and the dependence of porosity on the roasting temperature and the fiber concentration and dimensions are plotted. In making dense ceramics, porosity is controlled by comprehensively manipulating the slip properties and roasting conditions; the principal factors affecting the

ceramic material porosity are discussed and the methods of producing dense pore-free ceramics and ceramics with a specified porosity are outlined. An analysis of the production practices and material properties reveals that products with a specified porosity within a 0-95% range can be made from amorphous silicon oxide and complex items with various combinations of ceramic and modifying materials can be produced. Figures 3; references 7: 5 Russian, 2 Western.

Biological Implant Glass Ceramics

927D0236G Moscow STEKLO I KERAMIKA in Russian No 4, Apr 92 pp 26-28

[Article by L.M. Silich, N.I. Zayats, O.P. Chudakov, M.A. Shandyukova, S.A. Gaylevich, Belarussian Polytechnic Institute and Minsk Medical School; UDC 666.263.2:61]

[Abstract] The increasing application of glass- and glass ceramic-based materials in surgical and dental orthopedic practices as implants prompted a study of the effect of various mechanical, chemical, and physical factors on the implant and the resulting stringent requirements imposed on the implant materials. Two types of bioimplants—bioinert and bioactive—are considered and their characteristics are outlined. The advantages of glass ceramics over traditional implant materials are discussed and the problem of developing and studying new crystalline glass materials with a specified range of properties is formulated. In particular, a glass ceramic system consisting of silicon, phosphorus, aluminum, calcium, and potassium oxides and fluorine is used in the study. The phase formation in the system under study at a 1,000°C temperature, the glass ceramic leaching kinetics, and the X-ray and electron diffraction patterns of the glass ceramic sample surfaces exposed to blood plasma are plotted. The glass ceramic material produced as a result of the study has good physical-chemical and mechanical properties: a density of 2,700 kg/m^3, a microhardness of 2,450 MPa, a thermal coefficient of linear expansion of 87 x $10^{-7}°C^{-1}$ (TKLR), a compressive strength of 240 MPa, a chemical resistance to a 1 $mole/dm^3$ HCl solution of 12.6% and 0.8% for NaOH, and an attrition of 0.7 x 10^{-3} kg/m^2. The material has a complex dependence of properties on composition due to the phase separation. The material's toxicological and hygienic properties meet the requirements imposed on implants, making it possible to recommend the material for prosthetic devices and use in facial surgery. Figures 4; references 2: 1 Russian, 1 Western.

Chill Casting of Large-Size Pig Iron Castings With Complex Shape

927D0234E Moscow LITEYNOYE PROIZVODSTVO in Russian No 4, Apr 92 pp 18-20

[Article by L.B. Goldshteyn, Ye.M. Podkovyrin, V.A. Fedorov-Bakal, V.P. Burba, V.N. Belyy, All-Union Scientific Research Institute of Ferrous Metallurgy Machines; UDC 621.74.043]

[Abstract] A range of problems which must be solved comprehensively for making large group 1-3 casting with a complex configuration by chill casting is outlined: increasing the tooling resistance, attaining the necessary strength in combination with good machinability, ensuring mold filling with killed metal and its uniform solidification, and improving the casting moldability and practicability. The casting parameters are examined and refined using a special metal mold unit designed and manufactured at the pilot plant of the All-Union Scientific Research Institute of Ferrous Metallurgy Machines and methods of solving each individual problem are discussed. A new trend in increasing the metal mold attachment resistance by an evaporative metal mold cooling method developed by the institute together with the Energostal plant is considered. The mold and core temperature variation during the cycle and the dependence of the ultimate rupture strength on the steel scrap concentration in the charge and the pig iron's eutectic ratio are plotted. The use of evaporative cooling makes it possible to lower the peak temperature loads in the mold walls and decrease their amplitude thus reducing the probability of defects and thermal stresses which lead to warping. The study also shows that in addition to the physical and mechanical properties, the metal's liquid state before pouring has a significant effect on the casting quality. The possibility of substituting grey cast iron with high-strength cast iron is examined. Such a substitution makes it possible to decrease the casting mass by 27%. For illustration, sand mold casting indicators are compared to those of chill (permanent) mold casting. An analysis demonstrates the advantages of chill casting of large complex-shaped parts. Figures 3.

Improving Quality of Castings Made by Oriented Crystallization Method

927D0234D Moscow LITEYNOYE PROIZVODSTVO in Russian No 4, Apr 92 pp 16-18

[Article by B.A. Kulakov, V.M. Aleksandrov, V.K. Dubrovin, Chelyabinsk State Engineering University; UDC 621.74.002.6:669.14.018.44]

[Abstract] The high level of defects (a 75-82% rejection rate) of cast gas turbine engine blades made in PMP-2 continuous oriented crystallization furnaces from ZhS30-VI superalloys using ceramic molds prompted attempts to improve the casting quality and determine the principal factors affecting the defect formation. It is speculated that the principal factor responsible for nonmetallic inclusions (32-43% of rejects) is the interaction of chemically active alloy components with the mold's silica leading to the development of oxide films. Silicon precipitating as a result of the reaction diffuses into the poured metal since its maximum solubility in Ni reaches 15% at a 1873K temperature. The possibility of these processes is examined allowing for aluminum's activity in the melt using thermodynamic analyses. The silicon distribution in the casting cross section is measured by a REM-100U spectral X-ray diffraction analyzer and the Si distribution and high-temperature layer silicon saturation depth as a function of the SiO_2 concentration in the binder with the aggregate are plotted. Silicon saturation can be prevented by decreasing the silicon dioxide content or by using other silicon dioxide-free refractory materials. Moreover, given the same silica content in the casting binder, filled molds with a mullitized disthene-sillimanite are not saturated with silicon almost at all. Commercial tests of a procedure of turbine blade production demonstrate the possibility of decreasing casting rejects due to surface defects by 10-15% and preventing the alloy saturation with silicon. Figures 3; references 3.

Effect of Physical and Chemical Melting Conditions on Titanium Casting Quality

927D0234C Moscow LITEYNOYE PROIZVODSTVO in Russian No 4, Apr 92 pp 10-11

[Article by V.G. Mishanova, G.L. Khodorovskiy; UDC 621.74:669.295]

[Abstract] The urgency of using castings with good mechanical properties and a high reliability and the need to optimize the most important physical and chemical processes accompanying the alloy melting in a vacuum arc slag autocrucible unit (VDGU) are noted and the effect of the physical and chemical smelting conditions on the quality of titanium alloy casting is examined. To this end, the ranges of residual pressure during the vacuum arc autocrucible melting (VGDP) of titanium alloys and the effect of external in-leaks on the metal quality are analyzed. The effect of the residual pressure on the gas content behavior in alloys VT1 and VT5l and an alignment chart for determining the permissible external in-leak are plotted. An analysis reveals that it is necessary to take into account not only the effect of the gaseous atmosphere on the chemical composition of the alloy but also the inverse effect. Tests of the effect of hydrogen and a method of removing it at the end of the smelting process indicate that its concentration decreases by roughly 2-2.5 times compared to traditional smelting. Tests of samples cut from castings show that their strength varies by 3-15% and ductility—by 10-38% as a function of the physical and chemical conditions. A comparison of the effect of residual gas pressure and the gas in-leak shows that the former is much greater; thus, the titanium alloy properties can be controlled by manipulating the residual pressure. Figures 2.

Development of Accelerated YuNDK35T5AA Alloy Single Crystal Growth Conditions

927D0234B Moscow LITEYNOYE PROIZVODSTVO in Russian No 4, Apr 92 pp 9-10

[Article by Ye.V. Sidorov, Magneton Scientific Production Association; UDC 621.746:669.15.71]

[Abstract] The slow speed of making single crystal castings from YuNDK magnetic alloys by oriented controlled solidification using single crystal seed prompted the development of the solidification conditions which make it possible to produce single crystal ingots from the YuNDK35T5AA alloy at higher growth rates. To this end, single crystal castings with a 24 mm diameter and 140-150 mm height grown in aluminum oxide ceramic tubes with 1.5 and 5 mm thick walls using the Kristall YeM unit with a graphite resistance heater are investigated. The temperature gradient in the liquid on the leading edge of the crystallization front is manipulated and the temperature field is measured by six thermocouples. The single crystal structure formation in the directionally crystallizing sample largely depends on the heat removal while a decrease in the wall thickness lowers the melt overheating and reduces the temperature gradient. It is shown that in order to increase the growth rate of single crystal castings to 800-840 mm/h, one has to decrease the melt's temperature gradient on the leading edge to 2-4 deg/mm and reduce the ceramic mold wall thickness to 1-1.5 mm. The level of magnetic properties in a sample after a thermomagnetic treatment pursuant to GOST 17809-72 is the same regardless of the growth rate, thus confirming the expediency of speeding up the solidification process.

Effect of Cast Surface Purity on Mechanical Properties of High-Strength Pig Iron

927D0234A Moscow LITEYNOYE PROIZVODSTVO in Russian No 4, Apr 92 pp 4-5

[Article by V.I. Litovka, M.P. Bubnov, IPL at Ukrainian Academy of Sciences and TsISI; UDC 621.74:669.131.7]

[Abstract] The effect of the cast surface cleanliness on the mechanical properties of high-strength pig iron is discussed and the effect of surface layers of cast iron with globular graphite (ChShG) prior to machining on the mechanical properties of the castings is investigated by investment casting in order to reveal the extent of this effect. The pig iron is inoculated prior to casting with the FSMg alloying composition while the molds are heated to various temperatures within a 20-650°C range to ensure the necessary ingot cooling rate. The samples are tested in the cast state and following heat treatment; the structure and properties of the cast samples after annealing and the wear and wear rate of the samples as a function of the test duration are summarized. The dependence of the ultimate strength and reduction in area as a function of the ChShG pig iron cooling rate and the dependence of the cyclical toughness on the stress amplitude are plotted. An analysis of the findings shows that common estimates of the mechanical properties of globular graphite pig iron using samples cut from specially cast ingots are generally understated and do not fully reflect the high operating potential of products from this pig iron. It is suggested that ingots with a cast surface be used for maximizing the reliability of pig iron with globular graphite. Figures 2; tables 2.

Production of Complex Aluminum Casting by Backpressure Die Casting

927D0233H Moscow LITEYNOYE PROIZVODSTVO in Russian No 3, Mar 92 p 28

[Article by L.M. Markov, Ya.K. Kovchazliyev, Metal Science and Metallurgy Institute, Bulgaria; UDC 621:74.043]

[Abstract] The need for marine research instruments which operate at a great depth and must therefore be encased in strong, corrosion resistant, and light housings prompted an investigation into the possibility of producing aluminum hemispheres for such housings with a 30 mm thick wall by backpressure die casting. The alloy composition suitable for such castings is summarized and an experiment carried out in a VP400 backpressure die casting machines is described. The effect of dye on the heat exchange between the casting and the mold due to the development of "warm" and "cold" mold surfaces is examined: to this end, heat conducting Dyecoat 38 F and Dyecoat 11 dyes or heat insulating Dyecoat and Simpson dyes are applied to the metal mold by a sprayer. A study of the samples cut from the castings reveals that the cast parts with a 0.025 m wall can be used successfully at a depth of up to 6,000 m. They have an ultimate strength of 490-520 MPa, a bending strength of 530-560 MPa, an elongation of 0.5-0.7%, and a hardness of 160-170.

Ecological Aspect of Titanium Alloy Mold Production

927D0233G Moscow LITEYNOYE PROIZVODSTVO in Russian No 3, Mar 92 pp 26-27

[Article by V.G. Antashov, A.I. Trunov, V.A. Chernikov, Scientific Research Institute of Aviation Engineering and Saturn Scientific Production Association; UDC 621.744:669.294]

[Abstract] The ecological impact of mold preparation for titanium alloy casting whereby a carbon composition mixed with a resin is heat-treated in a gaseous medium, resulting in a release of toxic substances and a graphite dust and phenol concentration of 50 and 300-300 times higher than the safe level, respectively, prompted a study of ways to solve this problem. Two principal methods are identified—capturing, neutralizing, and burying or reusing the toxic substances or using a waste-free technology. Due to the difficulties of implementing the former method, the latter is considered in detail and its stages are outlined. The state of aggregation, safe level, hazard

category, and toxicological characteristics of acetone, benzapyrene, benzene, phenol, formaldehyde, graphite, and hydrochloric acid are summarized. The conclusion is drawn that the most expedient procedure calls for eliminating the casting pickling thus improving the safety conditions. The methods of accomplishing this task are described, e.g., increasing the chemical inertness of ceramic molds or using protective coats. The principal possibility of developing environmentally clean waste-free titanium casting mold-making practices is demonstrated. The need for further research is stressed. Tables 1.

Hygienic Assessment of Liquid Aluminum Alloy Refining

927D0233F Moscow LITEYNOYE PROIZVODSTVO in Russian No 3, Mar 92 pp 25-26

[Article by A.Ye. Yermolenko, A.A. Grinberg, S.A. Savichev, A.M. Rabinovich, Scientific Research Institute of Occupational Health and Occupational Safety at Russia's Academy of Medical Sciences and All-Union Scientific Research and Design Institute of Electric Machine Building, Vladimir; UDC 621.74:669.714]

[Abstract] The FRAM 02 flux developed by the All-Union Scientific Research and Design Institute of Electric Machine Building (VNIPTIEM) which has a high refining and modifying ability and is capable of improving the foundry air quality by decreasing the liberation of toxic substances from the molten metal prompted a comparative hygienic assessment of the aluminum alloy refining processes using this flux as well as the Universal No. 3 flux and the Degazer degassing preparation and an analysis of the total and unit levels of the most toxic chemical substances. The composition, addition method, ratio to the metal weight, melt temperature, and suggested treatment duration are analyzed for three flux brands and the refining ability and slag removal of the three flux brands are summarized for the most toxic substances forming during the casting. The hygienic estimate is made while refining the AK 12 (P.Ch. grade) alloy in an induction furnace. A comparison of the data shows that the FRAM 02 flux is vastly superior to the other brands from the viewpoint of improving the air quality. When it is used, no group 1 toxic substances are detected. The specific substances which must be monitoring for each flux are specified. Tables 2; references 1.

Plasma Coats for Magnesium Casting Metal Molds

927D0233E Moscow LITEYNOYE PROIZVODSTVO in Russian No 3, Mar 92 pp 19-20

[Article by D.G. Isayev, G.S. Isayev, N.A. Serova, L.M. Patrushev, V.N. Shkrob, Moscow Steel and Alloy Institute and Rubin Plant; UDC 621.74.043:669.721]

[Abstract] A persistent trend toward increasing the output of various parts and units from magnesium alloys due to their relatively low specific gravity and good performance indicators and the shortcomings of magnesium alloys, especially their high cost and low corrosion resistance combined with a large number of defects, are noted. The use of spinel-type oxide materials for plasma spraying of antisticking ceramic coats on the metal mold surfaces is discussed and a procedure of producing fused disperse materials on the basis of $MgAl_2O_4$ spinel for this purpose developed at the Moscow Steel and Alloy Institute is described. The resulting plasma sprayed coats are characterized by a low porosity and an absence of microporosity and poorly visible intergranular boundaries. The chemical and phase composition of three coating materials and their microhardness, adhesion strength, heat resistance, and strength are summarized; the surface roughness profilograms of the ML-10 castings are plotted and the microstructure of antisticking coatings is shown. The study demonstrates that the coats have an extended service life and make it possible to produce cast corrosion-resistant parts from magnesium alloys which do not require additional finishing process stages. Figures 2; tables 2; references 4: 2 Russian, 2 Western.

Chemically Inert Ceramic Molds for Making Titanium Castings

927D0233D Moscow LITEYNOYE PROIZVODSTVO in Russian No 3, Mar 92 pp 15-16

[Article by V.A. Chernikov, G.L. Khodorovskiy, V.N. Larionov, Ye.N. Khlystov, Saturn Scientific Production Association and Scientific Research Institute of Aviation Technology; UDC 621.74.045:669.295]

[Abstract] The advantages of steady-state metal casting into molds heated to a temperature of 1,000°C or higher which makes it possible to avoid spin casting in producing thin-walled large-sized titanium alloy blanks, fill the mold with a compact flow of killed metal, eliminate certain types of defects, and prolong the crystallization span thus improving the filling conditions of thin extended internal mold cavities and creating favorable conditions for secondary H_2 dissolution, are discussed. The conditions necessary to ensure the gas bubble stability are examined and the effect of the initial mold temperature on the filling of its internal cavities and the quality of cast titanium blanks is investigated. The experimental procedure is outlined in detail and the dependence of the titanium blank's cast structure, density, and roughness on the initial mold temperature and silicon dioxide concentration in the binder and the effect of the modified layer depth in titanium castings on the initial mold temperature and SiO_2 concentration in the binder are plotted. The efficacy of using protective mold coatings, especially from yttrium oxide, is demonstrated. An analysis reveals that due to the high cost of yttrium for making inert ceramic mold coatings, the use of

corundum mold coats combined with mold heating is still acceptable for titanium alloy castings with a complex shape. Figures 2.

High-Temperature Gasostatic Treatment of Cast Structural Materials: Discussion

927D0233C Moscow LITEYNOYE PROIZVODSTVO in Russian No 3, Mar 92 pp 12-14

[Article by S.I. Kruk, V.M. Sagalevich, Delfin Central Scientific Research Institute and Moscow State Engineering University; UDC 621.74]

[Abstract] The advantages of hot isostatic pressing (VGO) of HIPing—an integral part of the shaped casting production process in various industries, particularly aerospace—are discussed and the experience of leading foreign companies in this field, e.g., Industrial Materials Technology and General Electric, is reviewed. Gasostatic pressing makes it possible to eliminate the metal microporosity and thus increase its fatigue strength and service life at elevated temperatures. The mechanism of isostatic pressing is explained and it is noted that it facilitates internal defect curing and improves the metal structure in general. The effect of the cooling rate after HIPing on the metal structure and mechanical properties is outlined. The specific uses of HIPing for making stainless steel castings is illustrated. HIPing lowers the crystal anisotropy of casting steel H12 and weldability of steel 316L. The uses of HIPing for titanium alloys are described and it is shown that the elimination of defect in titanium alloys during HIPing makes it possible to save metal by decreasing the number of gates while maintaining the metal quality. It is stressed that HIPing is especially efficient with aluminum alloys; it eliminates their porosity and increases fatigue strength by 30-50% while increasing toughness somewhat. HIPing also improves the ductility of castings. The outlook for future uses of HIPing is assessed. References: 14 Western.

Modern Methods of High-Strength Aluminum Alloy Casting Production and Machining

927D0233B Moscow LITEYNOYE PROIZVODSTVO in Russian No 3, Mar 92 pp 6-8

[Article by N.S. Postnikov, All-Union Aviation Materials Institute; UDC 621.74.04:669.715]

[Abstract] The patterns of the reliability characteristics of aluminum alloy casting which are related to the chemical and phase composition and structure of cast parts and the new aluminum alloys developed in recent years as well as the processes which ensure the necessary performance of modern aluminum castings are discussed. The ultimate strength, elongation, loss of strength due to welding, long-term strength, and other mechanical properties of the VAL-T5, VAL12-T5, and VAL16-T5 alloys and the mechanical properties of T-joints, lids, beds, and cassettes made from these alloys are summarized; the properties of parts produced by permanent mold casting and liquid extrusion are compared. Compared to permanent mold casting, the dynamic effect of pressure during liquid extrusion increases the solidification rate by two- to threefold. The effect of machining, particularly surface deformation or cold working, is examined and it is shown that surface machining increases the fatigue resistance by 1.5-2 times and stress corrosion cracking by two- to threefold as well as decreases general corrosion losses by 20-25%. The effect of vacuum heat treatment (TVO) is considered and the comparative characteristics of the properties of samples cut from various alloys after heat treatment with or without hot isostatic pressing (GIU) are cited. The findings demonstrate that modern aluminum alloys and advanced casting methods can make it possible to replace not only deformable aluminum alloys but also brass, pig iron, and steels. Tables 8.

Copper Alloy Casting Production Trends and Problems

927D0233A Moscow LITEYNOYE PROIZVODSTVO in Russian No 3, Mar 92 pp 4-6

[Article by V.M. Chursin, Moscow Evening Metallurgical Institute; UDC 621.74:669.35]

[Abstract] The relatively steady production level of shaped copper alloy castings, both at home and abroad, despite numerous efforts to minimize the Cu consumption is attributed to the alloys' good heat and electric conductivity, corrosion resistance, antifriction properties, nonmagnetic properties, shape memory, and general reliability. The copper alloy casting production outlook and problems are investigated. To this end, attention is focused on the alloy composition, furnace design and operation, charge composition and properties, casting methods, and specialty casting practices. The effect of various process, design, and composition factors on the mechanical and physical properties of copper alloy castings is considered in detail. The efficiency of using secondary raw materials and scrap is assessed. It is noted that the use of secondary pig alloys considerably reduces charge and smelting outlays and saves copper. References 5: 4 Russian, 1 Western.

Oxidation of Fine-Disperse Cu and Zn Powders During Heating

927D0251B Kiev POROSHKOVAYA METALLURGIYA in Russian No 7, Jul 92 (manuscript received 2 Aug 90) pp 9-13

[Article by I.V. Gribovskaya and S.V. Zhidovinova, Institute of Metallurgy, Ural Department, Russian Academy of Sciences, Yekaterinburg; UDC 669.3'5-492.094.3]

[Abstract] An experimental study of fine-disperse Cu and Zn powders was made concerning their oxidation during heating from 293 K room temperature to 973 K

in air. The powders produced by evaporation and condensation in an argon or nitrogen atmosphere, the copper target being vaporized at 2073 K and the zinc target being vaporized at 1183 K. Copper powder of the 0.02-0.5 μm grain size fraction (specific surface of 9500 m^2/kg) with a 1 % oxide content and zinc powder of the 1-5 μm grain size fraction (specific surface 1400 m^2/kg) with a 10.7 % oxide content were deposited by condensation, both powders consisting of spherical grains. Following measurements with an OD-102 derivatograph, 0.5 g specimens of Cu powder and 1 g specimens of Zn powder were poured into alundum beakers for heating from room temperature up at a rate of 0.167-0.250°C/s. They were at each temperature photographed in a UDV-2000 x-ray camera and analyzed in a DRON-3 x-ray diffractometer for phase composition of the oxide films which had formed on the grain surfaces. Oxidation of Cu powder was found to begin at 503 K and end at 793 K, an exothermic effect occurring within this temperature range. Neither "free" metallic copper nor Cu_2 but only CuO were recorded at 623 K. Differential thermal analysis revealed a cyclic cracking of films and formation of new films on the copper grain surfaces at temperatures above 503 K. While both Cu and CuO oxides were forming as the temperature was raised, there also took place a $Cu_2 \rightarrow$ CuO transformation. This transformation was completed at 623 K on flat specimens, at 793 K on massive ones. Oxidation of Zn powder was found to begin at 608 K, to gradually slow down above 723 K, and to stabilize at 973 K. Differential thermal analysis revealed that the rate of zinc powder oxidation had peaked to a maximum at 683 K and then again at 758 K after having dipped to a minimum at 693 K. The oxidation resistance of zinc powder in humid air below 608 K may be due to protective action of chemosorbed water films on the grain surfaces. The high ZnO content in the powder at high temperatures is evidently due to hydration of this oxide into $ZN(OH)_2$ in humid air, the oxide otherwise not undergoing any phase transformations but remaining in its either amorphous or crystalline form. Figures 2; references 11.

Producing Mixtures of Ultrafine-Disperse Ni, Co, and Cu Powders

927D0251A Kiev POROSHKOVAYA METALLURGIYA in Russian No 7, Jul 92 (manuscript received 26 Jun 89) pp 5-9

[Article by N.M. Khokhlacheva, A.V. Lyushinskiy, V.N. Paderno, T.G. Khokhlacheva, M.P. Gryunvald, and M.Ye. Belchikova, Ramenskoye Engineering Office of Instrument Design and Institute of Problems in Material Science at Ukrainian Academy of Sciences, Kiev; UDC 621.792]

[Abstract] Preparation of ultrafine-disperse metal powders by thermal decomposition of their salts of organic acids at low temperatures is examined, specifically preparation of Ni, Co, and Cu powders from formates of these metals to be mixed for production of Ni-Co, Ni-Cu, and Co-Cu powder composites with various weight ratios of their components. The process consists of five stages: 1) mixing of the formates, 2) homogenization of the mixture, 3) thermal decomposition (pyrolysis) of the formates at a constant temperature in an inert atmosphere, 4) cooling, 5) protection of the mixture against oxidation during storage. In an experimental study of this process solid solutions of the formates were obtained from nitrates of these metals by precipitating their cations with sodium carbonate and then from their carbonates by precipitating them with formic acid. The solid solutions of the three (Ni,Co,Cu) formates differed from the original formates in both color and crystal structure. They dehydrated at 140°C and decomposed at 160°C. The thermal decomposition in an inert atmosphere was tracked with a derivatograph, the specific surface of the powders being measured by thermal desorption of argon. The microstructure of powder particles was examined under a "Stereoscan-150" electron microscope and their phase composition was analyzed in a DRON-2 x-ray diffractometer with Fe-line radiation. The results of this study indicate the best technology for making intricate inserts of a powder-metal composite material approximately the same as that of parts to be joined by cold welding without degradation of quality. Figures 4; tables 1; references 3.

Compactability of Ni and Co Powders Forming by Decomposition of Salts Under Vacuum

927D0251C Kiev POROSHKOVAYA METALLURGIYA in Russian No 7, Jul 92 (manuscript received 9 Oct 90) pp 30-33

[Article by V.N. Kolesnikov, Kharkov University; UDC 621.762]

[Abstract] Intergrowth of metal crystals from one salt crystal during its decomposition under vacuum was studied in an experiment with Ni and Co formates and oxalates, these salts decomposing at low temperatures within the 550-650 K range so that powder formation can be observed under an electron microscope as crystals of these salts are being heated to those temperatures. They were so heated with an electron beam, conversion of salt into metal powder proceeding in two stages: chemical decomposition reaction followed by interdiffusion of metal atoms resulting in an "atoms → clusters → nuclei → crystals → aggregates" sequence of transitions, with an attendant large increase of density and a bifurcated spatial distribution of components in the new solid solution. Decomposition of a salt crystal was found to be accompanied by formation of fine of metal crystals in the 0.01-0.1 μm size range, these microcrystals sticking to one another and thus forming an unbalanced structure similar to that of a powder compact. Evidently, the curvature gradients at contact sites give rise to Laplacian pressure fields which combine to cause cubic compression of the powder mass as the microcrystals slip against one another. The effective pressure is proportional to the porosity of the powder and to the surface energy of its particles, both decreasing in the process. The process relaxation time and the boundary viscosity of powder in

this process have been estimated on the basis of the experimental data in accordance with the theory of diffusion-viscous flow. Figures 3; references 10.

New Metallurgical Processes

927D0243E Moscow STAL in Russian
No 4, Apr 92 pp 30-31

[Article by V.I. Kashin, Metallurgy Institute imeni A.A. Baykov; UDC 621.746.27.047]

[Abstract] The proceedings of a Soviet-German seminar on new metallurgical processes held in November 1991 in Duesseldorf are reviewed; representatives from the Metallurgy Institute imeni A.A. Baykov, the Central Scientific Research Institute of Ferrous Metallurgy, the Metallurgy Institute at the Urals Department of the USSR Academy of Sciences, and Electric Welding Institute imeni Ye.O. Paton as well as leading research centers and a number of German industrial companies participated in its activities. The German scientists discussed the patterns of steel resulfurization with an abrupt change in the slag oxidation and noted that the resulfurization rate greatly exceeds the desulfurization rate; an experimental procedure of investigating the thermodynamics of diluted sulfur solutions in molten iron and slag and sulfur distribution is presented. Three reports dealt with the problem of making steel with a specified nitrogen content; the issues of steel smelting and refining practices and coke substitution with bituminous coal are discussed. "Cold" physical and mathematical simulation of the gas- and hydrodynamics of metallurgical processes and practical applications of the studies of the combustion and heat and mass transfer process are discussed; special attention is focused on making thin slabs and sheets by the continuous casting method; the experience of continuous casting machine (MNLZ) operation (U.S. made) in Germany is summarized. Reports on the thin sheet rolling technology were presented. An analysis of German reports shows that much of the German scientific effort is aimed at continuous casting and thin sheet casting.

Development of Slag-Forming Mixtures for Continuous Casting Machines at Belarussian Metal Works

927D0243D Moscow STAL in Russian
No 4, Apr 92 pp 22-24

[Article by A.V. Kuklev, A.M. Toptygin, I.I. Sheynfeld, A.V. Maslennikov, A.V. Olenchenko, Central Scientific Research Institute of Ferrous Metallurgy and Belarussian Metal Works; UDC 621.746.27.047]

[Abstract] Efforts to substitute imports of the "Metallurgika" powder from Germany with domestic products after the commissioning of phase II of the Belarussian Metal Works (BMZ) prompted the development of slag-forming mixtures (ShOS) for steel casting in the ESPTs continuous casting machine (MNLZ-3); under contract to the Fest Alpine company, phase II products include low and medium alloyed steel and manganese steel. The client specified that Scorialit C163-79/H, Scorialit C163-79/E, and Scorialit C114-74 powder mixtures or their analogs be used for this purpose. Commercial tests of the Tsentr 1BM, 3BM, 4BM, 5BM, and 7BM powders are conducted at the BMZ. The volume of gas liberated from the metal, the amount of fluorides released during the mixture melting and slag interaction with water vapors in the course of steel casting in a continuous casting machine using the five domestic slag-forming mixtures, and the volume of semifinished rolled stock produced from the blanks cast in the continuous casting machine using the three imported and five domestic slag-forming mixtures are summarized. A comparison shows that neither foreign nor domestic mixtures meet the slag viscosity requirements for the 1,300°C temperature. The study reveals that from the environmental viewpoint, the Tsentr 1BM and Tsentr 7BM mixtures are preferable while the use of the Tsentr 3BM, 4BM, and 7BM slag-forming mixtures ensures a higher quality of continuously cast blank and semifinished rolled stock surfaces. The study confirms the possibility of developing new mixture compositions with improved ecological characteristics from cheap and easily available components and waste products. Tables 2; references 3: 1 Russian, 1 Western.

Melt Refining by Filtering

927D0243C Moscow STAL in Russian
No 4, Apr 92 pp 21-22

[Article by S.A. Suvorov, V.N. Fishchev, N.B. Tebuyev, A.S. Kondratyev, V.N. Popov; UDC 620.192.41]

[Abstract] The use of filtering for fine refining of melts in order to attain a low level of nonmetallic inclusions (NV) and reduce the amount of blow holes in the castings is discussed and it is shown that the so-called cellular foam filters which are characterized by a low mass, a high effective filtering surface area, a low friction loss, acceptable thermal and mechanical properties, and a sufficient capacity are the most promising for realizing the filtration refining process. The outcome of an examination of the filtering capacity of highly porous oxide cellular foam filters in filtering molten steel St3 is presented; the filtering coefficient expressed through the total oxygen concentration in the metal before and after filtering is used as the estimation criterion. A deep filtering mechanism is realized in the foam filters whereby the nonmetallic inclusions are separated from the melt and precipitate on the filter surface within the entire medium volume; the particles are retained under the effect of inertial displacement forces, diffusion, and adhesion, making it possible to retain particles with a size of up to 5-10 μm. The effect of the filter cell diameter and links on the filtering coefficient is plotted and the oxygen content before and after filtering in four samples is statistically summarized using Fisher's and Student's criteria. The findings indicate that the use of cellular

foam filters made from a corundum-zirconium composite makes it possible to lower the oxygen content in steel by 42%. Figures 2; tables 1; references 7: 4 Russian, 3 Western.

Efficiency of Stainless Steel and Nickel-Based Alloy Filtering Method

927D0243B Moscow STAL in Russian
No 4, Apr 92 pp 18-21

[Article by D.A. Soskov, T.A. Topilina, Al.G. Shalimov, A.V. Laktionov, V.P. Stepanov, Central Scientific Research Institute of Ferrous Metallurgy and Elektrostal Metal Works; UDC 620.192.41]

[Abstract] The use of refractory ceramic filters for removing nonmetal inclusions from steel and alloys is discussed and the efficiency of stainless steel and Ni-based alloy filtering in vacuum induction furnaces in specialty electrometallurgy is studied both in a lab and in commercial furnaces. In the former case, the effect of the metal deoxidation, material, and structural features of the filters on the efficiency of complex alloyed stainless steel refining is examined in a 10 kg induction vacuum furnace using bulk filters with fused magnesium oxide, aluminum oxide, and zirconium dioxide; in the latter, studies are conducted in a medium-size vacuum induction furnace (VIP) using screen-type channel filters. The Al and Ce additions are manipulated in the experiment while the concentration of the oxide nonmetallic inclusions and the amount of inclusions in each size group are used as the optimization variables. The factors which determine the optimum filtering conditions for steel Kh16N15M3 are determined by staging a 6-3/IV fractional factorial experiment. The filtering parameters of stainless steel in a 10 kg furnace and the filter matrix characteristics are summarized and the oxide inclusion concentration and distribution in steel before and after filtering and the effect of the filter height on the filtering efficiency and kinetic parameter are plotted. An analysis confirms the possibility of filtering off high alumina oxide inclusions with a size of >8 μm by using screen channel filters in commercial furnaces and of reducing the high alumina inclusion content by 20-70% in lab conditions by using 30-80 mm bulk filters and by deoxidizing stainless steel with 0.25% Al and 0.05% Ce. The oxide inclusion content can be decreased by 50-44% in Ni-based alloys and by 45% in stainless steel in vacuum induction furnaces. Figures 3; tables 2; references 4: 3 Russian, 1 Western.

Steel Filtering During Continuous Casting

927D0243A Moscow STAL in Russian
No 4, Apr 92 pp 16-18

[Article by A.L. Liberman, I.V. Dubrovin, V.A. Korzhavin, V.A. Zubov, T.N. Popova, A.I. Ustinov, Central Scientific Research Institute of Ferrous Metallurgy, ITF Dnepromet, and Oskol Electrometallurgy Works; UDC 620.192.41]

[Abstract] The need for high-quality continuously cast metal, especially in making "pure steel," prompted an investigation into the use of filters for additional removal of nonmetal inclusions by means of coagulation rather than simple precipitation. The use of filters made as a stack of thin ceramic plates positioned parallel to each other with a clearance between them is described. The filters used for ladle refining are self-cleaning while favorable conditions for coagulation are created due to the metal flow turbulization in the slots between the plates as a result of the vertical channels and due to a forced inert gas delivery through the base of the filter. The self-cleaning filter design is optimized by hydraulic simulation of casting from a 150 t pouring ladle into a 22 t intermediate ladle in a four-stream radial continuous casting machine (MNLZ). The design efficiency is estimated by the mean duration of the elementary metal volume stay in the intermediate ladle. The filter quality is assessed by examining the fractures of "blue" samples and measuring the contamination index. The service life of the filtering elements makes it possible to use the new system for large-scale long-term casting. Figures 3; tables 2.

Investigation of Spin Casting of Ceramics. Properties of Castings

927D0221B Moscow OGNEUPORY in Russian
No 3, Mar 92 pp 6-9

[Article by Yu.Ye. Pivinskiy, T.I. Litovskaya, O.N. Samarina, F.S. Kaplan, All-Union Refractories Institute; UDC 666.762.2.032.5:539.217.1]

[Abstract] The discussion of the principal patterns of spin casting of highly concentrated ceramic binding suspensions (VKVS) of fused quartz (see *Ogneupory* No 11, 1991) and its parameters is continued. In so doing, attention is focused on establishing the effect of the performance and rheological parameters of fused quartz VKSK on the porosity and strength indicators of casting and the possibility of hardening the castings in the process of nonfired quartz ceramics production. The effect of the circumferential velocity during centrifugal molding on the porosity indicators and bending strength in the dried and hydrothermally hardened state, the dependence of the effective viscosity of fused quartz VKSK on the shear stress at various pH, the effect of the

initial fused quartz VKSK pH on the porosity indicator under slip and spin casting, the range of porosity indices and bending strength of dried and hydrothermally hardened castings, the dependence of compressive strength and bending strength of dried castings produced by slip and spin casting on the pH of the original fused quartz VKSK, and the effect of the pH of the original fused quartz VKSK on the bending and compressive strength of spin casting in the dried and hardened states and after heat treatment are plotted. The porosity patterns of pilot ceramics castings are examined. The study reveals a significant effect of the circumferential velocity on the porosity indicators and shows that quartz ceramics whose properties can be improved by hydrothermy treatment or hardening in an alkali solution can be produced by a nonfiring method. The possibility of using the spin casting method for producing casting system refractories with a granular filler (e.g., ceramic concrete) by spin casting is established. Figures 9; references 10: 9 Russian, 1 Western.

New Heat Treatment Technology for Truck Spring Leaf

927D0210D Moscow METALLOVEDENIYE I TERMICHESKAYA OBRABOTKA METALLOV in Russian No 2, Feb 92 pp 11-14

[Article by K.Z. Shepelyakovskiy, R.R. Ismailov, A.N. Litvin, N.I. Vishnevetskiy, V.I. Tabaka, V.A. Rusin, Tekhmash Scientific Production Association and Sinelnikovo Spring Works; UDC 621.785.545:621.771.23/24]

[Abstract] The characteristic features of induction through-superficial hardening (OPZ) in general and its use for truck spring blades in particular are discussed. Instead of the through heat treatment aimed at attaining a moderate strength of 1,500 N/mm^2, superficial hardening for a high-strength state with simultaneous core hardening is used; as a result, favorable residual compressive stresses are retained in the surface layer, making it possible to improve the spring performance. The hardness distribution in a 45S steel spring cross section after through-superficial hardening, the static bending curve of steel 60S2KhG and steel 45S springs, and the fatigue curves of spring leaves from steel 60S2KhG are plotted. The new technology makes it possible in a single pass to produce a high-strength hardened layer with an ultimate strength of 2,500 N/mm^2 and a hardened core with a 1,200 N/mm^2 strength which, together with the residual compressive stress in the surface layers makes it possible to improve the spring performance and decrease the spring mass by 15-25%, radically automate the heat treatment process and improve the working conditions, lessen the environmental impact, and eliminate shot-blast cold working. Figures 6; references 3.

Spring Leaf Hardening Using Induction Heating

927D0210E Moscow METALLOVEDENIYE I TERMICHESKAYA OBRABOTKA METALLOV in Russian No 2, Feb 92 pp 17-19

[Article by Shuo Bong-Zuwen, Liu Di-Bin, Peoples Republic of China; UDC 621.785.545:621.771.23/24]

[Abstract] The use of induction heat treatment of spring leaves in China is discussed and the design of the production line for spring leaf bending and hardening, an induction heater for spring leaf hardening, and an induction coil used for heating spring leaves for hardening are described. The induction heating technology is characterized by a higher heating rate which makes it possible to attain a fine-grain hardened steel structure without increasing the decarburized layer thickness; improves the working condition and lessens the environmental due to eliminating the use of gas; and ensures very stable heating in accordance with the selected rate and results in a high process maneuverability. The operating experience of production lines for induction hardening of spring leaves demonstrates the reliability of the heating equipment and high automotive spring quality. Figures 4.

Stabilizing Hardened State of Cold-Strained Low-Carbon Steel

927D0210G Moscow METALLOVEDENIYE I TERMICHESKAYA OBRABOTKA METALLOV in Russian No 2, Feb 92 pp 26-30

[Article by Yu.P. Gul, G.I. Perchun, Dnepropetrovsk Metallurgical Institute; UDC 669.14.018.298: 539.388.22]

[Abstract] The use of cold straining, particularly cold working, for structural hardening of low-carbon steel and the relationship between the thermal stability of the material and its hardenability are discussed and the lack of published data on stabilizing the hardened state of highly strained metals and alloys and noted. Unsuccessful attempts of using cold straining as the final stage operation in making mass-produced carbon steel items prompted an investigation of the possibility of increasing the thermal stability of highly strained (80%) drawn plain steel in the hardened state by carrying out special relaxing strain treatment. The behavior of the mechanical and physical properties of cold-strained wire under cyclical deformation is plotted and the thermal stability of the highly strained steel in the hardened state after various types of treatment is compared. An analysis of these methods demonstrates that cyclical deformation by means of alternating bending leads to a substantial thermal stabilization whereby the resulting effect is due to a decrease in the integral energy and volume gradient of this energy under cyclical deformation which slows down both the primary and cumulative recrystallization processes. Without subsequent heating, cyclical deformation does not cause noticeable microstructural changes while after heating, the stabilized steel maintains an elevated dislocation density and a reduced ferrite grain size. Figures 3; tables 1; references 3.

Effect of Doping and Heat Treatment on Structure and Properties of Fe-Ni-Be Invar Alloys

927D0210H Moscow METALLOVEDENIYE I TERMICHESKAYA OBRABOTKA METALLOV in Russian No 2, Feb 92 pp 33-36

[Article by Ye.L. Svistunova, A.A. Gulyayev, Central Scientific Research Institute of Ferrous Metallurgy imeni I.P. Bardin; UDC 669.018.472]

[Abstract] The structure and hardness of Fe-Ni-Be alloys with a narrow Be concentration range is discussed and the need for examining the mechanical and physical properties and structure of Invar alloys as a function of the Ni and Be concentration in order to facilitate high-strength alloy development is noted. To this end, 10 kg Invar ingots with various Ni and Be concentrations smelted in a lab and 300 kg ingots of the 40NL alloy containing 40% Ni and 0.75% Be commercially produced at the Sibelektrostal Plant in Krasnoyarsk are forged into rods with an 8 mm diameter from which test samples are made. The samples are then water hardened at a 1,000-1,250°C temperature for 0.5 h and aged at

450-700°C for 1-16 h. The dilatometry studies are carried out in a Sincu-Rico instrument at a 2°C/min rate; static tensile tests are carried out in an Instron tester at a 3.3 x 10^{-5} m/s rate, hardness is measured in a Vickers tester, the microstructure is examined under a Neophot optical microscope and a Tesla BS-540 electron microscope at a 120 kV accelerating voltage, and the X-ray diffraction study is carried out by an URS-55 instrument using an RKU-114 chamber in Fe*K* radiation. The dependence of the discontinuous decay fraction behavior on the aging temperature, the effect of the Be and Ni concentration on the thermal coefficient of linear expansion (TLKR), the alloy hardness after quenching and aging at various temperatures, and the dependence of the mechanical properties and mean thermal coefficient of linear expansion on the aging duration are plotted. An analysis of the findings reveals that Be-doping of Fe-Ni Invar alloys leads to their age hardening after quenching and aging while low values of the thermal coefficient of linear expansion is maintained. An increase in the Be concentration in the 36N alloy increases is TKLR both in the hardened and aged state while an increase in the Ni content to 38-41% at a fixed Be concentration lowers the TKLR of aged alloys and brings it closer to that of the 36N alloy. The 40NL alloy with 40% Ni and 0.8% Be is suggested for use as a high-strength Invar alloy. Figures 5; tables 2; references 6: 4 Russian, 2 Western.

Effect of Heat Treatment Conditions on Properties of Cast Steel VNL-3

927D0211D Moscow METALLOVEDENIYE I TERMICHESKAYA OBRABOTKA METALLOV in Russian No 3, Mar 92 pp 9-10

[Article by A.G. Bratukhin; UDC 621.785.3:669.15-194.3]

[Abstract] The effect of heat treatment conditions on the properties of transition-class cast steel VNL-3 (containing ≥0.8% C, 13-14% Cr, 4.4-5.5% Ni, 1.5-2.0% Mo, and 1.2-1.75

Cu) used for making large aircraft parts by the precision casting method is investigated. This steel is characterized by a high strength of 1,350 N/mm^2, a good ductility of $\delta \geq 12\%$ and $\psi \geq 30\%$, and a relatively high toughness of 60 J/cm^2 due to complex multiple heat treatment. The study demonstrates that an optimum combination of mechanical properties is attained by double heat treatment: heating to 1,100°C for 1 h with air cooling, tempering at 600°C for 0.5 h with hardening at 970°C, cold treatment at -50°C to -70°C, and tempering at 450°C. This heat treatment procedure is recommended for ensuring high strength rather than high ductility. Otherwise, the following heat treatment condition is suggested: hardening at 970°C, tempering at 450°C, and cold treatment at -50°C to -70°C. It is stressed that steel VNL-3 should be heated in a shielding gas or in a vacuum; in addition, the part surface can be protected by applying the EVT-10 enamel. References 1.

Effect of Heat Pretreatment and Cold Plastic Working on Mechanical Properties of Steel 50RA

927D0211E Moscow METALLOVEDENIYE I TERMICHESKAYA OBRABOTKA METALLOV in Russian No 3, Mar 92 pp 10-12

[Article by A.L. Bakhmatov, Engineering Physics Institute at the Urals Scientific Center of Russia's Academy of Sciences; UDC 621.785.796:620.17:669.14.018.298]

[Abstract] The effect of heat pretreatment of structural steels prior to cold plastic working—regular hardening and hardening from the intergranular temperature range—on the mechanical properties of forged and hydroextruded steel 50RA is investigated. To this end, tubular blanks with a 30 and 10 outside and inside diameter, respectively, and 300 mm length are made from cold drawn and annealed steel sections and subjected to heat treatment under two conditions. The critical temperatures are measured dilatometrically; after the heat treatment and machining, the samples are forged and extruded in a hydraulic press. After the heat treatment, the steel microstructure is examined under a Neophot-2 optical microscope using etching to reveal the "new" ferrite. Then longitudinal samples are cut from the billets for tensile tests pursuant to GOST 1497-84 and impact tests pursuant to GOST 9454-78. The steel toughness in the transverse direction is determined by impact bending tests using special semicircular samples with a U-notch. The strain hardening coefficient is calculated using a formula derived on the basis yield stress before and after plastic strain and the relative straining degree. Analyses of the test results and microstructural studies show that after hardening with high tempering, the steel structure represents temper sorbite with a 285 HB hardness and 18-25% "new" ferrite with a 255 HB hardness. This structure after hot quenching from the upper bound of the intercrystalline temperature range and tempering ensures a higher ductility and toughness at a sufficiently high strength level than tempered sorbite formed after conventional hardening and tempering. This technology is recommended for improving the ductility, toughness, and service properties of steel 50RA parts produced by cold straining. Figures 1; tables 1; references 4: 3 Russian, 1 Western.

Effect of Heat Treatment on Structure of Cobalt Alloys Used for Making Orthopaedic Implants

927D0211K Moscow METALLOVEDENIYE I TERMICHESKAYA OBRABOTKA METALLOV in Russian No 3, Mar 92 pp 38-41

[Article by A. Weronski, B.M. Surowska, Lublin Polytechnic Institute, Poland; UDC 669.25:616-089.843]

[Abstract] The special requirements imposed on the metallic materials used as surgical and orthopedic implants under the effect of alternating loads inside the human body, particularly sufficient static and dynamic strength and wear resistance as well as nonrejection by the organism, are outlined and the need for corrosion

and biological assimilation testing is stressed. The effect of heat treatment on the structure of cobalt alloys used for making biological implant materials is investigated and the chemical composition of the Vitallium, MP35N, 3162 ASTM, Medpol 1, and Medpol 2 cobalt alloys as well as the concentration ranges are summarized. The dependence of the forces picked up by the knee joint of a 70 kg person on the bending angle is analyzed graphically and the anode polarization curves (passivation and repassivation) in a ringer solution at body temperature of alloys after water-hardening at 1,200°C for 1 h and aging is plotted. Microstructural studies and an analysis of the curves show that cobalt alloys are corrosion resistant in human body while plastic strained alloys have the best operating properties. In the single-phase alloys with an FCC (GTsK) lattice under study, the grain size depends on the hardening reheat temperature while aging after hardening does not cause secondary precipitation and does not lower the pitting and intercrystalline corrosion resistance. Figures 5; tables 2; references: 9 Western.

Causes and Characteristics of High-Temperature Failure of Nickel-Based Casting Superalloys

927D0222A Moscow METALLOVEDENIYE I TERMICHESKAYA OBRABOTKA METALLOV in Russian No 4, Apr 92 pp 10-12

[Article by V.M. Vorobyev, Moscow State Engineering University imeni N.E. Bauman; UDC 669.245: 620.172.251.2]

[Abstract] The increased tendency toward failure during casing, welding, and other hot working which greatly lowers the realization efficiency of many industrial technologies involving nickel-based high-temperature alloys used for making parts and units of today's power plants operating at elevated temperatures and stresses necessitates a comprehensive investigation of this type of alloys aimed at determining the mechanism of hot crack development and propagation and ways of preventing these phenomena. To this end, samples from the ZhS6U alloy cut from cast blanks after diffusion annealing are tested; the mechanical properties of the samples are measured at various temperatures in an LTP-3-5 unit. The chemical composition of the alloys is summarized and the temperature dependence of their mechanical properties is plotted. An analysis of the fractograms of the samples which failed at 700-800°C shows that an intergranular viscous failure is dominant within this temperature range; in the samples which failed at normal temperatures, local cold spalling sections are observed against the backdrop of intergranular viscous failure; within 400-500°C—brittle intercrystalline failure areas are observed; within 500-600°C—failure occurs mostly at the grain boundaries; within 600-700°C—sulfide eutectics are fused at the grain boundaries resulting a decrease in the alloy ductility; and within 800-1,000°C—failure is characterized by a number of structural and phase transformations and the alloy's integral ductility decreases sharply due to the structural element boundary fusing. The findings show that the increased tendency of this alloy toward failure is due to the presence of eutectics and the brittle and fusible phase precipitation in the intergranular space and dendrite axes as well as the grain boundary fusing. The importance of taking these factors into account in developing machining and treatment processes is stressed. The author is grateful to N.N. Prokhorov and V.B. Garipov for assistance and advice. Figures 2; references 15.

Effect of Nonferrous Metal Additions on Nickel-Based Casting Alloy Structure and High-Temperature Strength

927D0222B Moscow METALLOVEDENIYE I TERMICHESKAYA OBRABOTKA METALLOV in Russian No 4, Apr 92 pp 12-15

[Article by V.V. Sidorov, A.M. Kulebyakina, Scientific Production Association of the All-Union Institute of Aviation Materials; UDC 620.17:620.18:669.245'26'25' 27'28'4'76]

[Abstract] The negative effect of nonferrous metal impurities on the properties of nickel-based high-temperature alloys prompted a study of the effect of Pb and Bi additions on the structure formation and high-temperature properties of casting nickel alloys with 5% Cr, 9% Bi, 12% W, and 1% Mo doped with C, Ti, and Al and produced by the method of uniaxial or oriented casting. The impurity segregation degree near the grain boundaries depends on the boundary formation mechanism; if the grains are oriented in a certain way, the impurity is displaced into the melt by the growing grains in which case both processes may occur simultaneously. The effect of the Pb impurity on the relative life of the above nickel alloy and a eutectic alloy with various compositions is plotted. The effect of impurities is especially severe under unidirectional solidification of nickel alloys with a eutectic structure. An analysis demonstrates that nickel alloys with 5% Cr, 9% Bi, 12% W, and 1% Mo with a uniaxial structure are more sensitive no nonferrous metal impurities than the alloys cast with an oriented columnar structure due to the structure formation characteristics of these alloys; the effect of impurities is especially negative on the formation of a composite structure during the casting of eutectic alloys. In this case the concentrational overcooling leads to a loss of the planar crystallization front stability and the development of a cellular structure which is characterized by a shorter alloy life. Figures 4; tables 1; references 6: 5 Russian, 1 Western.

Effect of Ytterbium Ion Implantation on Nickel's High-Temperature Strength

927D0222C Moscow METALLOVEDENIYE I TERMICHESKAYA OBRABOTKA METALLOV in Russian No 4, Apr 92 pp 15-17

[Article by Yu.D. Yagodkin, A.A. Dalskiy, O.A. Shadrin, Moscow Aviation Institute; UDC 621.793.184:669.24: 669.018.6]

[Abstract] The positive effect of rare earth elements on the high-temperature oxidation resistance of nickel alloys is discussed and the effect of the Yb ion implantation condition on the physical and chemical state of the Ni surface layer and its high-temperature resistance are studied. To this end, 99.9% pure Ni plate samples made from an ingot by forging and subsequent planing, grinding, and polishing are degreased and irradiated by an Yb ion beam at a 1 x 10^{17}-1 x 10^{19} ion/cm^2 dose, a 30 keV energy, and a current density of 0.05-0.5 mA/cm^2. The Yb distribution in the surface layer and the dependence of the surface layer state variables after Yb implantation and the NiO film thickness after high-temperature strength tests on the irradiation dose are plotted. The findings indicate that Yb ion implantation makes it possible to alter considerably the surface state of nickel samples and, as a consequence, control their high-temperature strength. This strength increases at a $\leq$6 x 10^{17} ion/cm^2 dose and decreases at a $\geq 10^{18}$ ion/cm^2 dose. The conclusion is drawn that the Yb concentration in the surface layer and the surface irregularities developing as a result of the ion beam sputtering are the principal factors which determine the high-temperature strength of nickel alloys. Figures 2; references 8.

Effect of B and Hf on Corrosion Resistance of High-Temperature Nickel Alloys

927D0222D Moscow METALLOVEDENIYE I TERMICHESKAYA OBRABOTKA METALLOV in Russian No 4, Apr 92 pp 17-20

[Article by V.M. Beglov, B.K. Pisarev, G.G. Reznikova, Prometey Central Scientific Research Institute of Composites, St. Petersburg; UDC 669.245'781'297:620.193]

[Abstract] The possibility of increasing the corrosion resistance of nickel superalloys by adding B and Hf in an amount which has no negative impact on the high-temperature strength is discussed due to the fact that the main corrosion mechanism in such alloys is intergranular whereby the boundary zone's Al and Ti are depleted due to their diffusion toward the metal/reagent interface, so the corrosion resistance can thus be increased by doping the alloy with metals with a low solubility in the matrix. An alloy with 15% Cr, 10.0% Co, 5% W, 2% Mo, 3.0% Al, 4.5% Ti, 0.1% C, 0.02% B, 0.05% Zr, and 0,05% Y is smelted in an induction furnace and 14x70 mm ingots are made by investment casting; the ingots are subsequently subjected to diffusion annealing and aging. Corrosion tests are carried out using two procedures; the alloying element distribution in the boundary corrosion zone, the frontal corrosion behavior of alloys with a varying carbon and boron concentration, and the corrosion resistance of alloys doped with hafnium and hafnium with boron are plotted. The chemical composition of the corrosion zone is analyzed and plotted. Additional doping of low carbon corrosion resistant nickel alloys with 0.1% B and 1% Hf makes it possible to increase their resistance to high-temperature corrosion and salt attack and raise their high-temperature strength while maintaining high corrosion resistance by increasing the Ti and Al content; this makes the alloys suitable for use in gas turbine engine blades. Figures 5; references 3.

Development of Maraging Steel Compositions for Liquid State Quenching

927D0222E Moscow METALLOVEDENIYE I TERMICHESKAYA OBRABOTKA METALLOV in Russian No 4, Apr 92 pp 22-25

[Article by T.A. Chernyshova, T.V. Lyulkina, L.M. Tribunskiy, Metallurgy Institute imeni A.A. Baykov and Ulyanovsk Polytechnic Institute; UDC 621.785.6:621.745.56: 669.15-194.55]

[Abstract] The use of rapid quenching for widening the range of maraging steel (MSS) properties and the effect of alloying elements on the structure and properties of maraging steels produced by rapid melt quenching as well as the alloying element ratios which facilitate the maximum hardening of maraging steels during aging are discussed. An attempt is made to develop maraging steels specially intended for subsequent rapid quenching and demonstrate the possibility of improving their service properties by adjusting the composition allowing for the quenching conditions. The MSS microhardness is used as the optimization variable while the alloying element (Co, Ti, Al, and Si) content is used as the manipulated variables. The dependence of the rapidly quenched maraging steel microhardness after aging on the Al and Ti concentration, the microhardness increment of maraging steels containing 11-12% Ni after aging as a function of Ti and Al additions, and the dependence of the microhardness of model alloys on the Co, Ti, Al, and Si concentration are plotted. The tests reveal that the pilot MSS have an ultimate rupture strength of 3,500 to 3,500 N/mm^2 while maintaining the viscous failure mechanism; electric resistance measurements show that aging is accelerated at the early stages and is retarded at the concluding stages. The use of rapid quenching also makes it possible to facilitate an intensive precipitation of disperse phased during aging. Figures 4; tables 2; references 3.

Structure and Mechanical Properties of Microcrystalline Ni-Fe-Zr System Alloys

927D0222F Moscow METALLOVEDENIYE I TERMICHESKAYA OBRABOTKA METALLOV in Russian No 4, Apr 92 pp 25-28

[Article by O.M. Zhigalina, V.V. Sosnin, A.M. Glezer, Central Scientific Research Institute of Ferrous Metallurgy imeni I.P. Bardin; UDC 620.172.2:620.18: 669.245'1'296]

[Abstract] The high mechanical properties and magnetic characteristics (at high frequencies 0.5-1 MHz) of the Ni-Fe-Nb(Mo) microcrystalline alloys produced by melt quenching, compared to the alloys smelted by conventional technologies, which are due to the solid solution hardening, grain refinement, formation of a specific microstructure, and disperse phase precipitation, are discussed and the effect of Zr-doping on the structure, phase composition, and mechanical properties of Ni-Fe-Zr alloy tapes in which the Ni concentration is manipulated within 76.5-85% and the Zr concentration—within 0.3-8.5% is investigated. To this end, 60-80 μm thick tapes are made by spin casting in an atmosphere of argon using a Rotor-3M unit. The dependence of the mean grain size in rapidly quenched Ni+15% Fe alloys on the added Zr content, the effect of the mean grain size on the annealing temperature and the dependence of ultimate rupture strength and microhardness of rapidly quenched Ni-Fe-Zr alloys on the annealing temperature and Zr concentration are plotted. The alloy properties are measured using transmission electron microscopy and X-ray diffraction analysis. The results reveal that alloys with less than 0.5% Zr crystallize from the melt by the cellular mechanism and by the dendritic mechanisms at a 3-8.5% Zr content. The grain size does not increase during the annealing in alloys with $\leq$0.5% Zr at temperatures under 900°C. The Ni-Fe microcrystalline alloys are hardened by additions of zirconium due to the grain refinement and the development of Ni_5Zr particles while the microhardness reaches 1,250 N after annealing at 600°C. Figures 6; tables 1; references 7: 5 Russian, 2 Western.

Properties of Ti- and Al-Doped Co-Fe-V-Ni Alloys

927D0222G Moscow METALLOVEDENIYE I TERMICHESKAYA OBRABOTKA METALLOV in Russian No 4, Apr 92 pp 29-32

[Article by L.A. Matyushenko, B.N. Mokhov, Ye.Z. Vintaykin, N.A. Polyakova, O.V. Basargin, Central Scientific Research Institute of Ferrous Metallurgy imeni I.P. Bardin; UDC 669.225:620.17]

[Abstract] The use Co-Fe-V-Ni alloys with a given combination of elastic and thermal properties as the material for elastic pressure gauge sensors prompted an investigation of the effect of age hardening on the properties of Co-Fe-V-Ni alloys using aluminum and titanium as the elements which trigger age hardening. The alloying element concentration in eight test samples and the heat treatment and forging conditions are listed. The alloys are smelted in an induction furnace, then 8.0 mm dia. rods are forged from the ingots and the blanks are hardened at 1,000°C at 1 h. The mechanical tests and hardness measurements are performed using standard procedures and the modulus of elasticity is determined dynamically using an Elastomat unit. The temperature coefficient of linear expansion (TKLR) is assessed by a quartz dilatometer using a relative method. The magnetic properties are measured in a dynamic susceptibility unit at a 3 kHz frequency within a -200 to +730°C range while phase transformations are tracked by a X-ray diffraction analysis, electron microscopy, and neutron diffraction analysis. The effect of the tempering temperature on the HV hardness of alloys doped with Ti and Al in the forged and hardened state, the dependence of the neutron current intensity on the scattering angle, the temperature dependence of the Young modulus after various types of treatment, and the temperature dependence of the modulus of elasticity after hardening and tempering are plotted. A comparative analysis shows that an alloy with 50.2% Co, 5.7% V, and 8.6% Ni has the optimum properties after hardening and tempering and is characterized by the lowest temperature coefficient of the elasticity modulus as well as the highest Curie temperature and a low temperature coefficient of thermal expansion. This alloy is recommended for use as the material for flexible pressure gauge sensor. Figures 6; tables 4; references 4.

String Wire With High Acoustic Properties

927D0222H Moscow METALLOVEDENIYE I TERMICHESKAYA OBRABOTKA METALLOV in Russian No 4, Apr 92 pp 41-43

[Article by V.R. Baraz, N.A. Rundkvist, A.V. Belov, Urals Polytechnic Institute and All-Union Metalware Scientific Research Institute; UDC 534.321.9]

[Abstract] Existing notions about the factors affecting the musical string vibration frequency and its tone, i.e, the type of material used, are discussed and it is noted that thus far, the effect of the chemical content, particularly the carbon concentration, on the acoustic properties of strings has not been considered in sufficient detail. Consequently, an attempt is made to establish a correlation between various physical and mechanical characteristics of steel and the acoustic properties of strings and develop more reliable acoustic indicators for objective quantitative assessment of the sound quality. Samples with a 1.05 mm diameter made from carbon steels with 0.51, 0.61, 0.74, 0.79, and 0.92% C produced by patenting an initial blank with a 4.20 mm diameter are subjected to mechanical tests by standard procedures while the residual macrostresses are measured by an X-ray method by the shift in the $(211)_\alpha$ line relative to the standard line in the course of successive electrolytic etching. The dependence of the mechanical, physical, and acoustic properties of a 94% strained wire on the carbon concentration and the residual stress distribution in the strained U9A string

cross section are plotted and the heat treatment conditions are summarized. An analysis confirms the relationship between the extremal type of the mechanical and physical properties of cold strained carbon steel wire on the carbon concentration within a 0.51-0.92% range whereby the properties peak at a close-to-eutectoid carbon concentration; the integral acoustic parameter displays a similar concentration dependence. The study established a correlation between the mechanical and physical properties and the acoustic parameter. It is shown that a low level and uniform distribution of residual macrostresses has a beneficial effect on the sound quality. Figures 2; tables 1; references 9.

Properties of Porous Materials From Copper and Ni-Cr Alloy Fibers

927D0222I Moscow METALLOVEDENIYE I TERMICHESKAYA OBRABOTKA METALLOV in Russian No 4, Apr 92 pp 46-48

[Article by L.I. Kartashova, V.I. Salo, Lugansk Mechanical Engineering Institute; UDC 621.763:663.3:669.245'26]

[Abstract] The advantages of porous fiber materials (PVM) made from thin wire over metal powder (PPM) or mesh (PSM) materials and the principal methods of manufacturing porous fiber materials are discussed and the characteristic features of the elastic aftereffect during the compaction of sinusoidal copper and Ni-Cr alloy fibers with a 50 μm diameter as well as the mechanical and hydraulic properties of the resulting materials with a 0.4-0.8 porosity are investigated using round and flat samples. The dependence of the mechanical properties of porous fiber materials on the fiber porosity and configuration, the dependence of the hydraulic drag coefficient on the sample porosity and thickness, and the dependence of the pore size on the material porosity are plotted. The sinusoidal fiber shape ensures a more uniform fiber distribution in the material which can be used in filtering elements operating within a broad temperature range both in neutral and corrosive media. Tests of such filters have been conducted under industrial conditions. Figures 3; tables 1; references 5.

Effect of Alloying on Medium Carbon Steel Properties After Rolling

927D0223A Moscow METALLOVEDENIYE I TERMICHESKAYA OBRABOTKA METALLOV in Russian No 5, May 92 pp 6-7

[Article by G.I. Sokolova, L.M. Panfilova, M.I. Goldshteyn, V.G. Cheremnykh, Urals Scientific Research Institute of Ferrous Metallurgy and Urals Polytechnic Institute; UDC 669.14.018.298:621.771.016]

[Abstract] The structure, strength, ductility, toughness, reduction, and other properties of medium carbon steel 30Kh3, 30Kh3F, 30KhsAF, 30Kh3FB, 30Kh3NMAF, and 30Kh3NMAFB with 3% Cr doped by carbide- and nitride-forming elements, cast into 200 kg ingots, rolled into 30x30 mm blanks and heat treated, are examined after controlled rolling under varying conditions. The rolling and heat treatment conditions are summarized. The carbonitride phase precipitation under straining is studied and the carbide and nitride phase composition is examined after water quenching using X-ray diffraction analysis by a DRON-3.0 diffractometer in Cu*K* radiation. The findings indicate that disperse complex (VNb)N nitride particles precipitate under straining while the grain becomes more refined. Medium carbon steel alloying with Cr and V, Nb, N, Ni, and Mo combined with controlled rolling makes it possible to increase the steel strength by 70% while maintaining the necessary ductility due to the formation of a fine grain austenitic structure during straining and age-hardening by niobium and vanadium carbides. In some cases, the use of controlled rolling makes it possible to eliminate the hardening and normalizing operations when making parts from steels containing Nb, V, and N. Figures 4; tables 3; references 4.

Increasing Toughness of Pipe Main Fastening Parts

927D0223B Moscow METALLOVEDENIYE I TERMICHESKAYA OBRABOTKA METALLOV in Russian No 5, May 92 pp 8-10

[Article by V.I. Bolshakov, L.N. Deyneko, A.G. Shcherbakov, R.G. Gubaydulin, A.K. Tingayev, Dnepropetrovsk Civil Engineering Institute, Dnepropetrovsk Metallurgy Institute, Trubodetal Production Association, and Chelyabinsk State Polytechnic University; UDC 621.774:620.178.72]

[Abstract] Frequent pipeline failures due to the insufficient metal viscosity and corrosion resistance and the increasingly stringent requirements imposed on the mechanical properties of pipes and fastening parts during the construction of main pipelines operating under severe climatic conditions and under elevated pressures prompted an investigation into ways of increasing the toughness of joining parts. The toughness and cold shortness threshold of 30 and 14 mm thick sheets of steel 09G2S and 15KhSND used for making fasteners with a diameter of up to 1,420 mm is measured after thermal hardening by two methods—the base condition currently used in the industry and the condition proposed by the authors. Both heat treatment conditions are summarized and compared. Toughness is separated into components by the maximum load value and the crack development and propagation work is measured. An analysis shows that the proposed hardening method makes it possible to ensure stable and high toughness levels under the most complex operating conditions thus greatly reducing the failure probability. The new technology has passed pilot and commercial tests. Today, a section for thermal hardening of pipe joints is being set up at the Trubodetal Production Association for making transmission pipes for a broad range of light hydrocarbon fractions. Tables 2; references 7.

Structural Transformations Under Hot Deformation in Stainless Steel

927D0223C Moscow METALLOVEDENIYE I TERMICHESKAYA OBRABOTKA METALLOV in Russian No 5, May 92 pp 19-23

[Article by A.N. Belyakov, R.O. Kaybyshev, Institute of Metal Superplasticity Problems, Ufa; UDC 669.14.018.8: 621.77.016.2]

[Abstract] The importance of attaining a superfine-grain structure in steel in order to improve its mechanical properties and the shortcomings of static recrystallization which makes it impossible to produce a grain with less that 10 μm in size prompted an investigation of the structural changes in ferritic, austenitic, and ferrite-austenite steel under hot deformation in the absence of polymorphous transformations. The chemical and phase content of steels 15Kh25T, 12Kh18N9, and EK-72 and the grain boundary distribution in the disorientation angles are plotted. Samples cut from steel annealed at 1,200-1,250°C for 4 h are deformed by upsetting in an Instron unit within a 900-1,100°C range at a 10^{-2}-10^{-3} s^{-1} straining rate, then water quenched. A metallographic analysis is carried out under a Neophot-2 optical microscope and Epiquant structural analyzer while the fine structure is examined under a Tesla BS-540 electron microscope. The findings show that hot deformation of corrosion-resistant steels of these classes leads to dynamic recrystallization: various types of substructures are formed depending on the straining conditions and crystal lattice type at the initial stages of plastic flow and, consequently, different mechanisms of dynamic recrystallization are realized. The substructure formation in the initial grain and the gradual transformation of the low angle grain boundaries into high grain boundaries are the principal mechanisms of the recrystallized grain formation. The role of collective processes in the structure formation is noted. Figures 3; tables 2; references 13: 6 Russian, 7 Western.

Effect of Second Phase Amount on Texture and Superplasticity Indicator Anisotropy of Microduplex Steel 03Kh26N6T Sheets

927D0223D Moscow METALLOVEDENIYE I TERMICHESKAYA OBRABOTKA METALLOV in Russian No 5, May 92 pp 24-28

[Article by G.Yu. Glebova, A.A. Alalykin, V.K. Portnoy, Moscow Steel and Alloy Institute; UDC 669.15'24'26'-194:620.18.4]

[Abstract] The anisotropy of mechanical properties of sheet steel and its relation to the crystallographic texture developing under rolling and heat treatment and the effect of texture on the superplasticity (SP) indicators of sheet steel are discussed and the effect of the amount of austenite before cold rolling on the texture formation and anisotropy of superplasticity indices of sheets of 03Kh26N6T steel produced by three separate smelting are examined; the elemental composition of the three batches is summarized. The inverse pole figures (OPF) of steel 03Kh26N6T after cold and hot rolling and after heating for superplastic deformation (SPD) are plotted. An analysis shows that the presence of up to 25% austenite in steel prior to cold rolling does not affect the texture formation process; rather, the differences in the rolling texture are due primarily to the amount of hard titanium carbonitride inclusions. The presence of austenite before cold rolling leads to a decrease in the metallographic texture after the superplastic deformation heating. The greater the austenite amount, the finer the austenite particle and the more uniaxial its shape. The level of superplasticity characteristics and their anisotropy are largely determined by the axial misalignment of the austenite particles forming during the SPD heating. Figures 6; tables 3; references 18: 11 Russian, 7 Western.

Iron's Plasticity Near Curie Point

927D0223E Moscow METALLOVEDENIYE I TERMICHESKAYA OBRABOTKA METALLOV in Russian No 5, May 92 pp 29-30

[Article by G.A. Maksimova, V.P. Mayboroda, Materials Science Problems Institute, Kiev; UDC 669.12:620.187]

[Abstract] The origin of disperse pitting elements discovered on the iron fracture surface near the Curie point (700-855°C) is debated and the microdeformation process which accompanies twinning resulting from the grain disorientation is divided into two stages: twinning observed at the first stage which is preserved of up to 10 min under exposure and formation of cellular dislocations structures under subsequent exposure to 30-80 min. The dependence of the strength and ductility of 99.9% pure iron containing 0.005% C on exposure to a 720-870°C temperature is examined using standard samples. Tensile tests are carried out in a type 1246 NIKIMP machine in a vacuum. The heat treatment conditions are described. An analysis of the data shows that an increase in exposure to 720°C leads to a considerable decrease in strength and increase in plasticity which is attributed to the fact that the 720°C temperature corresponds to the onset of subcritical superplasticity; an increase in the testing temperature to 820°C leads only to a decrease in strength. The findings indicate that pits of a greater diameter form after a 6 min exposure than after 15 min exposure on the fracture surface. A decrease in the α-Fe ductility with an increase in the testing temperature under a single-phase structural state attests to structural transformations resulting in an abnormal ductility increase within the 720-820°C range. Figures 1; tables 1; references 5.

Case Hardening of Titanium Alloys by Thermic Spontaneous Ignition

927D0224B Moscow METALLOVEDENIYE I TERMICHESKAYA OBRABOTKA METALLOV in Russian No 6, Jun 92)

[Article by Ya.D. Kogan, Ye.P. Kostogorov, N.E. Struve, and A.A. Inyakin, Moscow Institute of Automobile

Roads; Institute of Structural Macrokinetics at Russian Academy of Sciences; UDC 621.785:539:669.295.5]

[Abstract] Case hardening of titanium alloys by combining chemical transport reactions with thermic spontaneous ignition of powder mixtures heat was studied in an experiment with W0Ti pure titanium (tungstenless) and the W20Ti (20 % W) alloy. This thermochemical treatment was performed in an open reactor with an argon (inert gas) blast and with a mixture of Ti, polyboride, Al_2O_3, AlF_3 powders added as impregnating agents. The microstructure of the surface layers was examined under a Neophot-30 optical microscope. Their phase composition was examined in a Dron-3 x-ray diffractometer and in a Jeol "Superprobe-733" x-ray microanalyzer. Their microhardness was measured with a PMT-3 tester under a 1 N load on the indenter. Case hardening by this method can be tentatively regarded as proceeding in four stages. In the first stage the reactant mixture is heated to its ignition temperature. In the second stage there takes place spontaneous ignition, titanium and polyboride powders interact so that the temperature in the reactor rises to the highest level at a rate ranging from 30°/s to 200°/s, and gaseous fluorides (MgF_2, BF_3 are formed. These fluorides, driven by the temperature difference between powder mixture and metal surface, flow to the latter. A layer of precipitate then forms on the surface as a result of exchange reactions and disproportionation. In the third stage there takes place temperature equalization over the reactor volume and active atoms (Mg,B,Al,Ti) begin to diffuse into the substrate. In the fourth stage, isothermal soaking, the diffusion layer coating the surface continues to grow. This treatment of W0Ti pure titanium was found to have produced a case with a 15-20 μm thick TiB layer (microhardness 1100-1300 H) on top of 30-50 μm thick Ti_α(B,Mg) layer (microhardness 300-500 H). This treatment of W20Ti titanium-tungsten alloy was found to have produced a transition layer (microhardness 700-900 H) under a 20-40 μm thick layer (microhardness 900-1100 H) containing not only TiB but also a solid solution of B and Mg in α-Ti along with Al_2Mg_3, $TiAl_3$ and other intermetallic compounds. The results of wear tests performed in a reciprocating friction machine indicate that case hardening titanium and titanium alloys by this method can increase their wear resistance in dry friction by a factor of up to 6 and thus about twice as much as conventional nitriding. Figures 2; references 2.

Structure and Properties of High-Speed Tool Steels Carbonitrided by Ion Implantation in Hydrogen-Free Atmosphere

927D0224A Moscow METALLOVEDENIYE IN TERMICHESKAYA OBRABOTKA METALLOV in Russian No 6, Jun 92 pp 13-15

[Article by G.V. Shcherbedinskiy, L.A. Zhelanova, S,V, Zemskiy, and A.I. Sumakov, Central Scientific Research Institute of Ferrous Metallurgy imeni I.P. Bardin and Kursk Polytechnic Institute; UDC 669.14.018.252.3: 621.793.184]

[Abstract] The effects of carbonitriding high-speed tool steels by ion implantation in a hydrogen-free glow-discharge plasma so as to avoid subsequent hydrogen embrittlement was studied in an experiment with three such steels (R-6Mo5, R-6Mo5V3-MP, R-06Mo5V2-MP). The gaseous medium for this process was produced by thermal decomposition of ferrocyanides under a vacuum of 0.1-1.5 kPa, the thus formed cyanogen then being ionized upon its entry into the interelectrode space. The discharge current in the plasma was varied over the 1-50 mA/cm^2 range and the potential difference between the electrodes was varied from 300 V to 600 V. Such a treatment was found to increase the microhardness of surface layers to 1400 H and to raise the red hardness temperature of these steels by 30-40°C. Specimens carbonitrided by this process at 540-580°C for 30 min and specimens nitrided in an ammonia atmosphere were tested for wear resistance in abrasion by the Skoda-Savan loss-of-mass method and for impact strength. The carbonitrided specimens had a higher wear resistance, in terms of smaller volume of material removed within a given time, and 1.2-1.4 times higher impact strength than the nitrided ones. The phase composition of the steels after carbonitriding was examined in a DRON-3 x-ray diffractometer, an analysis of the data indicating the presence of $(Fe,Cr)_3$ $(Mo,W,V)_3C$ (Me_6C) carbides and (V,Mo)(C,N) carbonitrides with a NaCl crystal structure. Figures 1; tables 4; references 2.

Characteristics of Pre-Recrystallization Processes in Highly Deformed Nickel Foils

927D0224F Moscow METALLOVEDENIYE I TERMICHESKAYA OBRABOTKA METALLOV in Russian No 6, Jun 92 pp 44-45

[Article by A.K. Butylenko, Ya.N. Vovk, V.I. Kolomytsev, and V.V. Nevdacha, Institute of Metal Physics at Ukrainian Academy of Sciences; UDC 620.186.5: 669.24]

[Abstract] An experimental study of nickel foils cold rolled from 3 mm to 5 μm thickness was made concerning the processes taking place during the initial stages of annealing prior to recrystalization. Specimens of NP-1 nickel foils were annealed under a vacuum of about 10 mPa at temperatures ranging from 200°C to 800°C in about 100°C steps, for 1 h at each temperature. The specimens were then examined in a DRON-2 x-ray diffractometer, in an IRIS-3 x-ray spectrometer, and under an EM-200 electron microscope. Their electrical resistance was measured at room temperature. The results indicate that in such foils with a cellular structure recrystallization is preceded by polygonization, recrystallization then only beginning at 350-400°C and complete recrystallization taking place only after heat treatment at about 600°C. The electrical resistivity of these foils was the same after heat treatment at temperatures from 200°C to about 500°C and was about 2 % higher after heat treatment at all higher temperatures. For use as structural elements in thermal transducers, therefore, these foils should be annealed at 350-450°C so as to ensure stabilization of their elasticity and electrical properties. Figures 2; references 8.

Use of Laser Treatment for Conversion of Metastable Austenitic Invar Alloys Into Thermal Bimetals

927D0224D Moscow METALLOVEDENIYE I TERMICHESKAYA OBRABOTKA METALLOV in Russian No 6, Jun 92 pp 21-22

[Article by I.I. Kositsyna, S.V. Kositsyn, and Sagaradze, Institute of Metal Physics; Central Scientific Research Institute of Metallurgy and Materials, Yekaterinburg; UDC 621.9.048.7:669.018.472]

[Abstract] The feasibility converting metastable austenitic invar alloys by laser treatment into thermal bimetals, quasi-composites consisting of two layers with identical chemical and phase compositions but different magnitudes of the coefficient of linear thermal expansion, was studied in an experiment with the Ni32 alloy (67.7 Fe - 32.2 % Ni, 0.01 % C). Specimens of this alloy, 60 mm long bars with 4 mm square cross-section, were quenched from 1100°C in water and then cooled with liquid nitrogen. This treatment produced a material containing 80 % α-martensite. The specimens were subsequently treated on one side only with an LGN-702 "Kardamon" continuous-wave CO_2-laser, its 2.5-3 mm wide beam being made to scan this surface at various speeds from 530 to 1030 mm/min. This treatment austenitized this side 1-3 mm deep, while the other side retained its martensite content. An austenitic structure within the martensitic layer with microsegregation of the Ni content was produced next by heating to 470°C at a rate of 0.2°C/min, Ni-rich ultrafine-disperse austenite particles having precipitated and left a Ni-poor residual martensite. Diffusionless transformation of this residual martensite into austenite was finally achieved by soaking at 600°C for 10 min so as to retain the chemical micrononhomogeneity of the austenite. The coefficient of linear thermal expansion was measured with a Chevenard dilatometer using a normal HVS head, the specimens being heated and cooled at a rate of 8°C/min. By this method were produced monolithic purely austenitic double-layers of this Fe-Ni alloy behaving as thermal bimetals over the -100-(+140)°C temperature with a $6x10^{-6}$/°C and becoming paramagnetic with a $16x10^{-6}$/°C coefficient of linear thermal expansion above the 140°C Curie point. Figures 2; references 3.

Relations Characterizing Breakup of Residual Austenite Under Shock Waves Generated by Laser Pulses

927D0224C Moscow METALLOVEDENIYE I TERMICHESKAYA OBRABOTKA METALLOV in Russian No 6, Jun 92 pp 20-21

[Article by N.G. Varenova, P.Yu. Kikin, A.I. Pchelintsev, and Ye.Ye. Rusin, Institute of Machine Science, Nizhegorod branch; UDC 621.048.7:669.14.018]

[Abstract] An experimental study of carbon steels and alloy steels hardened by laser treatment was made concerning subsequent breakup of residual austenite in their surface layer under shock waves generated during a second laser treatment. Specimens of 45 plain carbon steel, U8 straight-carbon tool steel, and R-6Mo5 high-speed tool steel were hardened by radiation pulses of 25 J energy and 5 ms duration with an overlap factor of 2.0 from a YAG-laser operating in the free mode. They were then treated with 5-25 radiation pulses of up to 1.5 J energy and 20-30 ns duration from a ruby laser, the amplitude of shock waves generated by these pulses being varied over the 0.1-1 GPa range by regulating the energy of these laser pulses. A phase analysis in a DRON-3 x-ray diffractometer with filtered CoK_α radiation revealed a linear dependence of the fraction of residual austenite in the surface layer on both the energy of these laser pulses and on their number. As the shock pressure was raised from 0.1 GPa to 1 GPa, the percentage of austenite in the surface layer of 45 steel decreased at a constant slow rate throughout the entire pressure range, while in the surface layer of the two other steels it decreased first at a constant slower rate and then at a constant faster rate after the shock pressure due to laser pulses had exceeded a threshold level: 0.35 GPa for U8 steel and 0.53 GPa for R-6Mo5 steel. As the number of pulses was increased from 5 to 25, the percentage of austenite in the surface layer of all three steels decreased at a constant rate: fastest in R-6Mo5 steel and slowest in 45 steel. Figures 2. references 3.

Improving Properties of Low-Alloy Cr-Mo Steel by Out-Of-Furnace Treatment

927D0224E Moscow METALLOVEDENIYE I TERMICHESKAYA OBRABOTKA METALLOV in Russian No 6, Jun 92 pp 37-40

[Article by M. Tripkovich, Metallurgical Combine, Niksic (Yugoslavia), and A.N. Smirnov, Donetsk Polytechnic Institute; UDC 669.046.55:669.14.018.298]

[Abstract] An experimental study of low-alloy Cr-Mo steel was made concerning its comprehensive out-of-furnace treatment and the effect of such a treatment on its mechanical properties. Ingots of this steel were produced in a 60-ton electric-arc furnace, 90 % of the oxidizing slag having been removed upon conclusion of the oxidation preriod and $CaO-CaF_2$ reducing slag having then been added after preliminary deoxidation with ferromanganese and ferrosilicon. The steel with this reducing slag was poured from the crucible into a 60-ton ladle at a temperature of 1605°C. A part of the steel was poured into one mold and there split into four 2.8-ton ingots. The remainder underwent a comprehensive treatment in an ASEA-SKF facility: 1) removal of residual furnace slag with a mechanical tool during electromagnetic stirring (10 min); 2) desulfurization and removal of nonmetallic oxides with synthetic $CaO-CF_2-Al_2O_3-SiO_2$ in a heating chamber (52 min), 3) pouring into three molds at a temperature of 1580°C. This process was found to have somewhat increased the C,Si,P content

but appreciably decreased the S,O content with the oxygen, moreover, having become more uniformly distributed. It increased the plasticity and the ductility of the steel after hot rolling at temperatures ranging from 900°C to 1300°C and after hot tempering at temperatures ranging from 350°C to 600°C. It did not significantly increase the torsional strength but appreciably lengthened the life of the steel specimens under a cyclic load. The torsional strength of both refined and unrefined steel decreased steadily with higher rolling temperature. The number of load cycles till fracture increased to a maximum for both refined and unrefined steel rolled at 1280°C, remaining consistently larger for refined steel and decreasing for both steels rolled at still higher temperatures. According to the results of impact tests, hot tempering increased the toughness of refined steel more than the toughness of unrefined steel. Their difference in toughness was, moreover, found to be larger than their difference in ductility under a static load. For use of this steel, therefore, the importance of purity evidently increases when the loading rate is increased. Figures 3; tables 3; references 4.

Features of Laser Surfacing With Different Methods of Feeding the Powder

927D0232B Moscow SVAROCHNOYE PROIZVODSTVO in Russian No 3, Mar 92 pp 4-6

[Article by V.Ye. Arkhipov, A.A. Ablayev, I.V. Geletin, L.T. Krasnov, Remdetal All-Union Scientific Research Institute; UDC 621.791.927.2:621.373.826]

[Abstract] The authors of this study examined the characteristic features of laser surfaces when different methods of feeding the powder were used. During the course of the studies, the researchers examined Ni-Cr-B self-fluxing powders with slightly different chemical compositions. Seven powders were compared: PG-12N-01, NChP-2, PG-10N-04, PG-12N-02, PR-N73Kh16S3P3, PR-N77Kh15S3P2, and PG-10N-01. Special attention was paid to the effect that the surfacing materials' chemical composition and the surfacing process used had on the tendency of the resultant coatings to crack. The tests performed established that surfacing to cylindrical specimens in a spiral motion resulted in the development of axial stresses reaching 190 MPa and tangential stresses reaching 120 MPa. When coatings were surfaced after preliminary application of the surfacing material (powder) in slurry coats, the structure of the slurry coat resulted in intensive absorption of the laser energy by the binding component (adhesive) with low heat removal. This technique resulted in the formation of a single metallurgical bath with removal of the oxide (slag) compounds on the surface. This in turn generally resulted in the formation of a structure with a uniform chemical composition and phase component with a minimum amount of disperse carbide or boride compounds, which in turn enabled the resultant coatings to withstand the significant stresses of the surfacing process without cracking. The technique of surfacing by feeding the powder through a batcher-feeder, on the other hand, generally resulted in coatings with numerous surface cracks. The said surface cracks were observed to form at power densities of 1.5 to 2 x 10^8 W/m^2. When the power density was increased to 2.5-3 x 10^8 W/m^2, the cracks became deeper, extending beyond the surface layers into the depths of the test specimens. Next, the researchers compared the relative effectiveness of three surfacing regimens: the use of a substrate without fusion, the use of a substrate and fusion, and the use of a substrate with a low tendency toward crack formation followed by the application of the basic surface material. Tests comparing the three regimens demonstrated that the composition of the material used as a substrate is extremely important. Using a substrate with a chemical composition analogous to the coating or an iron-based material (e.g., PG0S27) not only did not result in any improvement in surfacing quality, but actually resulted in a worse surface layer in certain cases. Powders that made it possible to increase the dimensions of the transition zone with a smooth increase in the amount of iron (the first regimen) or powders resulting in a reduced tendency toward crack formation (the third regimen) made it possible to virtually eliminate crack formation in the applied coating. Tests comparing the different powders established that PG-10N-04 powder results in a coating that has a hardness [HRC] of 25 to 27 and that is, for all practical purposes, not prone to crack formation. The powders NPCh-2 and PR-N77Kh15S3P2 result in a coating with an HRC of 30 to 35 with a reduced tendency toward crack formation. The powders PG12N-02 and PR-N77-Kh15S3P2 resulted in coatings with HRC values of 40 or greater. Figure 1, table 1; references 3 (Russian).

Stresses in Female Joints of Aluminum Oxide-Based Ceramic With Metals Welded by an Electron Beam

927D0232D Moscow SVAROCHNOYE PROIZVODSTVO in Russian No 3, Mar 92 pp 8-10

[Article by M.P. Maloletov, I.I. Metelkin, V.P. Skalskaya, V.A. Kazakov, O.N. Kudryashov, and Ye.M. Borisov; UDC 621.791.72.052:539.4.014:669.3/.7]

[Abstract] The authors of this study examined the stresses that develop in female joints of aluminum oxide-based ceramics with metals and alloys that are produced by electron beam welding. Specifically, they developed a technique for calculating the stresses developing in electron beam-welded female joints of aluminum oxide-based ceramics with aluminum alloys, titanium, and 12Cr18Ni10Ti corrosion-resistant steel. The analysis presented was performed without any consideration of the transition layer formed during the welding process. A series of mathematical expressions have been presented that are based in part on the theory of thin shells. The expressions have been used to perform a series of calculations that are said to be usable as specific recommendations regarding the design of female joints to be produced by the technique of electron beam welding. Specific recommendations are given regarding joint length, wall thickness, and length of the protruding end. Figures 2; references 7 (Russian).

Activation of the Process of Flame Dusting by Air Jets

927D0232C Moscow SVAROCHNOYE PROIZVODSTVO in Russian No 3, Mar 92 pp 7-8

[Article by M.A. Belotserkovskiy and V.T. Sakhnovich, Institute of Problems of Machine Reliability and Durability, BSSR Academy of Sciences; UDC 621.793.71]

[Abstract] The authors of this study examined the effectiveness of using air jets to activate the process of flame-dusting powder materials as a method of producing wear-resistant protective coatings. Two pieces of equipment, the UPTR-1-85 and UPTR-1-90, developed at the Institute of Problems of Machine Reliability and Durability, were used to test the air jet activation technique. The activator was designed so that the attack angle of the air jet in relation to the flame jet axis could be varied from 0 to 70°. The nozzles were configured so

that they could be moved along the longitudinal axis, and they were equipped with removable nozzles with different flow areas. Nickel-clad aluminum oxide and chromium carbide powders with particle sizes of 40-50, 50-63, and 63-100 μm were tested. Oxygen, acetylene, and compressed air were used as working gases. The tests demonstrated that activation modes resulting in the highest powder particle flight speeds were best (the highest particle flight speeds were achieved at an attack angle of about 30°). As the particle size of the powder increased, the maximum particle flight speed decreased, and the distance to the point of maximum acceleration increased. For these reasons, the use of an air activator was deemed feasible for applying coatings of powders of refractory metals, oxides, and carbides with a particle size of less than 50 μm. The method of air jet activation was not feasible with large-sized particles of powder because the larger particles do not have time to heat to the temperature usually reached in conventional spraying at optimal distances. The air jet activation method is also not feasible for use in applying powders of lower-melting materials (such as bronzes or nickel-based self-fluxing alloys with a particle size of about 100 mm) because of the reduced powder utilization factors associated with the use of lower-melting materials. The activation scheme by crossed jets, which is used in the UPTR units (and by the firm Metco), was shown to be preferable to activation by parallel jets (the scheme used in the activators produced by the firm Castolin). Figures 2; references 6: 4 Russian, 2 Western.

The Experience of Introducing Friction Welding in the Manufacture of Equipment for the Oil and Gas Industry

927D0232A Moscow SVAROCHNOYE PROIZVODSTVO in Russian No 3, Mar 92 pp 2-4

[Article by R.D. Dzhabarov, N.S. Fataliyev, Yu.A. Tkachev, V.I. Timofeyev, and S.K. Rakhimov, Azerbaijan Petroleum Machine Building Scientific Research Institute; UDC 621.791.14-03:622.276-012]

[Abstract] Researchers at the Azerbaijan Petroleum Machine Building Scientific Research Institute conducted a series of studies to determine the effectiveness of incorporating the technique of friction welding into the process of manufacturing equipment for use in the oil and gas industry. They proposed a new friction welding technique entailing induced welding compound formation and also developed and manufactured a special welding unit to perform the new method. This new equipment has been patented in the United States, England, Japan, Canada, Italy, and France. Comprehensive research studies of the strength of pipe connections produced by the new technique that was conducted jointly by the Azerbaijan Petroleum Machine Building Scientific Research Institute and Central Scientific Research Institute of Machine Building Technology confirmed that the new friction welding technique results in better pipe joints than butt resistance does. The superiority of friction welding was confirmed in tests involving specimens of pipe made of steels from four different strength classes. The friction welding research studies conducted at the Azerbaijan Petroleum Machine Building Scientific Research Institute confirmed that friction welding is highly effective in the manufacture of geological-prospecting and drilling pipes (with welded seams), gate valves for high-pressure gusher fittings, and welded pump rods (with welded nipples and heads). Special updated welding machines were developed specifically for these products and were demonstrated to be economically feasible for production on a series-production basis. Additional studies performed at the Azerbaijan Petroleum Machine Building Scientific Research Institute established that friction welding is promising as a method of repairing pipe and continuous and pump rods, as well as for laying commercial pipelines both on land and underwater. The Azerbaijan Petroleum Machine Building Scientific Research Institute is currently working jointly with the firm Corod (Canada) to manufacture a prototype machine for friction-welding continuous rods with an oval cross section. The welding unit developed at the Azerbaijan Petroleum Machine Building Scientific Research Institute to friction-weld pipes has been installed at the Lanchou Machine Building Plant in the People's Republic of China. Figures 2, tables 2; references 7 (Russian).

An Investigation of the Process of the Gas-Laser Cutting of Metals

927D0232E Moscow SVAROCHNOYE PROIZVODSTVO in Russian No 3, Mar 92 pp 31-32

[Article by S.G. Gornyy, I.R. Yemelchenkov, D.V. Kuzmichev, I.V. Matyushin, A.P. Chekmezov, Yu.T. Sukhov; UDC 621.791.947.72:621.375.826]

[Abstract] The main problems arising during both theoretical and experimental studies of the process of gas-laser cutting lie in the need to simultaneously consider the results of the effect of the laser radiation on the metal, the dynamic effect of the jet of cutting gas, and the additional heat released in the vicinity of the cut due to thermochemical reactions. In an effort to overcome these problems, the authors of the study reported herein performed a theoretical analysis of the process of the gas-laser cutting of metals that is based on a scheme incorporating experimentally obtained information regarding the two characteristic zones, i.e., an oxidation and a fusion zone, that form when metal is broken down during the process of gas-laser cutting. The scheme presented, which is based on the experimental finding that the metal breakdown products contain $\geq$40% unoxidized metal, makes it possible to estimate the heat content of the fusion in the cut zone with consideration for superheating to some temperature designated T_*. According to the analysis presented, superheating of the material in the cut zone is determined not only by the intensity of the laser

radiation but also by the thermochemical and dynamic effects of the gas jet. The calculations of the dependence of thickness of the cut material on cutting speed performed on the basis of the expressions derived during the course of the analysis presented are shown to virtually coincide with the results of experiments performed on EFA-53 and LTN-102V laser cutting units. The expressions presented were thus recommended for use in estimating the basic characteristics of the process of gas-laser cutting of metals in both active and neutral gases. Figures 3; references 3 : 2 Russian, 1 Western.

Investigation of Weathering Crust Olivinites in Kovdor Massif as Raw Material for Refractory Production

927D0221F Moscow OGNEUPORY in Russian No 3, Mar 92 pp 22-24

[Article by M.Ye. Kononov, A.P. Protsyuk, N.G. Nikitenko, T.N. Levchenko, G.V. Cheremnykh, IKhTrems at Russia's Academy of Sciences and Kovdorslyuda Mica Ore Dressing Works; UDC 549.753.314:666.762.34]

[Abstract] The use of mantle olivinites from the Kovdor massif for making forsterite refractories makes it possible to forego crushing the lump material and firing it at 1,300-1,350°C; moreover, olivinite can be used as a charge component in making fused phosphate and magnesium fertilizers from various phosphate feedstocks. These features prompted an investigation of the mineral composition of the mantle olivinites from the Sevenaya Mountain; to this end, microscopic, X-ray phase, and differential thermal analysis and infrared spectroscopy methods are used to identify the minerals and determine the composition of 27 samples from various areas. The chemical composition of the mantle olivinites and the mineral composition of the ore are summarized and a thermodynamic study of the likely mechanisms of calcium and magnesium incorporation into olivine's crystal lattice is carried out. Olivinite with magnesite additions has a refractoriness of 1,750°C. The study shows that the use of olivinites is the principal trend in developing a raw material base for the forsterite refractory production. The need to develop specifications and procedures for using Kovdor massif mantle olivinites is stressed. Tables 2; references 16: 15 Russian, 1 Western.

Characteristics of Troshkovskiy Clays as Refractory Production Material

927D0221G Moscow OGNEUPORY in Russian No 3, Mar 92 pp 24-28

[Article by A.P. Shelest (deceased); UDC 666.762:622.361.1.001.4]

[Abstract] Troshkovskiy deposit clays are classified by texture and the chemical composition of four representative types of clay are summarized. The thermograms of refractory kaolin clay and loose kaolinite-montmorillonite clay and the dependence of the water absorption on the kaolinite:montmorillonite ratio are plotted. The mineral composition and chemical content of Eastern Siberian clays are determined by a range of microscopy, electron microscopy, and thermal studies and the properties of roasted clays, i.e., the roasting temperature, Al_2O_3 concentration, refractoriness, porosity, and compressive strength as a function of the binder type and roasting temperature are investigated. According to their mineral composition, clays are divided into three categories. An analysis of the findings indicates that the peculiar behavior of Troshkovskiy clays during dispersion, drying, and roasting is due to their chemical and mineral composition. Figures 6; tables 2; references 10.

Paleostructural Characteristics of Tonezh Brown Coal Deposit in Pripyat Basin

927D0230A Moscow RAZVEDKA I OKHRANA NEDR in Russian No 3, Mar 92 pp 7-8

[Article by P.V. Vinichenko, Kirovgeologiya Association; UDC 553.96(477)]

[Abstract] The Paleostructural characteristics of the Neogene-age brown coal deposit in the southwestern corner of the Pripyat basin located in the vicinity of Tonezh in Lelchitsy rayon of the Gomel oblast in Belarus which was discovered by the Kirovgeologiya association in 1981 and surveyed by the Belarusgeologiya association in 1983-1984 are described and it is noted that in a plan view, the Cretaceous erosion incision has not fully inherited the Jurassic linear depression. A geological section of the Neogene coal control paleovalley is plotted and the depression's elongation and its likely causes are discussed. It is noted that the Neogene deposit thickness in the deepest part of the depression reaches 190 m vs. a typical figure of 20-40 m for the region. The total thickness of commercial coal seams in the cross section reaches 23.8 m at a depth of up to 140 m. Deposit localization monitoring is identified as the most important prospecting criterion; other exploration criteria are reviewed and the conclusion is drawn that by taking into account the prospecting criteria fully, it is possible to substantially improve the coal exploration efficiency in the Pripyat region. Figures 1; references 1.

On Classifying Mineral Reserves

927D0230B Moscow RAZVEDKA I OKHRANA NEDR in Russian No 3, Mar 92 pp 13-14

[Article by L.I. Chetverikov, Voronezh State University; UDC 553.042]

[Abstract] The results of analyses of commercial mineral reserves are discussed and the suggested limit of error in computing the reserves for four categories of deposits according to various sources are summarized. The commercial reserves are divided into four categories according to their geological structure—simple, complex, very complex, and highly complex—which correspond to four different accuracy levels. Recommendations are made regarding the optimum density of the exploration and surveying net for each category of deposits and it is suggested that the net density be increased by fourfold. It is shown that the requirements imposed on the commercial reserve assessment accuracy and detail at various exploration stages can be made consistent with the customary fourfold surveying net extension only in the framework of correct error analysis. Tables 2; references 5.

Using Microcomputer for Analyzing Basic Situations in Field

927D0230C Moscow RAZVEDKA I OKHRANA NEDR in Russian No 3, Mar 92 pp 18-20

[Article by O.V. Oshkordin, A.A. Metsger, S.G. Frolov, A.V. Sukhanov, Urals Mining Institute imeni V.V. Vakhrushev and Uraltsvetmetrazvedka Nonferrous Metal Exploration Trust; UDC 681.3:622.24]

[Abstract] The specific features of geological exploration objects, e.g., their attributively inherent uncertainty and hierarchical structure, prompted the development of a procedure for analyzing work-related basic situations of geological exploration and prospecting directly in the field using a microcomputer. To a great extent, the proposed technique takes into account the systemic nature of the drilling process and makes it possible to fully find and to comprehensively utilize existing professional experience and personal expert knowledge. The main elements incorporated in the procedure, i.e., the knowledge base, the database, and software, are outlined and the principal operations involved in soundly justifying the designs and policies and procedures are described; these include analyzing the possible exploration object versions, estimating the efficiency of procedures and designs, and selecting the optimum design. An algorithm of arriving at the design and procedure decision and selecting the sequence of necessary steps is cited. The analytical software is realized in the Basic language for the Iskra-1030 microcomputers. The use of PCs makes it possible to make sound decisions and raise the technical culture level as well as leads to considerable savings. Figures 1; references 3.

State and Future Mineral Resource Exploration Trends of Kara-Bogaz-Gol Bay

927D0230D Moscow RAZVEDKA I OKHRANA NEDR in Russian No 3, Mar 92 pp 22-24

[Article by V.P. Fedin, Turkmen Geological Surveying Expedition; UDC 553.63(575.5)]

[Abstract] The consequences of the Kara-Bogaz-Gol Bay transition from a Caspian Sea bay into an inland lake and the resulting rapid evaporation of the brine and development of a 50 cm deep layer of chloride-magnesium salts prompted an attempt to revert the bay to its original status. Currently, the "bay" receives seawater over a pipeline in the amount of 2 cubic kilometers per year. Consequently, the principal factor in restoring Kara-Bogaz-Gol to its original state is identified as increasing the volume of water feeding it and developing a sound supply schedule. The parameters of the Kara-Bogaz-Gol water area under a regulated water supply condition, the average monthly air temperature at the Bekdash weather station on the coast, the brine evaporation data for 1986 and 1987 measured by a GGI-300 evaporator, and the necessary amount of water delivery for equalizing water losses to evaporation from a 3,500 km^2 area are summarized. The existing raw material base of the "bay" is analyzed and is future utilization trends are outlined. The conclusion is drawn that the current brine intake level of 60,000 cubic meters per day is not defensible and should be decreased to 28,800 cubic meters per day on an annual basis. The importance of adjusting the investments in R&D, support, construction, and commissioning of new facilities for solving the problem of Kara-Bogaz-Gol is stressed. Tables 3; references 3.

Effect of Coal Deposit Exploration on Ground Water Condition

927D0230E Moscow RAZVEDKA I OKHRANA NEDR in Russian No 3, Mar 92 pp 31-32

[Article by Ye.P. Kotelevets, N.A. Kashirina, Luganskgeologiya Association; UDC 553.94/.96.004:556.332.52]

[Abstract] The hydrogeological and mining conditions of coal exploration and the problem of water inflow into coal mines and collieries are discussed and the effect of the coal deposit mining and exploration on the ground water conditions is investigated. Attention is focused in the gradual sinking of the earth surface and the resulting loss of homes built on top of coal mine workings. According to the ground water circulation and natural ground water occurrence patterns in various types of rock in the vertical cross section, three hydrodynamic zones are identified and their specific features are described. The effect of coal exploration in each of the hydrodynamic zone on the ground water condition is analyzed. An increase in the mean weighted mine water mineralization since the 1970's is noted; most of the mineralized water pumped out of coal mines reaches the Severnyy Donets and Mius rivers; today, the mineralization, hardness, and sulfate and phenol content in the surface waters of these rivers exceeds safe levels by two- to threefold. A degradation of the ground water quality in the Severnyy Donets Valley due to contaminated surface water infiltration and the danger this phenomenon poses to drinking water are pointed out; the danger from the water accumulation in abandoned mines is also discussed.

25IZG Core Drill Bit Sets With AKON Synthetic Polycrystal Diamonds

927D0230F Moscow RAZVEDKA I OKHRANA NEDR in Russian No 3, Mar 92 pp 33-34

[Article by A.I. Osetskiy, G.A. Blinov, V.Sh. Khazhuyev, A.S. Kushkhabiyev, All-Union Exploration Technology Institute and KBZAI; UDC 622.24.051.71:679.826]

[Abstract] The use of drill bits and diamond tools with natural diamonds is prevalent today despite their high cost due to the low efficiency of synthetic diamond (SA) tools for drilling hard rock. This fact prompted the All-Union Exploration Technology Institute (VITR) together with KBZAI to develop the 25IZG core drill bit sets using the AKON synthetic diamonds; the drill bit set

specifications are summarized. The new drill bits with a 59 mm diameter passed acceptance tests at the Nevskgeologiya and Yuzhkazgeologiya associations; to this end, 500-700 m deep wells were drilled using the SKB-4, SKB-5, and ZIF-650M drilling rigs at a 390-800 min^{-1} speed, an axial load of 800-1,500 daN, and a 19-40 dm^3/min drilling emulsion rate. The test results are compared to the output of standard ZAI drill bits with natural diamonds. Tests reveal that it is expedient to use the new drill bits for category VII-X hard and very hard rock, including abrasive and crumbling rock. Large-scale production of the new drill bits is expected to commence in 992. Tables 2; references 3.

Outfitting Mine Shafts With Preliminary Rock Freezing

927D0232E Moscow RAZVEDKA I OKHRANA NEDR in Russian No 5, May 92 pp 27-28

[Article by A.V. Rudchenko and V.S. Zakharov, Geologorazvedka Concern; UDC 622.012.2:622.234.3]

[Abstract] Two shafts, 91 and 140 m deep, were sunk during the course of prospecting for ore bodies covered with sea sediments (including flooded quicksands) measuring 40 to 80 m thick. Samples pumped up from the shaft bottoms established that the submerged sand horizons had a filtration factor of 1.3 m/day, the gravel-pebble horizon had a filtration factor of 8.6 m/day, the influx of water into the first shaft ranged from 85 to 120 m^3/h, and the influx into the second shaft was between 130 and 160 m^3/h. In view of these findings, specifications were developed for freezing equipment to freeze the rock to be mined while it was still in the shaft. The equipment set for freezing the rock, sinking the wells, and erecting the freezing columns took 45 days to construct. Compressor pump tubes 114 mm in diameter were used in erecting the freezing columns. Threaded connections and a sealant were used to join the tubes. A PKhS-100 portable refrigeration unit consisting of two PKhU-50 units to cool the aqueous brine solution was used. At the outlet from the evaporator, the coolant used had a temperature between -15 and 135°C. The process of freezing the rock to form an ice-and-rock shaft enclosure took 45 days. The process of sinking the mine shaft was begun when the temperature of the brine entering the freezing columns reached -30°C. The temperature in the thermometric boreholes located along the axis of the freezing column ranged from -12 to -17°C, and the temperature in the well located 1 m from the axis of the freezing columns was -10°C. A total of 22 freezing columns sunk to a depth of 120 m were used to form the ice-and-rock shaft enclosure. Under the conditions provided, the rock in the shaft's cross section was completely frozen, which created additional problems. Jack hammers and manual loading of the rock to a depth of 60 m were required, after which explosive drilling operations were required. Blastholes measuring 42 mm in diameter were drilled by PR-30 perforators. A continuous wooden lining (200 x 200 mm) was used in sinking the shafts. The explosive drilling operations were conducted at an average rate of 37 m/month. Despite the additional problems created by the frozen rock, the technique of using portable refrigeration units to freeze submerged rock made it possible to implement mining conditions under very complex geological and mining conditions in the time frame required for similar operations under normal conditions. Figures 2, table 1.

Uranium Deposits in Regions of Continental Volcanism

927D0232B Moscow RAZVEDKA I OKHRANA NEDR in Russian No 5, May 92 pp 8-11

[Article by A.D. Kondratyukin, Sosnovgeologiya GGP, and A.G. Yevstratov, I.S. Modnikov, and I.V. Sychev, All-Union Crude Minerals Scientific Research Institute; UDC 553.495:551.263.037]

[Abstract] Uneven-aged continental volcanic belts are unique regional structures of the earth's crust that are distinguished by their high yields of certain rare, nonferrous, and noble metals. The efforts of specialized organizations of the former USSR Ministry of Power and Electrification in the Eastern Transbaykal region, central and southern Kazakhstan, and Central Asia have uncovered, prospected, and launched the commercial exploitation of a large amount of uranium deposits in such belts. These deposits are distinguished by the high quality of their ores and by the relative ease with which they may be recovered on a commercial basis. The uranium deposits in regions of continental volcanism have a similar ore composition with a specified sequence of mineral associates, i.e., preore (quartz-chlorite-pyrite or, more rarely, ankerite-polymetallic), ore (pitchblende-molybdenite or, more rarely, pitchblende-coffinite-brannerite and pitchblende-polymetallic), and postore (quartz-fluorite-calcite with sphalerite, galenite, chalcopyrite, and other sulfides). The clearest representatives of such ore objects are the uranium-molybdenum deposits of the Strelitsa ore-bearing region, which is located in the southern part of Priargunye of the eastern Transbaykal region. Ore-bearing volcanic structures of this type were formed during the process of the tectonic-magmatic activation of the granitized dome emergence of the foundation over the course of 35 to 50 million years. The uranium concentration in the acidic effusions of the porphyric structure reaches 11 g/t or more, with most (60 to 90%) occurring in the glassy base of the rock. Volcanic glasses with an acidic composition have the highest uranium (20 to 25 g/t) and thorium (40-50 g/t) contents. Longitudinal fractures in the foundation are the main tectonic structure indicating that uranium ore is present within the confines of a given volcanic-tectonic structure. In a volcanogenic-sedimentary section, these structures generally appear in the form of rather wide (many hundreds of meters) intermittent zones with an increased incidence of cracking. The uranium deposits are located primarily in the central part of the depression in a band caused by a lengthwise

magma-controlling sedimentation fracture. Cracked-veined and stockwork types of ore bodies and stratal deposits are characteristic of uranium deposits. The formation of commercial uranium deposits within the confines of a volcanic-tectonic structure is the result of a protracted multiple-stage ore formation process. Two leading mineral types of ores develop depending on the specific conditions of ore deposition in the given beds. Uranium-molybdenum ores are the most prevalent. Uranium ores revealing a close temporal and spatial link to zones of low-temperature alkaline sodium metasomatism are less extensively developed. The vertical geochemical zonality of uranium deposits consists of enrichment of the upper portions of the ore-bearing zones with chalcophilic elements with respect to uranium. Physicochemical circumstances such as those described herein are characteristic of the volcanic-sedimentary hood of depressions and upper part of a granitized foundation characterized by maximum tectonic destruction. Figures 3; references 4 (Russian).

The Main Commercial Types of Uranium Deposits in the Countries of the CIS and the Experience of Searching for Them, Accelerated Prospecting for Them, and Preparing Them for Assimilation

927D0232A Moscow RAZVEDKA I OKHRANA NEDR in Russian No 5, May 92 pp 5-7

[Article by S.S. Naumov and M.V. Shumilin, Geologorazvedka Concern; UDC 553.495(47+57)]

[Abstract] Since 1971, prospecting for uranium has been confined to the southern, relatively assimilated regions of the former USSR. The northern and northeastern regions of Russia have remained virtually unexplored even though geological data indicate that this extensive territory probably contains uranium deposits with significant forecast reserves. The total raw material uranium base of the former Soviet Union has been estimated at 2 million tons, about 1,200,000 tons of which is thought to consist of category reserves and forecast category R_1 reserves. These uranium resources are located mainly in four republics of the CIS: Kazakhstan, Russia, Ukraine, and Uzbekistan, with most of the already prospected reserves being in Kazakhstan and most of the forecast reserves being in Russia. The uranium deposits of the aforesaid republics belong mainly to the four leading commercial types: stockwork-metasomatic deposits in albitites, veins-stockwork in folds and continental volcanic complexes, infiltration deposits in terrigenous platform complexes, and infiltration deposits in paleovalleys. Most of the stockwork-metasomatic deposits in albitites are ascribed to crystalline formations of the Ukraine craton and are associated with the era of Early Proteozoic (1.8 billion years) activation of Archean cratonized blocks. The ores in these deposits are primarily poor and standard (0.09 to 0.18%). The reserves of individual deposits of this type are estimated at 20,000 to 50,000 tons and are located in the vicinities of Kirovgrad and Krivoy Rog. Vein-stockwork deposits in folds and continental volcanic complexes deposits are known to exist in Kazakhstan (the Kokchetavskiy and Balkhashskiy regions) and Russia (the Transbaykal region). The deposits of the Zabaykalye region are the most interesting. In an area measuring only 20 km across, more than 10 uranium deposits of relatively rich contrast ores have been discovered (of the said deposits, the Streltsovskoye and Tulkuyevskoye have reserves of 60,000 and 35,000 tons, respectively). Infiltration deposits in terrigenous complexes are known to exist throughout the world; the scales of the deposits of this type in Kazakhstan and Uzbekistan are unique, however. The total amount of uranium resources of this class in the former Soviet Union are estimated at more than 500,000 tons, with individual deposits varying in size from 5,000-10,000 to more than 50,000 tons. Infiltration deposits in paleovalleys are most prevalent in Russia (the Transural region, Western Siberia, and the Northern Transbaykal region). These deposits are distinguished by their link to the surfaces of ancient peneplains submerged in the crystalline foundation. The geological enterprises of the concern Geologorazvedka, which is involved in uranium prospecting, have developed and manufactured their own drilling rigs (The PBU-800, TSBU-200, etc.) and have been focusing their attention on developing advanced engineering support for uranium prospecting operations. A number of publications have detailed the experience that has been gained in searching for, prospecting, and developing uranium deposits in the former Soviet Union. Unfortunately, however, none of these publications ties specific techniques to specific deposits. Figures 2; references 9 (Russian).

Uranium Deposits in the Paleovalleys of the Transural and Transbaykal Regions

927D0232C Moscow RAZVEDKA I OKHRANA NEDR in Russian No 5, May 92 pp 12-15

[Article by I.I. Kuchinin, Zelenogorskgeologiya GGP, P.A. Peshkov, Sosnovgeologiya GGP, P.K. Dementyev, A.V. Kochenov, A.Ye. Khaldey, and A.B. Khalezov, All-Union Crude Minerals Scientific Research Institute; UDC 553.49(57.54/.55)470.51/.56-32]

[Abstract] Included among the insulator uranium deposits localized in permeable sedimentary rock is a large group of ore objects associated with paleovalley structures. Such deposits have been termed "basal" deposits in the Western literature. Ore-bearing paleochannel structures are generally the result of erosion and often have zones of fault damage in the foundation. Such deposits are widely developed on nearly all continents among rock of different geologic ages. On Russian soil, the paleovalley deposits that are of commercial interest are located mainly in two regions, i.e., the Transural and Transbaykal regions. The ore-bearing paleovalleys of the Transbaykal region are concentrated primarily on the Vitim plateau, and the main node of development of paleovalley deposits with a high uranium content is located within the confines of the

Amalat plateau (the Khiagdinskaya group of deposits). The uranium-bearing structures are mainly short (1-2 to 10 km) side tributaries of the Bolsheamalat and Atalangin paleorivers. When viewed in a plane, the ore deposits of the region have a ribbon-like shape that roughly echoes the contours of the paleovalleys. The maximum uranium concentration is in relatively fine-grained layers and lenses that are in contact with larger-grain water-permeable horizons, along which superimposed oxidation and clarification processes developed. Besides containing uranium, the paleovalley deposits of the Transbaykal region also contain a broad spectrum of accompanying microelements (ranked in order of decreasing prevalence): Mo, Zn, Co, Zr, As, Th, Cu, Y, and Sc. Samples taken from the deposits are characterized not only by specialization for uranium (5 to 8 g/t) but also by an elevated percentage of a number of other elements present in uranium ore. From a geological standpoint, the ore-bearing deposits of the Transural region are quite different from those of the Transbaykal region. The Dolmatovskoye, Dobrovolnoye, and Tobolskoye deposits, which are located in connate valleys of the Late Jurassic period, are the best studied deposits of the group. The said deposits are located in the central Transbaykal region. The average content of organic carbon in the Dolmatovskoye deposit ranges from 0.5 to 1%, and the average pyrite content fluctuates from 0.2 to 2%. The maximum uranium content is fixed in gray unoxidized rock close to the point of contact with the former oxidation zone, forming a subzone of rich ore and often accompanied by accumulations of secondary sulfides. The uranium in this rock is present in the form of U(IV) oxides and coffinite and is associated with a number of more recently deposited minerals such as pyrite, jordisite, chalcopyrite, arsenopyrite, and sphalerite. The uranium is also accompanied by a broad spectrum of microelements (the main ones being Mo, Se, and Re in amounts of 0.06, 0.08, and 5 x 10^{-4}%, respectively). Figures 4; references 3 (Russian).

A Metrologic Support System for Exploration and Prospecting Operations at Uranium Deposits

927D0232A Moscow RAZVEDKA I OKHRANA NEDR in Russian No 5, May 92 pp 32-34

[Article by I.M. Khaykovich and A.S. Serykh, Rudgeofizika All-Union Scientific Research Institute of Prospecting Geophysics; UDC 550.812:553.495:389]

[Abstract] A new metrologic support system was developed for use in exploration and prospecting operations at uranium deposits. Contemporary uranium exploration and prospecting operations generally entail the use of nuclear geophysics sampling systems that are based on the principle of measuring fields of gamma-radiation from natural radioactive elements in integral and gamma-radiation spectrometry modes. Because measurements must be taken on the earth's surface, in boreholes, and in mines, a variety of measuring equipment must be used. Included among such equipment are special logging equipment, portable instruments, and instruments mounted in motor vehicles and on aircraft. It is crucial that the measurements taken by each of these diverse pieces of equipment be unified. The new metrologic support system described herein has been designed with this goal in mind. The new support system, which was designed at the All-Union Scientific Research Institute of Prospecting Geophysics, is based on the use of measuring equipment that maintains the dimensions of the units of mass fractions of natural radioactive elements (potassium, uranium [radium], and thorium) while also converting them to other measurement units, including working units and the units on which the operation of individual pieces of measuring equipment is based. The new metrologic support system is designed to operate in an integral gamma-radiation-counting mode, as well as in a gamma-radiation spectrometry mode. The new metrologic support system makes it possible to link the results obtained by logging and by ground and air photography, and the software and algorithms accompanying the new support system (which are based on the apparatus of mathematical statistics and linear algebra) make it possible, at each stage of the measurement process, to not only obtain estimates of the parameters being sought but to also obtain estimates of their errors, which is extremely important in isolated sections with different levels of natural radioactive elements and contamination levels, as well as in selecting the increment of isolines to be used when plotting maps. The system used for direct determination of uranium based on the method of logging prompt fission neutrons is based on the principle of measuring the field of prompt neutrons occurring during the fission of nuclei of uranium 235 by thermal neutrons. The new system makes it possible to judge radioactive equilibrium, which is very important from the standpoint of assessing the possibilities of using gamma-ray logging to estimate parameters. When calibrated, the new system makes it possible to determine the mass fraction of uranium with a basic error of up to 10%. The new metrologic support system is both simple and economical, and its use increases the reliability of the results of nuclear geophysical sampling without significant additional cost. References 9 (Russian).

A New Region With Deposits of Rich Complex Ores in Southern Karelia

927D0232D Moscow RAZVEDKA I OKHRANA NEDR in Russian No 5, May 92 pp 15-19

[Article by Ye.K. Melnikov, Yu.V. Petrov, and A.V. Savitskiy, Nevskegeoloya GGP; UDC 553.33/'9(470.22-13]

[Abstract] The Onezhskiy ore-bearing region, a region with rich deposits of complex ore, was discovered in the 1980's thanks to the intensive integrated forecasting and prospecting performed by the subdepartments of the Nevskgeologia PGO [not further identified] at the assignment of the concern Geologorazvedka. The new Onezhskiy ore-bearing region occupies about 50,000

km^2 and encompasses the most economically assimilated regions (Medvezhyegorsk, Kondopoga, and Pudozh) and adjacent portions of the Leningrad, Vologda, and Arkhangelsk oblasts. To date, five deposits have already been discovered in the Onezhskiy ore-bearing region, and more than 10 other sections appear to be promising sources of vanadium (with uranium, platinoid, gold, silver, and other valuable components) ore possessing unique mineralogical and geochemical features and technological properties. The Onezhskiy ore-bearing region is unique both in Russia and throughout the world because of the proximity of the ore deposits to established industrial activity. About 90% of the Onezhskiy ore-bearing region is located on the Baltic craton. The remaining 10% is located in the buffer zone where the craton and the Russian plate joint. The block has a two-tier structure, the lower structural tier consisting of deeply metamorphosed complexly dislocated supracrustal rock and granitoid Archean rock and weakly metamorphosed sedimentary and volcanic deposits and intrusive rock of the Lower Proterozoic period. The upper structural tier (the hood of the Russian plate) consists of phanerose sediments. In all, 95% of the territory is covered by Quaternary formations (mainly glacial). The Onezhskiy basin or depression is especially interesting. All of the complex ore deposits detected in the Onezhskiy ore-bearing region to date have been in zones of fold and fault dislocations. In a typical cross section, each of these zones of fold and fault dislocations consists of two to four tightly compressed steep or overturned anticlinal folds 0.8 to 1.8 km high and 10 or more km long. The ore-bearing zones of fold and fault dislocations are marked all over with zones of magnesial-alkaline-carbonate metasomatism. Uranium-noble metal-vanadium deposits are located in the most permeable intervals of the fold and fault dislocation zones. In addition to their main useful components (V, U, Pd, and Au), samples taken from the Onezhskiy ore-bearing region also contain more than 20 other valuable elements, including rhenium and rhodium. The Onezhskiy ore-bearing region has the objective geological and economic prerequisites for the creation of a new mining and industrial complex that would recover vanadium, gold, platinoids, uranium, and a number of other valuable components (magnesium, nickel, alkaline asbestos, and talc). Figure 1; references 8 (Russian).

Scientific and Engineering Progress in Environmental Protection in Ferrous Metallurgy

927D0243F Moscow STAL in Russian
No 4, Apr 92 pp 84-86

[Article by R.K. Veletskiy, Energostal Scientific Production Association; UDC 669.1:628.5]

[Abstract] The negative impact of ferrous metallurgy enterprises on the environment is discussed and it is noted that the industry contributes some 15 to 20% of all discharges into the air and water; moreover, the specific water consumption in the industry allowing for all process stages reaches 270 cubic meters per ton of steel. The efforts of the All-Union Research and Design Institute of Ferrous Metallurgy Energy and Cleanup and the Ferrous Metallurgy Energy Production Association in protecting the air and water from harmful discharges by ferrous metallurgy enterprises and setting up and adjusting gas scrubbers and water purification units as well as utilizing secondary energy resources (VER) and cooling steelmaking units and the metal itself are described. Implementation of the environmental technology developments in the past 25 years led to a 6.0 million ton decrease in atmospheric discharges and a 1.5 billion cubic meter drop in waste water effluents. The specific types of equipment and technologies designed in the field of air quality protection and waste water treatment are outlined in detail. The measures aimed at cooling the production units and utilizing secondary energy resources (from their thermal energy) are described. In all, the Energostal association's developments made it possible to double the secondary energy source utilization efficiency. The urgency of comprehensively addressing the issue of waste-free technology development is emphasized.

Principal Trends of Reservoir Protection at Metallurgical Enterprises

927D0243G Moscow STAL in Russian
No 4, Apr 92 pp 87-89

[Article by V.A. Kholodnyy, M.L. Kutsyshin, Energostal Scientific Production Association; UDC 628.1:669.1]

[Abstract] The principal trends in reservoir protection and efficient utilization of water resources under the ongoing development and retooling in the ferrous metallurgy industry, primarily decreasing the water consumption, developing more economic equipment, and implementing waste-free technologies, are identified and measures for removing mechanical impurities and stabilizing the water are outlined. New reagents developed for preventing carbonate deposits in water supply systems are reported and other methods of circulating water treatment, e.g., electrical, are discussed. The need for low-emulsion waste water treatment and utilization is stressed. Various methods of waste water utilization using lime and other compounds and physical and chemical methods of emulsion-containing waste water purification are presented. Tests of new filtering, flotation treatment, and electrochemical regeneration systems are reported. It is noted that comprehensive implementation of the above environmental engineering designs will make it possible to develop waste-free waste water treatment technologies and closed-loop (nondischarging) water supply systems for industrial enterprises.

State and Decontamination Trends for Water and Gas Treatment Product Utilization

927D0243H Moscow STAL in Russian
No 4, Apr 92 pp 89-90

[Article by V.G. Bratchikov, Energostal Scientific Production Association; UDC 628.544.13.001.537]

[Abstract] The increasing urgency of utilizing the trapped dust and sludge forming at ferrous metallurgy enterprises in addressing urgent environmental protection issues prompted an investigation into the state of water and gas purification product decontamination and utilization in the industry. These products are divided into two categories: standard and substandard. The latter include the products used as a raw material in ferrous metallurgy, those used after special processing in kindred areas, and products which are not utilized (30% of the total). A number of technologies developed by the Energostal Association for utilizing the sludge after neutralization are discussed and it is noted that a flexible standard power and basic process complex may be developed on the basis of the new technologies. A new management processing principle developed at the Energostal is reported; its implementation makes it possible to carry out comprehensive scientific and technical preparation for water and gas purification product utilization while the resulting products can be widely used in a regional basis. It is stressed that the iron-bearing sludge utilization practices developed by Energostal can be implemented at metallurgical enterprises.

Integrated Assessment of Electroplating Waste as Secondary Material Source for Silicate Materials

927D0236A Moscow STEKLO I KERAMIKA in Russian No 4, Apr 92 pp 2-4

[Article by Ye.M.Dyatlova, I.A. Levitskiy, V.V. Tizhovka, Belarussian Technological Institute imeni S.M. Kirov; UDC 66.087.7.002.68:666.3:666.1:66.293]

[Abstract] The lack of electroplating waste product utilization and the high concentration of heavy metal oxides and other toxic substances retarded its medical and health evaluation; thus, the need for an integrated assessment of the electroplating waste, including a toxicological analysis and a study of the feasibility of its use as a secondary raw material for making silicate products, is emphasized. The slurry forming in waste treatment facilities of mechanical plants during the rinse water neutralization is investigated. The chemical composition of oxygen and metals in waste samples examined by a scanning electron microscope with an Opton microanalyzer, the metal oxide concentrations in the samples, and the sieve residue fractions as a function of the mesh size

are summarized. An X-ray diffraction pattern of dried waste samples is plotted. The study shows that the waste product consists mostly of <0.063 mm particles whereby the total residue on the sieve amounts to 1.06% and the proportion of >0.5 mm inclusions is 0.35%. The results of a differential thermal analysis are plotted; the curves reveal the presence of two endoeffects attesting to decay processes. A toxicology study is carried out at the Belarussian Scientific Research Institute of Public Health and shows that the sludge is not a dangerous source of radioactive contamination pursuant to GOST 12.007-76. The above integrated assessment confirms the feasibility of using electroplating waste for making high-temperature synthesis products, such as glass, glaze, expanded clay aggregate, and other materials. Figures 3; tables 3; references 3.

Electrolytic Manganese Dioxide Byproducts in Glass Container Industry

927D0236B Moscow STEKLO I KERAMIKA in Russian No 4, Apr 92 pp 4-5

[Article by A.V. Sarukhanishvili, L. Shashek, Ye.V. Shapakidze, I.A. Sarukhanishvili, Georgian Engineering University and Prague Chemical Engineering Institute; UDC 666.171:666.123]

[Abstract] The chemical composition of the sludge from the production of electrolytic manganese dioxide (EMS) at the Rustavi Azot association—a waste byproduct resulting from the manganese ore heat treatment, milling, and processing—is summarized and it is noted that more than 4,000 t of sludge accumulates annually at the plant; moreover, its content's variation from the mean does not exceed 15%. The sludge suitability for use as a raw material in the glass container industry is assessed. To this end, a physical and chemical analysis is carried out; it reveals that the sludge consists of plagioclase minerals, aqueous sulfates of bivalent elements, and a water-bearing manganese oxide with a variable content (vad). The processes occurring at various temperatures in the charge with and without EDM sludge are compared and the technological properties of the glass produced using the EDM sludge are examined. The chemical stability, heat resistance, and solidification properties of the glass made with the EDM sludge are similar to those of commercial brands while the pilot glass exceeds commercial brands with respect to the body clarification and production temperatures; thus, the use of the sludge eliminates the need to use sodium sulfate and makes it possible to lower the quartz sand and Ca-bearing material content in the charge. Figures 1; tables 2; references 2: 1 Russian, 1 Western.

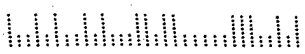

Foreign Broadcast Information Service (FBIS) and Joint Publications Research Service (JPRS) publications contain political, military, economic, environmental, and sociological news, commentary, and other information, as well as scientific and technical data and reports. All information has been obtained from foreign radio and television broadcasts, news agency transmissions, newspapers, books, and periodicals. Items generally are processed from the first or best available sources. It should not be inferred that they have been disseminated only in the medium, in the language, or to the area indicated. Items from foreign language sources are translated; those from English-language sources are transcribed. Except for excluding certain diacritics, FBIS renders personal names and place-names in accordance with the romanization systems approved for U.S. Government publications by the U.S. Board of Geographic Names.

Headlines, editorial reports, and material enclosed in brackets [] are supplied by FBIS/JPRS. Processing indicators such as [Text] or [Excerpts] in the first line of each item indicate how the information was processed from the original. Unfamiliar names rendered phonetically are enclosed in parentheses. Words or names preceded by a question mark and enclosed in parentheses were not clear from the original source but have been supplied as appropriate to the context. Other unattributed parenthetical notes within the body of an item originate with the source. Times within items are as given by the source. Passages in boldface or italics are as published.

SUBSCRIPTION/PROCUREMENT INFORMATION

The FBIS DAILY REPORT contains current news and information and is published Monday through Friday in eight volumes: China, East Europe, Central Eurasia, East Asia, Near East & South Asia, Sub-Saharan Africa, Latin America, and West Europe. Supplements to the DAILY REPORTs may also be available periodically and will be distributed to regular DAILY REPORT subscribers. JPRS publications, which include approximately 50 regional, worldwide, and topical reports, generally contain less time-sensitive information and are published periodically.

Current DAILY REPORTs and JPRS publications are listed in *Government Reports Announcements* issued semimonthly by the National Technical Information Service (NTIS), 5285 Port Royal Road, Springfield, Virginia 22161 and the *Monthly Catalog of U.S. Government Publications* issued by the Superintendent of Documents, U.S. Government Printing Office, Washington, D.C. 20402.

The public may subscribe to either hardcover or microfiche versions of the DAILY REPORTs and JPRS publications through NTIS at the above address or by calling (703) 487-4630. Subscription rates will be provided by NTIS upon request. Subscriptions are available outside the United States from NTIS or appointed foreign dealers. New subscribers should expect a 30-day delay in receipt of the first issue.

U.S. Government offices may obtain subscriptions to the DAILY REPORTs or JPRS publications (hardcover or microfiche) at no charge through their sponsoring organizations. For additional information or assistance, call FBIS, (202) 338-6735,or write to P.O. Box 2604, Washington, D.C. 20013. Department of Defense consumers are required to submit requests through appropriate command validation channels to DIA, RTS-2C, Washington, D.C. 20301. (Telephone: (202) 373-3771, Autovon: 243-3771.)

Back issues or single copies of the DAILY REPORTs and JPRS publications are not available. Both the DAILY REPORTs and the JPRS publications are on file for public reference at the Library of Congress and at many Federal Depository Libraries. Reference copies may also be seen at many public and university libraries throughout the United States.